

# **Generation of recombinant MVA encoding HBV core and CD70 and evaluation of the co-stimulatory effect of CD70 in protein-prime/MVA boost vaccination in mice**

Ann-Sophie Maria Margarita Stephan

Vollständiger Abdruck der von der TUM School of Medicine and Health der Technischen Universität München zur Erlangung einer Doktorin der Medizinischen Wissenschaft (Dr. med. sci.) genehmigten Dissertation.

Vorsitz: Prof. Dr. Jürgen Ruland

Prüfende der Dissertation:

1. Prof. Dr. Ulrike Protzer
2. Priv.-Doz. Dr. Jan P. Böttcher
3. Prof. Dr. Marc Schmidt-Supprian

Die Dissertation wurde am 19.10.2023 bei der Technischen Universität München eingereicht und durch die TUM School of Medicine and Health am 08.05.2024 angenommen.

## **Abstract**

Chronic hepatitis B infection, which can't be cured with currently available treatment options, and in particular the associated complications, are a global burden causing hundreds of thousands of deaths per year. Whereas the course of acute hepatitis B infection is often mild or asymptomatic, chronic infection causes liver cirrhosis and liver cancer and is exceptionally challenging to treat. In fact, in most of the cases, therapy with pegylated IFN $\alpha$  or nucleot(s)ide analogues can only control but not eliminate the viral infection. As a consequence, long-term treatment is required which entails the risk of development of drug resistances, adverse side effects, and high costs of treatment.

In studies in humans and animal models, the role of CD8 T cells in HBV (hepatitis B virus) infection was revealed. Disease control is associated with a strong and polyclonal response of CD8 T cells, which control and eliminate the infection. However, persistence of the virus and development of chronic infection is associated with a weak and narrowly focused cytotoxic T lymphocyte response with inhibitory molecules which are upregulated on HBV-specific cytotoxic lymphocytes. Therapeutic vaccination in chronic HBV infection aims at the enhancement of the patient's adaptive immune response to eliminate HBV. Several former studies have demonstrated this principle, and while reliable success is yet to be achieved, the plethora of potential vaccine formulations and administrations leaves a substantial margin for further improvement of therapeutic vaccines against chronic HBV. Previous results of the Institute of Virology of the Technical University of Munich strongly indicate a combination of heterologous protein-prime/MVA (modified vaccinia virus Ankara)-boost-vaccination regimen being a particularly auspicious approach to achieve such improvement.

This thesis examines the role of the co-stimulatory molecule CD70 during the boost in therapeutic vaccination by heterologous protein-prime/MVA-boost vaccination and reveals that CD70 could have a beneficial effect on the functionality of CD8 T cells that are specific for the target antigen. The study also provides evidence that the specific construction of the boost-vaccination vector with mutual temporal and spatial expression of target antigen and CD70 has a major impact on the specificity of the co-stimulatory function of CD70.

## Zusammenfassung

Die chronische Infektion mit dem Hepatitis B Virus (HBV) stellt ein großes globales Gesundheitsproblem dar: Während eine akute Hepatitis-B-Infektion oft mild oder asymptomatisch verläuft, verursacht die chronische Infektion Komplikationen wie Leberzirrhose und Leberkrebs, welche jährlich zu hunderttausenden Todesfällen führen. Darüber hinaus ist die chronische Hepatitis-B-Infektion äußerst schwer zu behandeln und mit den derzeit verfügbaren Behandlungsoptionen nicht heilbar. Die medikamentöse Behandlung mit pegyliertem IFN $\alpha$  oder Nukleot(s)id-Analoga kann die virale Infektion meist nur kontrollieren, aber nicht eliminieren. Dies bringt die Notwendigkeit einer langfristigen Behandlung mit sich, die das Risiko der Entwicklung von Arzneimittelresistenzen, unerwünschten Nebenwirkungen und hohen Behandlungskosten birgt.

In Studien an Menschen und in Tiermodellen wurde die Rolle von CD8-T-Zellen bei HBV-Infektionen gezeigt: Eine Kontrolle und Beseitigung der Infektion ist mit einer starken und polyklonalen Reaktion von CD8-T-Zellen verbunden. Die Persistenz des Virus und die Entwicklung einer chronischen Infektion sind hingegen mit einer schwachen und eng fokussierten zytotoxischen T-Lymphozyten-Reaktion assoziiert, bei der hemmende Moleküle auf HBV-spezifischen zytotoxischen Lymphozyten hochreguliert sind. Eine therapeutische Impfung bei einer chronischen Infektion zielt darauf ab, die adaptive Immunantwort des Patienten so zu stärken, dass eine Beseitigung von HBV erreicht wird. Frühere Studien zu therapeutischen Impfstoffen gegen chronische Hepatitis B haben dieses Prinzip bereits gezeigt. Obwohl dabei zuverlässige Erfolge noch nicht erzielt werden konnten, bietet die Vielzahl von Möglichkeiten der Impfstoffformulierung und -verabreichung einen Spielraum für weitere Verbesserungen. Die bisherigen Ergebnisse des Instituts für Virologie der Technischen Universität München zeigen, dass ein heterologes Impfschema mit Protein-Prime/MVA (modifiziertes Vaccinia Virus Ankara)-Booster-Impfung ein besonders vielversprechender Ansatz ist, um eine solche Verbesserung zu erreichen.

Diese Arbeit untersucht die Rolle des kostimulatorischen Moleküls CD70 während der MVA-Booster-Impfung einer therapeutischen heterologen Protein-Prime/MVA-Booster-Impfung und zeigt auf, dass CD70 eine positive Wirkung auf die Funktionalität von CD8 T-Zellen haben könnte, die spezifisch für das Zielantigen sind. Die Studie

liefert zudem Hinweise, dass die Konstruktion des MVA-Impfvektors mit zeitlich und räumlich gekoppelter Expression von Zielantigen und CD70 einen erheblichen Einfluss auf die Spezifität der kostimulatorischen Funktion von CD70 hat.

# INDEX

Abstract .....	2
Zusammenfassung.....	3
Abbreviations and Units .....	10
1. Introduction and background .....	12
1.1. Hepatitis B.....	12
1.1.1. The Hepatitis B virus .....	12
1.1.2. Epidemiology of HBV infection .....	16
1.1.3. Characteristics of HBV infection .....	17
1.1.4. The pathogenesis of chronic hepatitis B virus infection .....	22
1.1.5. Strategies to overcome immune tolerance in CHB by therapeutic vaccination .....	25
1.2. Modified vaccinia Ankara (MVA) as viral vector for therapeutic vaccination	27
1.2.1. Modified vaccinia Ankara: specifications and origin.....	27
1.2.2. MVA as viral vector for transgenes.....	28
1.2.3. Strategies of therapeutic vaccination by MVA immunization .....	29
1.2.4. Choice of the target antigen for vaccination: HBcAg.....	32
1.3. Co-stimulation of T cells via CD70/CD27 interaction.....	33
1.3.1. Characterization and biological function of CD27 and CD70 .....	33
1.3.2. CD70 as a promising co-stimulator in therapeutic vaccination .....	36
1.4. Aim of the study .....	38
2. Materials and Methods .....	39
2.1. Materials.....	39

2.1.1.	Reagents and Enzymes.....	39
2.1.2.	Buffers and solutions .....	39
2.1.3.	Chemicals.....	40
2.1.4.	Primers for PCR .....	41
2.1.5.	Cell lines and Bacteria.....	41
2.1.6.	Mouse strains .....	41
2.1.7.	Plasmids, viruses and DNA material .....	42
2.1.8.	Material for cell culture.....	42
2.1.9.	Antigens and Adjuvants .....	43
2.1.10.	Peptides, Antibodies and staining dyes.....	43
2.1.11.	Laboratory equipment / Devices.....	45
2.1.12.	Consumables .....	45
2.1.13.	Software .....	46
2.2.	Methods .....	47
2.2.1.	Cloning.....	47
2.2.1.1.	Vector design and cloning strategy .....	47
2.2.1.2.	Polymerase chain reaction (PCR) .....	48
2.2.1.3.	DNA digestion with restriction enzymes .....	50
2.2.1.4.	Agarose gel electrophoresis.....	51
2.2.1.5.	Purification of DNA (“spin purification”) .....	52
2.2.1.6.	Cloning by digestion and ligation.....	52
2.2.1.7.	Blunt-end cloning (TOPO cloning reaction) .....	53
2.2.1.8.	Transformation in TOP10 chemically competent cells.....	54

2.2.1.9.	Culturing and preservation of <i>E. coli</i> .....	54
2.2.1.10.	Plasmid extraction by Miniprep .....	54
2.2.1.11.	Specification of individual cloning steps.....	55
2.2.2.	Cell culture methods .....	56
2.2.2.1.	Culturing of eukaryotic cell lines .....	56
2.2.2.2.	Transfection of eukaryotic cells .....	56
2.2.3.	Verification of gene transcription in eukaryotic cells.....	57
2.2.3.1.	Flow cytometry analysis of transfected cells .....	57
2.2.3.2.	Immunoblotting of proteins .....	58
2.2.4.	Generation of recombinant MVA.....	60
2.2.4.1.	From Shuttle plasmid to pure and high concentrated vaccination stock of recombinant MVA.....	61
2.2.5.	Treatment of mice .....	65
2.2.5.1.	Mouse Strains .....	65
2.2.6.	Ex vivo immunological analysis.....	66
2.2.6.1.	Serological analysis.....	67
2.2.6.2.	Preparation of Splenocytes .....	67
2.2.6.3.	Preparation of liver associated lymphocytes (LAL).....	67
2.2.6.4.	Counting cells.....	68
2.2.6.5.	Analysis of cells by flow cytometry .....	68
2.2.7.	Immunohistochemistry .....	72
2.2.8.	Statistical analysis and visualization .....	73
3.	Results .....	74

3.1.	Immune response to rMVA-mediated antigens is not exclusively dependent on cross-presentation.....	74
3.2.	Generation of recombinant MVA vectors .....	76
3.2.1.	Cloning of rMVA-HBc-CD70 and rMVA-HBc .....	77
3.2.2.	Verification of correct transgene transcription in eukaryotic cells .....	80
3.3.	Comparison of rMVA-HBc and rMVA-HBc-CD70 in vivo.....	83
3.3.1.	CD70 co-expression in vaccination against HBc improves the number and function of HBV core-specific T cells in C57Bl/6 mice .....	83
3.3.2.	Vaccination of HBV1.3tg mice .....	88
3.3.2.1.	Co-expression of CD70 in protein-prime/MVA-boost vaccination increases the number of T-cell clusters in livers of HBV1.3tg mice .....	88
3.3.2.2.	The induction of the HBV core-specific T-cell immune response is dependent of antigenemia.....	90
3.3.2.2.2.	CD4 T-cell response of vaccinated HBV1.3tg mice .....	94
3.3.2.3.	CD70 co-expression during boost vaccination does not affect HBV-related serum markers in HBV1.3tg mice.....	95
3.3.2.4.	CD70 does not promote long-lasting immunopathology in the liver... 98	
3.3.2.5.	Tendency to reduced HBcAg expression in hepatocytes of HBV1.3tg mice after CD70 co-expression .....	98
4.	Discussion.....	101
4.1.	HBV core as target antigen in protein-prime/MVA-boost vaccination.....	101
4.2.	MVA is a suitable boost vector for therapeutic vaccination with a transgenic co-stimulatory component .....	102
4.2.1.	Recombinant MVA is preferably used as boost vector .....	102

4.2.2. rMVA infected cells present the transgene (HBV core) and the MVA-specific early antigen B8R mainly by direct presentation .....	103
4.2.3. CD70 and MVA is a suitable combination of co-stimulatory transgene and vector	104
4.3. CD70 co-stimulation improves the HBV core-specific T-cell response of vaccinated mice.....	105
4.4. Vaccination with transgenic HBc supports clusters of T cells in the livers of HBV1.3tg mice and CD70 enhances this effect .....	107
4.5. Therapeutic vaccination with transgenic CD70 boosts the immune response very specifically .....	109
4.6. Reduction of HBcAg-expression in the liver of vaccinated HBV1.3tg mice could not be observed in this study .....	110
4.7. An influence of CD70 co-stimulation on the HBV core-specific antibody response could not be observed .....	110
4.8. Outlook.....	111
4.9. Conclusion: CD70 co-stimulation is a potential improvement for therapeutic vaccination .....	111
Appendices .....	113
List of references.....	118
Danksagungen .....	127

## Abbreviations and Units

Abbreviation	Full term
AAV-MVA	Adenovirus which carries transgenic HBV
ALT	Alanine aminotransferase
anti-HBc(Ab)	Antibodies against the HBc antigen
anti-HBe(Ab)	Antibodies against the HBe antigen
anti-HBs	Antibodies against the HBs antigen
APC	Antigen presenting cell
BFA	Brefeldin A
bp	Base pairs
BSA	Bovine serum albumin
C93, C <sub>93</sub>	HBV core-derived dominant CD8 T-cell epitope
cccDNA	Covalently closed circular DNA
CD	Cluster of differentiation
cDNA	Complementary DNA
CHB	Chronic hepatitis B virus infection
CPE	Cytopathic effect
CpG	CpG Oligodesoxynucleotide
CTL	Cytotoxic T lymphocyte
DC(s)	Dendritic cell(s)
dH <sub>2</sub> O	Sterile distilled water
DNA	Deoxyribonucleic acid
dNTP	Deoxyribonucleotide triphosphate
ECL	Enhanced chemo luminescence
FCS	Fetal calf serum
FFPE	Formalin-fixed, Paraffin-embedded
HBc, HBV core	Hepatitis B virus core protein
HBcAg	Hepatitis B virus core antigen
HBe	Hepatitis B virus envelope protein
HBeAg	Hepatitis B virus envelope antigen
HBs	Hepatitis B virus surface protein
HBsAg	Hepatitis B virus surface antigen
HBV	Hepatitis B virus
HCC	Hepatocellular carcinoma
HE stain	Hematoxylin-eosin stain
HRP	Horseradish peroxidase
i.p.	Intraperitoneal
i.v.	Intravenous
ICS	Intracellular cytokine staining
IRES	Internal ribosomal entry site
LAL	Liver associated lymphocytes
Mean (SD)	Mean with standard deviation
MeOH	Methanol
MHC	Major histocompatibility complex
MOI	Multiplicity of infection (infectious particles per target cell)

MVA, rMVA	Modified vaccinia Ankara, recombinant modified vaccinia Ankara
MVA <sub>B8R</sub> , B8R	MVA-derived protein B8R (dominant CD8 T-cell epitope in C57BL/6 mice)
NA	Nucleoside/nucleotide-analogue reverse-transcriptase inhibitor
NIR	LIVE/DEAD Fixable Near-IR Dead Cell Stain Kit
ORF	Open reading frame
OVA	Ovalbumin Antigen
OVN	Over night
P/S	Penicillin/Streptomycin
PBMC	Peripheral blood mononuclear cells
PCEP	poly[di(sodiumcarboxylatoethylphenoxy)phosphazene]
PCR	Polymerase chain reaction
PD-1	Programmed cell death protein 1
pgRNA	Pre-genomic RNA
rcDNA	Relaxed circular DNA
RNA	Ribonucleic acid
RT	Room temperature
s.c.	Subcutaneous
SDS-PAGE	Sodium dodecyl sulfate polyacrylamide gel electrophoresis
SN	Supernatant
TCR	T-cell receptor
TNF / TNFR	Tumor necrosis factor / tumor necrosis factor receptor
ULN	Upper limit of normal
wt	Wildtype

## Units

°C	Degree celsius
µg	Microgram
µl	Microliter
d	Days
g	Gram
h	Hour
IU	Infectious units
kDa	Kilodalton
l	Liter
mg	Milligram
min	Minute
ml	Milliliter
mM	Millimolar
s	Second

# 1. Introduction and background

## 1.1. Hepatitis B

Hepatitis B is an inflammation of the liver caused by the hepatitis B virus (HBV) after transmission through infected body fluids, leading to acute and chronic disease. Chronic HBV infection (CHB) affects around 298 million people worldwide and can cause threatening complications as liver cirrhosis and liver cancer and thus is accountable for an estimated 820 000 deaths per year (data from 2019 (WHO 2022)).

### 1.1.1. The Hepatitis B virus

The hepatitis B virus is a small, DNA-containing, enveloped virus, that belongs to the Hepadnaviridae family (genus: Orthohepadnaviridae; species: HBV). It has a strong tissue and species tropism and infects hepatocytes of humans and some primates. Other family- and genus-members infect woodchucks, ground-squirrels, ducks, herons and storks. Though HBV is a DNA virus, the life cycle is dependent upon reverse transcription of a longer than full length RNA copy of its genome (the pgRNA). Therefore, HBV is a retrovirus with a DNA genome (Block et al. 2007).

### Composition of the viral DNA and proteins

One HBV virion holds a single copy of relaxed circular, partially double-stranded DNA (rcDNA) (Dandri und Locarnini 2012). On 3200 bp, the DNA offers four overlapping open reading frames (ORFs) that use one common polyadenylation signal motif (Block et al. 2007). Figure 1 shows the topological relation of DNA, RNA and the derived proteins.

The **envelope proteins** share the same C-terminal domain with N-terminal extensions, that make up three distinguishable proteins: HBsAg (the smallest envelope protein) and the M- and L-protein (Dandri und Locarnini 2012).

The structural protein **HBcAg** is translated from the same ORF as the precore protein and is the key component of the nucleocapsid.

**HBeAg**, that derives from pgRNA is a non-structural form of the nucleoprotein HBcAg. Since the start codon is upstream of the one for HBcAg, a sequence is translated, that directs the protein to the secretory pathway (Ganem und Prince 2004). HBeAg is not

required for viral replication but contributes to viral persistence by immune-modulating function (Dandri und Locarnini 2012).

The **X protein** is essential for viral replication and spread of the virus. It is involved in host and viral gene expression regulation (Dandri und Locarnini 2012; Ganem und Prince 2004).

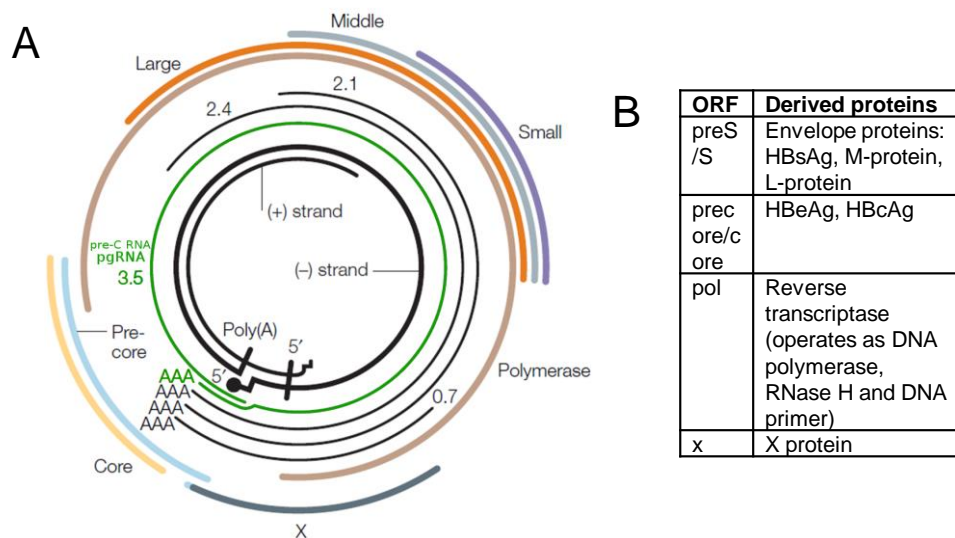


Figure 1 - **DNA, RNA and ORFs of the hepatitis B virus.** **(A)** The HBV-DNA (inner thicker lines) comprises of a full-length (-) strand and the (+) strand, which has a variable length of about 50% of the (-) strand (Block et al. 2007). Subgenomic (thin, black lines) and pre-genomic RNA (pgRNA, green line) have variable lengths and are templates for the viral proteins (colored, thick lines). Precore, core and polymerase derive from 3.5 kb long pre-C RNA. Envelope proteins (Large, Middle, Small=HBsAg) derive from 3.5, 2.4 and 2.1 kb RNA while 0.7 kb RNA is translated to X protein. *Poly(A)*: polyadenylation site. Figure taken and modified from (Rehermann und Nascimbeni 2005). **(B)** ORFs and respective proteins of the hepatitis B virus.

### Structure of HBV particles

Infectious HBV particles (Dane particles after discoverer David Dane, 1970) are built up from an envelope and a viral nucleocapsid, which encase a single copy of viral DNA covalently linked to the viral polymerase (Dandri und Locarnini 2012; Block et al. 2007). The nucleocapsid is usually an icosahedron assemble from 240 single HBcAg, that dimerize (Block et al. 2007). Apart from the Dane particles, infected hepatocytes secrete subviral particles in an  $10^3$ - $10^6$ -fold excess to Dane particles. They are built of envelope proteins (especially HBsAg and M-protein) and host-derived lipids in spherical and filamentous forms and contribute to immune-evasion in HBV infection (Block et al. 2007). The structure of HBV particles can be found in Figure 2.

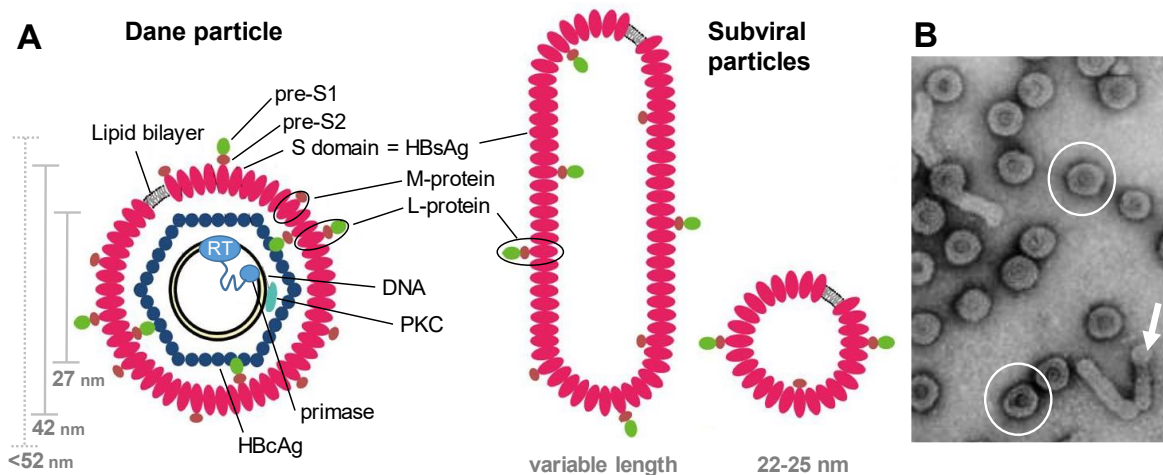


Figure 2 - **Structure of HBV particles.** (A) Schematic overview of infectious and non-infectious HBV particles (modified after (Tan 2014)). Infectious Dane particles (left) comprise of all structural proteins (*HBsAgs* and *HBcAg*) and contain the viral DNA, which is associated with the reverse transcriptase (*RT*) including the primer domain (*primase*) and the protein kinase C (*PKC*), that phosphorylates the *HBcAg* of the nucleocapsid. The full size of Dane particles ranges between 42 nm and 52 nm (Gerlich 2013). Subviral particles (middle: filament, right: sphere) are built up of envelope proteins (predominantly *HBsAg*) and host-derived lipids. (B) Electron microscopy of HBV particles (Gerlich 2013). Arrow: filamentous subviral particle. Circles: Dane particles.

## Organ tropism and replication of HBV

The organ tropism of HBV is determined by entry receptors that are expressed on hepatocytes. The envelope proteins attach to host cell surface proteoglycans and to NTCP receptors before they are internalized (Watashi et al. 2014; Yan et al. 2012). Species specificity is only partly caused by receptor-specificity but also by factors inside the cells that inhibit viral replication in others than the susceptible species (Meier et al. 2013). The amplification of genetic material and HBV particles is illustrated in Figure 3.

In viral replication and virus persistence, the covalently closed circular (cccDNA) plays a key role. In infected cells, there are many (~50) copies of cccDNA (Tuttleman et al. 1986) that derive from initial infection, genome amplification and nucleocapsid recycling (dotted arrow in Figure 3). They remain for months or even years even if virus replication is suppressed by antiviral treatment and can cause viral rebound, when therapy is stopped or under immunosuppression (Block et al. 2007). Usually, the cccDNA exists as an episomal minichromosome, but does also integrate into cellular chromosomes (Block et al. 2007). While those integrated forms of HBV DNA are not

responsible for generation of infectious virus (Barnes 2015), they are passed on by clonal expansion of hepatocytes and, as a source of HBsAg are considered to contribute to the development and maintenance of immune tolerance in chronic HBV infection (Wooddell et al. 2017; Mason et al. 2016).

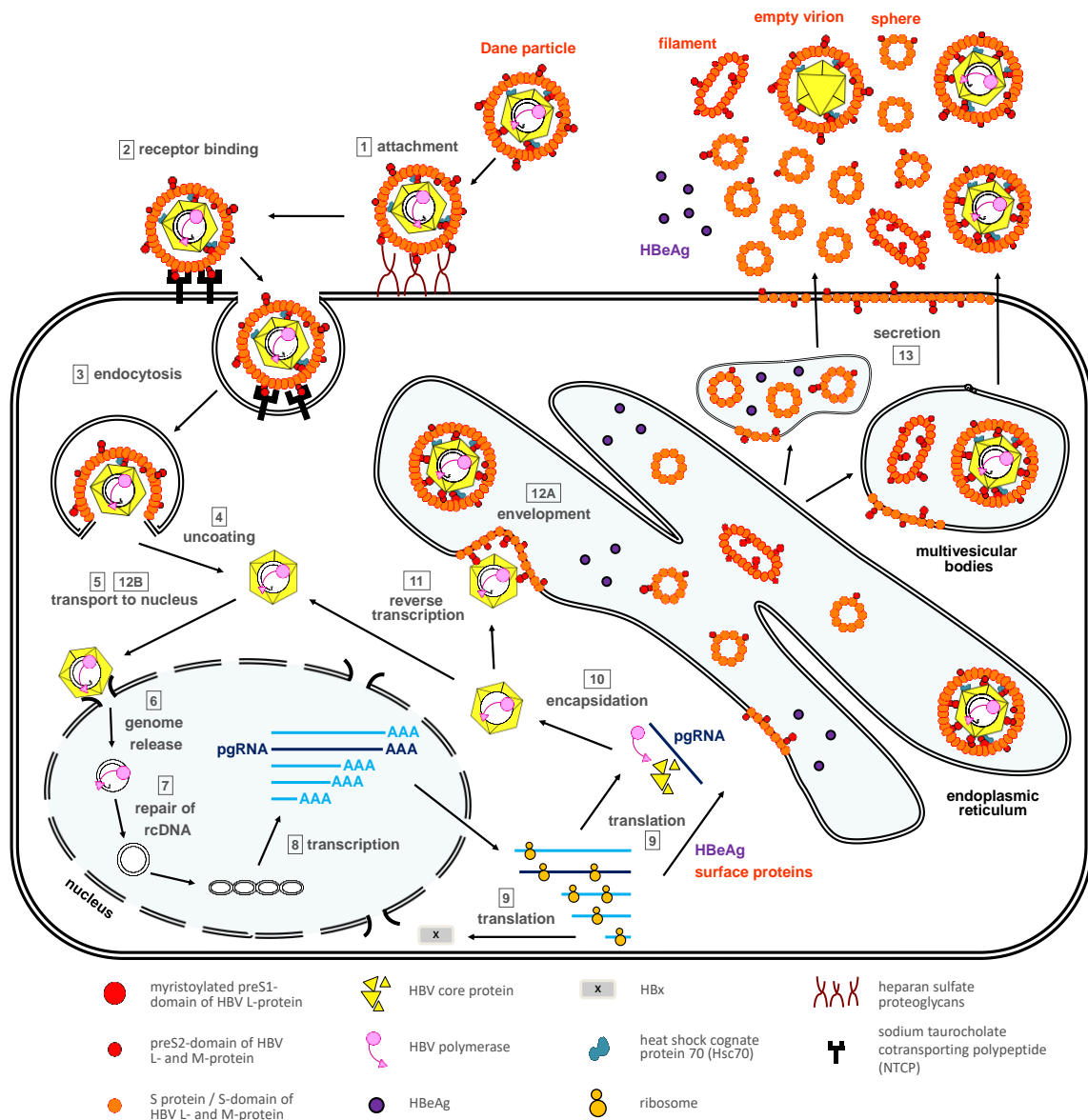


Figure 3 - **Replication of HBV inside a hepatocyte.** After attachment [1] and receptor-mediated internalization of the virus [2, 3], the viral DNA is transported into the nucleus where the relaxed circular DNA (*rcDNA*) is completed to double-stranded and covalently closed circular DNA (*cccDNA*) [4-7]. The host RNA polymerase II transcribes the *cccDNA* to subgenomic RNA sections and longer than full length pre-genomic RNA (*pgRNA*) [8], which are exported to the cytoplasm (Will et al. 1987). Viral proteins are synthesized in the cytosol and endoplasmic reticulum (*ER*) [9]. HBc proteins assemble to the nucleocapsids and each capsid loads one *pgRNA* with the attached reverse transcriptase (*HBV polymerase*). Then, the (-) DNA strand is synthesized along the *pgRNA* template [11] before it is

degraded to make room for the (+) strand with the (-) strand as template (Ganem und Prince 2004). Finally, the nucleocapsids are covered by envelope proteins [12] and released from the cell [13]. Surface proteins (envelope proteins, orange and reddish structures) and HBeAg are synthesized and also secreted from the cell [9,13]. Figure adapted from (Ko et al. 2017).

### 1.1.2. Epidemiology of HBV infection

Although there is a safe and effective vaccine, around 3.8% of the world population (296 million people) is chronically infected with HBV (estimated numbers in 2019 (WHO 2022)). Highest prevalence of any HBV infection (HBsAg positivity) is in sub-Saharan Africa and East Asia, while fewest people are infected in Western Europe, Central Latin America and North America (Razavi-Shearer et al. 2018). Figure 4 shows prevalence (acute or chronic HBV infection) in all age groups.

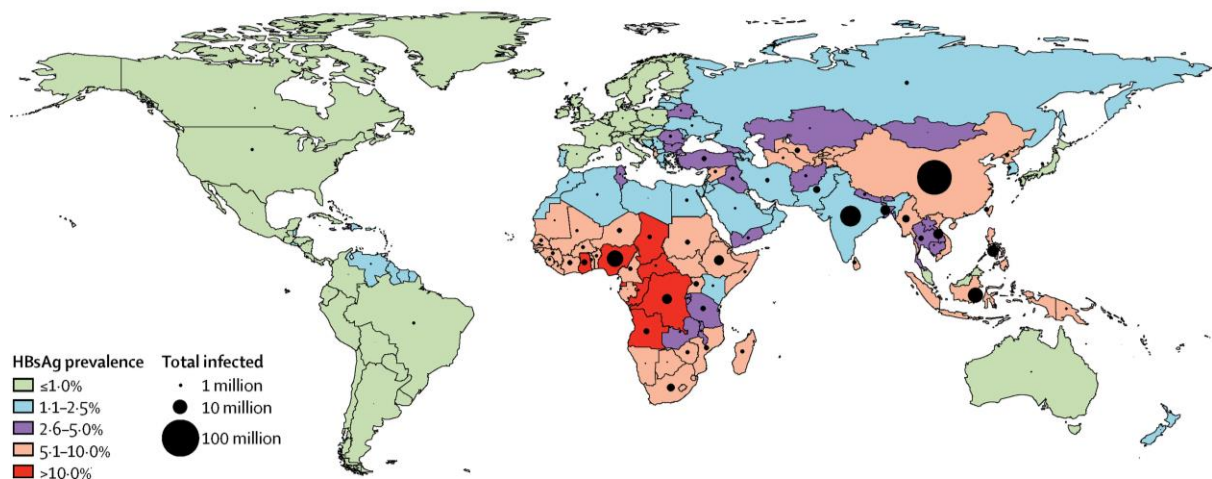


Figure 4 - HBs-Ag prevalence estimates for 2016 (all ages). Figure from (Razavi-Shearer et al. 2018).

In the last three decades, preventive hepatitis B vaccination has efficiently decreased the incidence of new hepatitis B virus (HBV) infections (especially in South East Asian children). But HBV prevalence is still high (>2%) in children in many countries for example in West Africa and still, about 1.5 million people get infected with HBV per year. (Razavi-Shearer et al. 2018; Flores et al. 2022; WHO 2022; Fofana et al. 2023)

The hepatitis B virus can be classified in various genotypes that are predominant in distinct regions of the world and in different population groups. Until now, 10 different genotypes A-J (>8% differences in genome) und several subgenotypes (4-8% difference) were identified (Sunbul 2014). The genotype is relevant for disease progression and treatment as the response to antiviral treatment and the tendency to mutation, chronification and progression towards liver cirrhosis and hepatocellular

carcinoma differ among the (sub-)genotypes (Sunbul 2014; Pol und Lampertico 2012; Song und Kim 2016).

### 1.1.3. Characteristics of HBV infection

#### Transmission

After percutaneous or mucosal exposure to infected body fluids, incubation period of HBV infection is 30-180 days. Virus can be detected in patients 30-60 days after infection. (WHO 2022) Most common transmission routes vary depending on age and local endemicity (Figure 5).

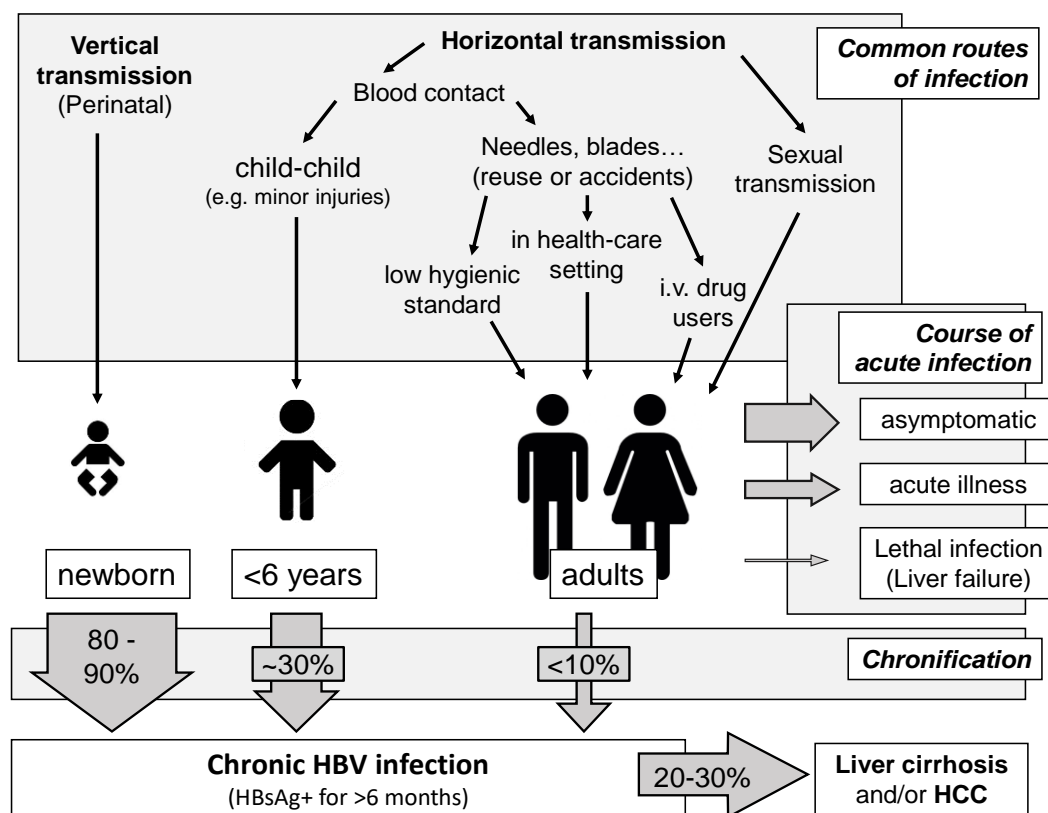


Figure 5 – **Transmission of HBV and natural course of HBV infection.** Percent values indicate the probability of transition into chronic disease or risk of complications (WHO 2022; Hyams 1995). *HCC*: hepatocellular carcinoma.

In high endemic regions, vertical transmission is predominant with highest rates of vertical transmission from HBsAg- and HBeAg-positive mothers to their newborns (without preventive treatment: up to 90%) (Gentile und Borgia 2014). Transmission rates can be lowered by active and passive immunization of the newborn and case-dependently by antiviral treatment of the mother before delivery (Bzowej 2010).

## **Diagnosis of HBV infection**

As acute HBV infection is often asymptomatic, diagnosis of HBV infection (chronic or acute) is often made after routine testing or when complications of chronic infection (liver cirrhosis, liver carcinoma) occur.

Confirmation of HBV infection and monitoring of disease activity is performed on blood tests using HBV-specific serum markers that distinguish the different phases of HBV infection (Figure 6) (Song und Kim 2016; EASL 2017; WHO 2022; Cornberg et al. 2021): Key antigen, which displays disease activity is the surface antigen (HBsAg). The replication activity and disease progression should be evaluated by determination of HBV-DNA titers. For further classification, HBeAg and anti-HBeAb are determined. The assessment of patients with chronic HBV infection further includes the evaluation of liver disease. By evaluation of ALT (alanin aminotransferase) in the serum, the extent of inflammation and liver damage are determined. Liver fibrosis is detected with non-invasive methods or liver biopsy.

## **Acute HBV infection**

Acute HBV infection is characterized by the presence of HBsAg and anti-HBcAg-IgM (IgM antibody against the core antigen) in the blood. Another marker that also might be detectable in the initial phase of infection and reflects high virus replication and high contagiousity, is hepatitis B e antigen (HBeAg). Some patients - in particular adults - develop symptoms of hepatitis (icterus, extreme fatigue, nausea and vomiting and abdominal pain), that last for several weeks (McMahon et al. 1985; WHO 2022).

## **Chronic HBV infection (CHB)**

If HBsAg is detectable for >6 months, HBV infection is defined as chronic hepatitis B (CHB) (WHO 2022). The disease progression can be classified into 5 phases (see Figure 6), depending on the presence of HBeAg and liver inflammation and the levels of HBV DNA levels and ALT (EASL 2017). The phases are not necessarily sequential and intermediate areas between phases obviously exist.

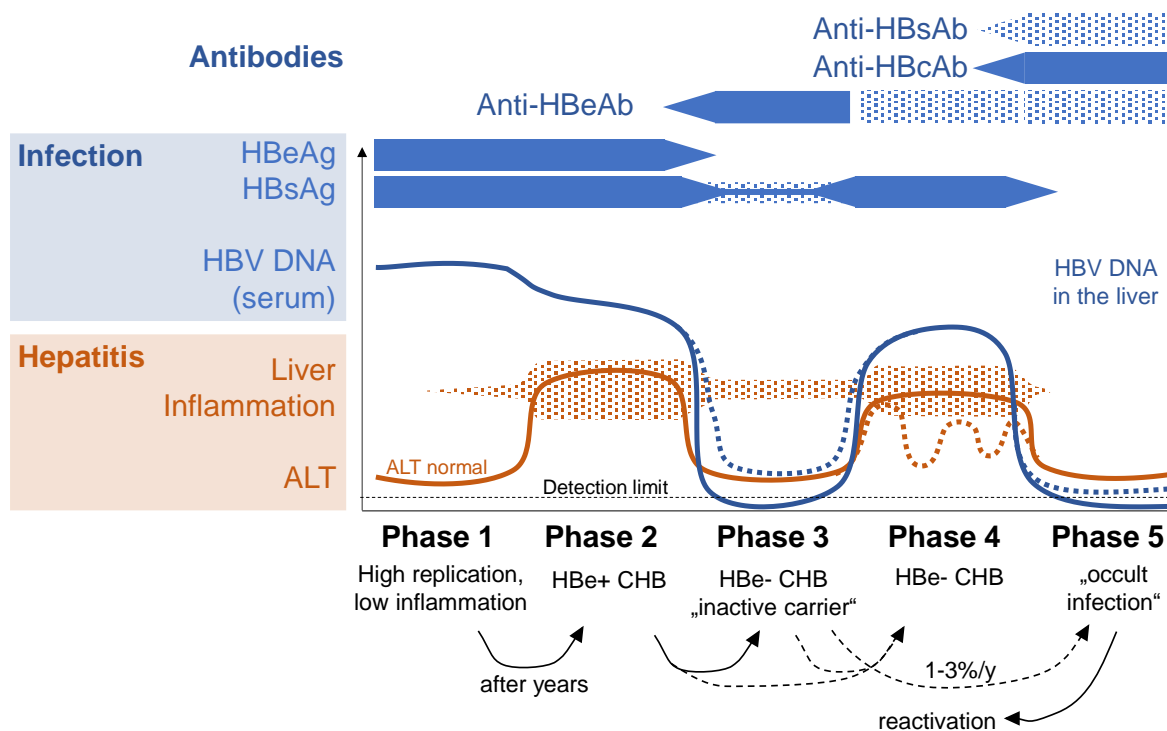


Figure 6 - **Phases of chronic HBV infection.** Most frequent transitions from one phase into another are indicated with arrows. *HBeAg*, *HBsAg*: HBeAg (precore antigen) or HBsAg in the serum; *Anti-HBcAb*, *Anti-HBsAb*, *Anti-HBeAb*: blue bars indicate presence of antibodies against HBc (HBV core antigen), HBs (HBV surface antigen) or HBe-Ag (HBV precore antigen), light blue: presence of antibodies not mandatory; *ALT*: alanin aminotransferase. Description of phases from (EASL 2017).

CHB most frequently occurs, when neonates get infected by an HBsAg-positive mother. In newborns with acute HBV infection, about 90% develop a chronic infection (Figure 5). When children older than 6 years or adults get infected with HBV, chronification occurs in 5-10% of patients and is overall more frequent in males and immunosuppressed individuals (Hyams 1995).

The following phase (**phase 1**), that mostly lasts for several years is characterized by high replication (high HBV DNA levels) and low inflammation (low ALT, minimal or low necroinflammation or fibrosis) (EASL 2017). It was formerly termed “immune-tolerant”, which was discussed as a misleading term as immune tolerance is a characteristic of all phases of CHB. Furthermore, Mason et al. showed that also in this early phase of infection, an HBV-specific T-cell response can be detected, and infection related histological changes (e.g. clonal expansion) are found in the liver and display disease progression (Mason et al. 2016; Protzer und Knolle 2016). **Phase 2** (HBeAg-positive CHB) is characterized by high HBV-DNA levels, the presence of serum HBeAg and

inflammation which leads to elevated ALT levels. In vertically infected patients, this phase is often entered after many years, in adults it is mostly reached earlier. Phase 2 normally lasts for weeks or even years. (EASL 2017)

During immune-activity, the selection of HBeAg-negative mutants can occur, which leads to an HBeAg-negative CHB (**phase 4**). This phase is characterized by high infection markers, no HBeAg and variable signs of hepatitis. The rate of spontaneous clearance and sustained remission under drug treatment are way lower and less frequent than in phase 2 while the rate of cirrhosis is 2-4 times higher. (Saikia et al. 2007; EASL 2017, 2017)

In **phase 3**, HBV-DNA levels as a marker for replication is low, hepatitis is minimal and seroconversion (loss of HBeAg and development of anti-HBeAb) takes place. Around 1-3% of phase 3 patients per year show a loss of HBsAg in the serum and enter **phase 5** (occult HBV infection). Characteristics of this phase are the presence of anti-HBcAb and absence of HBsAg, accompanied by normal ALT levels and (mostly) undetectable HBV-DNA in the serum. But trace amounts of HBV-DNA persist in the blood serum, in peripheral blood mononuclear cells and hepatocytes and maintain HBV-specific CTL responses for decades (Rehermann et al. 1996). Under immunosuppression or after transplantations and blood (product) donations, this may lead to reactivation of HBV infection / HBV infection.

### Complications of CHB

Most people dying from HBV infection, die from decompensated liver cirrhosis (200 000/year) or hepatocellular carcinoma (300 000/year worldwide) at an early age (43 median, (Peng et al. 2012)). HCC is the 3<sup>rd</sup> leading cause of cancer death worldwide and HBV infection is its etiology in 2/3 of all cases (Block et al. 2007; Chan und Sung 2006). Without treatment, prognosis of CHB is poor with a high risk of death by complications associated with liver failure and cancer (Figure 7).

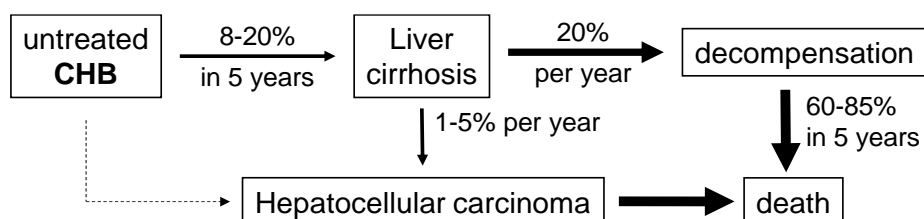


Figure 7 - **Natural course of complications in CHB.** Data from (WHO 2015).

## Prevention of HBV infection

An active, safe and effective vaccination with HBsAg is available since 1982. After vaccination, 95% of patients are protected against HBV infection. Immune evasion by mutation of the virus seems to be a rare event (Aghasadeghi et al. 2016). The WHO recommends vaccination of all infants within the first day after birth followed by 2-3 doses in first year of life. Especially in children, hepatitis B vaccination has already lowered the infection rates in many countries. (WHO 2022) To avoid perinatal transmission it is most important to identify HBsAg-positive pregnant women and to immunize the newborn infants actively and passively (Centers for Disease Control and Prevention 2016). Further effective prevention is done with safety strategies for blood (product) donations, safe injection practices and safer sex practices.

## Treatment of CHB

Due to integration of HBV DNA in the genome of hepatocytes and persistence of cccDNA, elimination of HBV infection (*complete cure*) is no feasible goal of CHB therapy (Lok et al. 2017). Though, an adequate immune response – or in some cases an effective treatment – can suppress infection markers to almost undetectable levels and can lead to complete healing of hepatitis. This status (phase 5, Figure 6) complies with a *functional cure*. A *partial cure* means that HBV DNA in the serum is undetectable after treatment but HBsAg is still present.

The goals of antiviral treatment aim at an improved survival and quality of life by prevention of complications as well as the prevention of reactivation and transmission (e.g. mother to child) (EASL 2017; Cornberg et al. 2021). In acute hepatitis, acute and subacute liver failure should be prevented and treated. Both the EASL and the S3 Guideline formulate four possible endpoints of treatment:

- HBsAg loss as the ideal endpoint of treatment (functional cure)
- Suppression of HBV DNA (partial/functional cure)
- Induction of HBeAg loss with a partial immune control
- Biochemical response (ALT normalization)

The indication for treatment and monitoring depends on the phase of infection, the age and health status of the patient, serum markers, family history of liver cirrhosis or HCC and the extent of liver disease: During all phases of CHB, monitoring of liver damage and virus replication (and if given adverse side effects of drug treatment) is indicated.

Shortly summarized, indication of treatment with antiviral drugs is given if there is a chronic hepatitis due to HBV infection (ALT elevation  $>2 \times \text{ULN}$ , presence of liver cirrhosis, moderate liver inflammation or fibrosis) (EASL 2017). In chronic HBV infection without hepatitis, treatment indication is given if there is a high virus replication (HBV DNA  $>20\,000$ ) in conjunction with risk factors (risk of HCC (e.g. positive family history), HBV reactivation, extrahepatic manifestations, risk of HBV transmission).

Current treatment options are directly acting antiviral drugs (nucleoside/nucleotide-analogue reverse-transcriptase inhibitor = NA) and pegylated IFN $\alpha$ : The initial treatment of choice is the long-term monotherapy with one potent NA. They can be administered orally, show few side-effects (compared to a therapy with IFN $\alpha$ ) and the preferred drugs entecavir and tenofovir have a low rate of selection of resistant mutants during treatment. The drawback of NA is their extensive incapacity of HBsAg clearance and thus requirement of long-term (often lifelong) treatment. In case of incomplete suppression of HBV replication, a switch to another NA or combination may be considered. A combination of NA and pegylated IFN $\alpha$  is not recommended (EASL 2017).

Pegylated IFN $\alpha$  is a second treatment option in mild and moderate CHB infection and shows a higher rate of HBsAg-loss than with oral antiviral treatment with NA. The treatment is limited in time with a standard treatment duration of 48 weeks, administration (injection) is more difficult and more expensive and indications are much more limited than those for NA. Adverse side effects are stronger and more frequent and require constant and careful monitoring. (WHO 2015; EASL 2017)

#### **1.1.4. The pathogenesis of chronic hepatitis B virus infection**

##### **Immune tolerance in chronic hepatitis B virus infection**

Immune tolerance is a physiological function of the immune system, which protects the organism from auto-immunity and can prevent organ failure by limiting an immune reaction during an acute infection. In the case of HBV infection, immune tolerance can lead to the development of a chronic infection.

Immune tolerance arises, when immune cells are impaired in quality and quantity. The function, amount or development of antigen-specific immune cells is altered when they

are deleted, their expansion is reduced, their maturation is impeded, or the cell function is altered in form of an “exhaustion” (Dembek et al. 2018). Exhausted T cells are characterized by a lowered proliferative potential, weaker effector function, expression of inhibitory receptors and an altered transcriptional profile in comparison to that of functional effector or memory T cells (Wherry und Kurachi 2015). It was shown, that the differentiation of T cells depends critically on the frequency of T-cell receptor engagement with a high frequency being accountable for the acquisition of an exhausted phenotype (Utzschneider et al. 2016).

One factor, which is presumed to cause immune tolerance in chronic hepatitis B infection is the presence of a high antigenic load. In HBV infection, HBsAg and HBeAg are secreted into the blood at high scales, where they circulate in form of subviral particles. Those particles have no apparent role in viral replication and are believed to be an immune evasive strategy to enable the establishment and maintenance of a chronic infection. This property is not singular for HBV infection as it has been shown for several noncytopathic viruses that cause persistent infections due to an overwhelming antigenic viral load. (Dembek et al. 2018) It explains, why antiviral suppression, which lowers the level of immune-modulating antigens, sometimes induces HBeAg seroconversion (Block et al. 2007).

A second circumstance, which supports the development of immune tolerance in HBV infection is the tolerogenic potential of the liver. It encourages development of immune tolerance by unique immune modulatory functions and a particular environment that limits inflammation and adaptive immune response. While these mechanisms prevent overwhelming tissue damage, they also facilitate the development of chronic infections of the liver like HBV and HCV. (Knolle und Thimme 2014) This might be particularly relevant in infants, where the probability of development of a CHB infection is much higher than in adults. This age-dependent rate of chronification may be caused by modified lymphoid organization in the liver and is particularly affected by the function of hepatic macrophages and their interaction with B lymphocytes. (Publicover et al. 2013) Also, the level of antigen expression in infected hepatocytes influences the outcome of antiviral immunity and persistence or clearance of an infection with weaker immune responses to slighter antigen expression on hepatocytes (Manske et al. 2018).

Immune tolerance in form of T-cell exhaustion prevents optimal control of infection, but the inhibitory pathways that are overexpressed in exhaustion offer opportunities for treatments (Wherry und Kurachi 2015): they can be modulated to reverse the dysfunctional state to elicit immune responses that suffice to control the infection and lead to viral clearance.

### **Viral clearance**

Nevertheless, spontaneous viral clearance also occurs in HBV infection – above all in acute resolved infection. To develop new approaches for treatment, it is important to examine the factors which lead to viral clearance in acute or chronic infection.

It was observed, that clearance of HBV in the acute phase is associated with a vigorous and polyclonal response of T helper and CTLs directed against multiple HBV antigens (Block et al. 2007). How this immune response is mediated is illustrated in Figure 8. In chronic HBV infection, spontaneous clearance also occurs, although it is very uncommon. When a potent T-cell response arises, elimination of the virus is achieved by direct killing of hepatocytes by CTLs (causing liver damage) and by noncytolytic reduction of viral gene products by cytokines as IFN $\gamma$  and TNF through elimination of HBV nucleocapsids and destabilization of viral RNA (Block et al. 2007; Guidotti et al. 1996; Ganem und Prince 2004). Those cytokines derive from HBV-specific CTLs, but also from antigen-nonspecific macrophages and T cells. Noncytolytic effects also occurred in mouse models for HBV and in human patients, chronically infected with HBV, when cytokines were present in the liver due to other viral infections (Cavanaugh et al. 1998; Ganem und Prince 2004).

When the balance of the HBV-specific immune response shifts from tolerance towards virus suppression during seroconversion, both minimal virus persistence and virus-specific CTL response can go on in the patient for decades (Rehermann et al. 1996). After recovery from acute HBV infection, HBV-DNA is detectable in the serum and PBMCs (peripheral blood mononuclear cells) of patients even after years with HBV-specific T cells showing markers of recent antigen contact (Rehermann et al. 1996; Michalak et al. 1994). Those findings suggest, that the treatment strategies in HBV infection rather aim at an effective immune control and thus functional cure than at a complete elimination of the virus, which is unlikely to be feasible (Lok et al. 2017). As antiviral therapies with NAs by now are very safe and well tolerated but mostly have

to be given life-long, new and safe treatments like immune modulatory therapies (e.g. therapeutic vaccination) are needed for treatment of CHB.

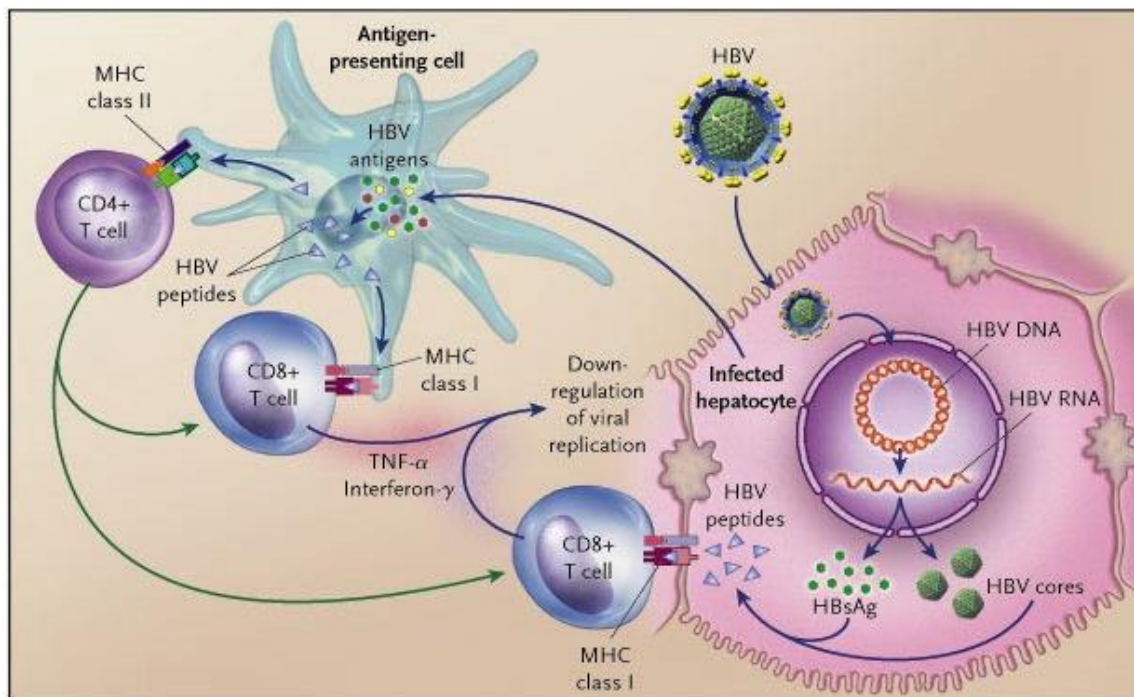


Figure 8 – **Cellular immune response to infection with HBV.** Antigen-presenting cells collect HBV antigens from infected hepatocytes and prime and activate CD4 and CD8 T cells, that are specific for HBV antigens. Activated CD8 T cells recognize HBV infected hepatocytes and control the infection by cytolytic effects or by non-cytolytic downregulation of viral replication. *HBsAg*, *HBV core*: viral antigens. (Ganem und Prince 2004).

### 1.1.5. Strategies to overcome immune tolerance in CHB by therapeutic vaccination

Considering the natural course of infection and clearance of HBV suggest, that a sustained and strong T-cell response might be a way to reach permanent suppression of viral replication and associated liver disease (Chisari und Ferrari 1995).

Many pre-clinical and clinical trials were conducted with the aim of evoking sustained T-cell responses against the target antigens, seroconversion and/or a decline of viral replication markers (Barnes 2015; Liu et al. 2014a; Backes et al. 2016; Pol et al. 2001; Yang et al. 2012). The first approaches in therapeutic vaccination against CHB were pre-clinical and clinical trials with HBs protein (the preventive HBV vaccine), which had no great effect in patients (Yalcin et al. 2003b; Yalcin et al. 2003a; Pol et al. 2001) Then, the vaccine was combined with antiviral treatment and/or different HBV antigens

were administered as a DNA vaccine with immunological effects in patients, which still were rather weak either (Mancini-Bourgine et al. 2006; Yang et al. 2006; Yang et al. 2012; Vandepapeliere et al. 2007). Therapeutic vaccinations in mice with distinct formulations revealed a benefit for heterologous vaccinations and of combinations with immune modulators (Kosinska et al. 2015; Liu et al. 2014a; Barnes 2015; Depla et al. 2008). Vaccines were designed as protein or DNA vaccines using different viral antigens or viral vaccination vectors (e.g. MVA). Partly, they were administered with checkpoint inhibitors, adjuvants or co-stimulators and/or combined with antiviral treatment (Liu et al. 2014b). There is also evidence, that therapeutic vaccination is particularly efficient in low viremic mice (Backes et al. 2016) or after knockdown of antigen production (Michler et al. 2020). Summarizing, therapeutic vaccination against CHB is challenging and needs the combination of vaccination against viral antigens with antiviral treatment, modulation of checkpoint inhibitors (e.g. targeting PD-1 or CTLA-4), combination with co-stimulators and/or the induction of intrahepatic cell clusters (intrahepatic myeloid aggregation for T-cell expansion = iMATEs) that work as local reinforcers of the HBV-specific immune response (Kosinska et al. 2015; Dembek et al. 2018; Bunse et al. 2022; Kosinska et al. 2019; Knolle et al. 2021).

There is evidence, that PD-1 plays a role in T-cell exhaustion in many human chronic infections (Liu et al. 2014a). In an animal model in the woodchuck, Liu et al. (Liu et al. 2014a) combined antiviral treatment, therapeutic vaccination with DNA plasmids (expressing core or surface antigen) and blocking of the PD-1 axis. They found that immunomodulation by blocking the PD-1/PD-L1 pathway has synergistic effects on the induction of virus-specific T cells. The combination therapy potently suppressed woodchuck hepatitis virus replication, resulted in immunological control of viral infection and even led to complete clearance in some woodchucks. Similar results have been seen, when siRNA interfering with PD-L1 was given during the protein prime in a protein-prime/MVA-boost vaccination (*TherVacB*) in a mouse model for chronic HBV (Bunse et al. 2022).

Thus, therapeutic vaccination strategies in general and in particular in combination with immunomodulating strategies are very promising in the difficult treatment of CHB. Backes et al. (Backes et al. 2016) developed a heterologous protein-prime/MVA-boost-vaccination regimen, that was evaluated in HBV1.3tg mice (a mouse model for vertically transmitted HBV) and showed, that vaccination is capable of breaking

tolerance even in high viremic mice. This vaccination (*TherVacB*) is currently evaluated in a phase 1/2 clinical study (TherVacB project 2020).

On this basis, in my study this vaccination regimen was combined with a T-cell co-stimulation by including CD70 in the MVA vector design.

## **1.2. Modified vaccinia Ankara (MVA) as viral vector for therapeutic vaccination**

For this work, a recombinant MVA (rMVA) was created, that encodes the HBV transgene HBV core (HBc) and the co-stimulatory molecule CD70. It was administered as a protein-prime/MVA-boost vaccination, following the vaccination scheme of Backes et al. (Backes et al. 2016). In the following chapters, the background on MVA is elucidated and the most important implications of vector design are discussed.

### **1.2.1. Modified vaccinia Ankara: specifications and origin**

Modified vaccinia Ankara, a replication-deficient virus belonging to the poxviridae family, was generated in the 1970s with the aim of developing a safe vaccine against smallpox. During more than 500 passages in primary chicken embryo cells, the original vaccinia virus lost about 15% of its DNA and the ability to replicate in most cells of mammalian origin (Antoine et al. 1998; Meyer et al. 1991; Drexler et al. 2004). It remained 178 kB of dsDNA that carries 177 genes of which about 25 genes do not encode functioning proteins due to mutations and/or splitting (Antoine et al. 1998).

The Vaccinia Virus is very large and brick-shaped with a size of 350x250 nm. Transcription and replication occur in the host-cell cytoplasm. Vaccinia virus as well as MVA are able to infect almost any cell line in culture and are presumed to have a broad cellular tropism. However, Chahroudi et al. demonstrated, that vaccinia virus exhibits a more restricted tropism for primary hematolymphoid human cells than has been previously recognized and preferentially infects antigen-presenting cells (dendritic cells, monocytes/macrophages, and B cells) and activated T cells. (Chahroudi et al. 2005)

### **1.2.2. MVA as viral vector for transgenes**

The suitability of MVA as a viral vector for transgenes has many aspects: it is safe, has a high package capacity for transgenes and is highly immunogenic.

MVA doesn't integrate into the host cell genome and can't replicate in human and most other mammalian cells (Drexler et al. 2004). Cells, which are infected with MVA undergo apoptosis within two days (Chahroudi et al. 2006). Thus, MVA is a very safe vector for transgenes. Those transgenes are inserted at the sites of naturally occurring deletions within the MVA genome or at the gene loci for certain vaccinia virus proteins (Drexler et al. 2004; Wyatt et al. 2009). MVA has a large packaging capacity for recombinant DNA and the ability to produce similar levels of viral and recombinant antigen in infected host cells (Drexler et al. 2004). Though MVA cannot replicate and drives the infected host cell into apoptosis soon after infection, it proved to be comparatively immunogenic as its replication-competent ancestor vaccinia virus (Chahroudi et al. 2006).

#### **Kinetics and cellular effects of MVA infection**

After infection with rMVA, the expression of a transgene under an early promoter starts within 30 min and has its peak in immature and mature dendritic cells (imDCs and mDCs) after about 10 h (Chahroudi et al. 2006; Baur et al. 2010). Within 4 h after infection, the shutdown of host cell protein synthesis begins (Chahroudi et al. 2006). Apoptosis of infected imDCs starts directly after infection and is in particular high 15-25 h after infection and dependent of the MOI (Chahroudi et al. 2006).

#### **Immunogenicity of recombinant MVA**

MVA as vaccine vector is highly immunogenic and stimulates the host immune system, for example by activation of innate immune mediators (Drexler et al. 2004; Barnes 2015). It was shown in various vaccination studies against cancers and viral infection, that immunization with recombinant MVA has the potential to activate robust cellular major histocompatibility complex (MHC) class I- and II-restricted CD8 and CD4 T-cell responses (Drexler et al. 2004).

One important finding highlights the importance of a suitable promoter in the design of rMVA vector: By choosing an immediate-early promoter, which leads to the expression of the transgene within 30 min, neoantigen-specific acute and memory CD8 T-cell

responses can be evoked more efficiently than under an early-late promoter (Baur et al. 2010).

For therapeutic vaccination against HBV, a viral vector seems to be advantageous for another reason: the stimulation of the immune system by innate immune responses alone may be associated with viral control (Barnes 2015). Also see chapter 1.1.4, “viral clearance” for this aspect of beneficial effects of immune stimulation by antigens that do not derive from HBV infection.

### **Dendritic cells and their role in immunization with vaccinia virus and MVA**

Vaccinia virus preferentially infects antigen-presenting cells and the main target after i.v. administration of MVA are antigen-presenting cells, mainly conventional dendritic cells (Bathke et al. 2018; Chahroudi et al. 2005). After therapeutic vaccination with a recombinant vaccinia virus in a tumor model, the antigen expression by dendritic cells correlates with the therapeutic effectiveness of the vaccination (Bronte et al. 1997). Thus, dendritic cells are presumed to be important mediators in therapeutic vaccination.

How dendritic cells react upon infection with MVA and other poxviruses is controversial: Some studies suggest, that infection leads to inhibition of maturation of immature dendritic cells (Kastenmuller et al. 2006; Engelmayer et al. 1999), while others state that the capacity of maturation is not impaired (Trevor et al. 2001). The inhibition of DC maturation possibly is an immune evasion mechanism of poxviruses as maturation of DCs with up-regulation of co-stimulatory and HLA molecules allows for efficient T-cell activation (Engelmayer et al. 1999). A transgenic co-stimulatory molecule as CD70 could counterbalance this detrimental effect. One study of a tumor model in the mouse provided evidence, that co-stimulation with CD70 on immature dendritic cells enabled activation of cytotoxic lymphocytes. While immature dendritic cells promote immune tolerance, CD70 expression by transgenesis converted them to an immunogenic state, that even uncoupled CD8 T-cell activation from CD4 T-cell help. (Keller et al. 2008)

#### **1.2.3. Strategies of therapeutic vaccination by MVA immunization**

Vaccinia-specific immune response during vaccination is assumed to affect immunogenicity of the transgene: specific T cells compete for viral or transgenic

epitopes on infected host cells (Kastenmuller et al. 2007). Those influencing effects can be avoided by prime-boost regimens. Thus, MVA vaccines are often combined with other forms of antigen application (as protein, in a DNA vaccine or via other viral vectors) in therapeutic approaches. (Drexler et al. 2004)

Dependent on vaccination regimen, rMVA is capable of eliciting humoral and cellular immunity and the potency of doing so can be influenced by formulation and composition of the vaccination components. For example, in a therapeutic vaccination against malaria in the mouse (Anderson et al. 2004), combination of a protein prime with the rMVA boost was more potent in activating IFN $\gamma$  secreting CD8 T cells than the combination with a DNA prime. Interestingly, those cells are important in malaria as they recognize and eliminate parasite infected hepatocytes, which is an analogy to the desired immune activation in CHB.

Apart from heterologous vaccination strategies, further possible elements of therapeutic vaccinations are components, that enhance the adaptive immunity. Those are for example cytokines as IL-2, co-stimulatory molecules as B7-1, blockade of immune inhibitory signals as CTLA-4 and cellular adjuvants as dendritic cells (Drexler et al. 2004). When they shall be delivered by the rMVA itself as a transgene, the details of MVA infection and associated immune activation are important – these components only can work as ligands/receptors if they are not degraded in the infected cells in the pathway of cross-presentation. This is discussed in the following paragraph.

### **Receptors as transgenes in MVA – the implication of cross-presentation and the role of promoters and administration routes**

Immune responses after MVA infection are mediated by direct presentation and cross-presentation (Gasteiger et al. 2007). In this work, a recombinant MVA was generated, that encodes HBc and the immune stimulatory molecule CD70. CD70 only can stimulate its receptor CD27 if it is transported to the host cell surface and presented to T cells intactly (see Figure 9), which is the case, if the transgenes are presented to T cells via direct presentation. If the MVA infected host cells undergo apoptosis and the antigens are taken up by antigen presenting cells and are cross-presented to specific immune cells, the stimulatory effect of transgenic CD70 would be wasted: it would be degraded in the process of uptake and cross-presentation (B in Figure 9).

The extent of how direct or cross-presentation contribute to specific immune responses in MVA immunization depends on multiple factors. Several studies have found different contribution of both ways (Gasteiger et al. 2007; Shen et al. 2002). An important element in vector design that would favor direct presentation seems to be the choice of the transgene promoter: immune responses to early MVA proteins as B8R rather derived from direct presentation (Iborra et al. 2012). Furthermore, several studies found, that early promoters for the transgenes work best for stimulation of a strong CD8 T-cell response against rMVA-delivered transgenes (Baur et al. 2010; Gasteiger et al. 2007; Bronte et al. 1997). Thus, the early promoter mH5 is an appropriate promoter for rMVA vector design.

Also, using i.p. application as vaccination route contributes to the preference of direct priming (Shen et al. 2002). They found, that in recombinant vaccinia virus vaccination in mice, i.v. and i.p. vaccinations were strongly dependent on direct presentation whereas this effect was much lower in i.m. administration and minimal after s.c. or intra dermal administration.

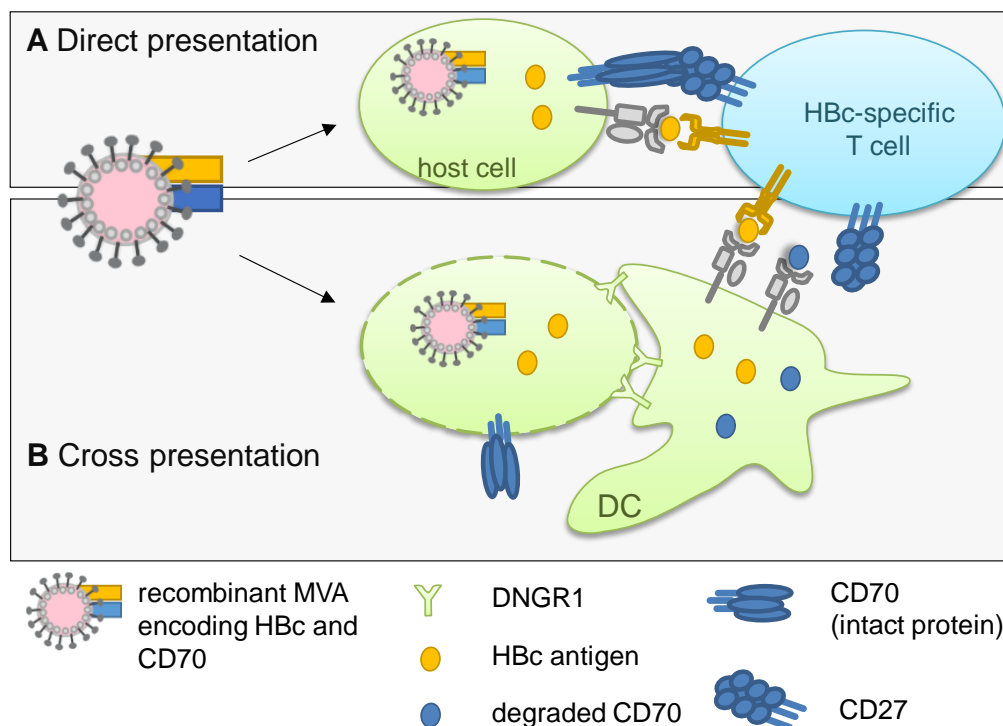


Figure 9 – **Direct presentation and cross presentation of transgenes to specific T cells.** The illustration shows a therapeutic vaccination with recombinant MVA (rMVA) containing 2 transgenes: the HBV antigen HBV core (*HBc*) and the co-stimulator CD70. **(A)** When the rMVA infects a host cell, the antigen HBc can be directly presented to a HBV core-specific T cell. Under these circumstances, the

co-stimulatory CD70 binds to its receptor on the T cell (CD27) and promotes the T-cell response. **(B)** When the infected host cell is lysed before it comes to T-cell activation, it can be taken up by an antigen presenting cell (e.g. dendritic cell = *DC*). This uptake is mediated by the receptor DNGR1. Then, the APC can cross-present the antigen to the specific T cell. Due to apoptosis and uptake in the antigen presenting cell, CD70 is degraded and can't bind to CD27.

Because of the central role of CD70 co-stimulation in this study, the role of cross-presentation was determined in a vaccination experiment with DNGR1 deficient mice, in which cross-presentation is impaired.

#### **1.2.4. Choice of the target antigen for vaccination: HBcAg**

Barnes et al. summarized in a review, that most therapeutic vaccination studies in the preclinical and clinical setting target HBs or HBc protein (Barnes 2015). For further investigation, they proposed a test and see approach which antigen works best in therapeutic vaccination. Still, there are indications that HBc – presumably in combination with other antigens – is a reasonable choice as antigen in therapeutic vaccination against CHB: Webster et al. proposed HBc as a promising antigen as HBV core-specific CTL-responses in patients correlated with viral control. But they consider that it is unclear if HBV core-specific responses are a cause or a consequence of viral control (Webster et al. 2004). Though, another study in patients with CHB suggests, that HBV core-specific cellular immune responses are a cause for control of CHB: they characterized specific T-cell responses of patients with CHB, who underwent seroconversion after bone marrow transplantation from donors with resolved HBV infection and found that CD4 and CD8 T cells against HBc were several-fold higher than those against surface proteins (HBs) (Lau et al. 2002).

HBc is a highly immunogenic protein both for humoral and cellular responses. This property is also exploited in its application as a carrier for foreign epitopes in vaccination against other diseases e.g. as fusion proteins (Francis et al. 1990; Liang et al. 2018; Pumpens und Grens 2001). Thus, the strong immunogenic properties of HBc can be conveyed to the linked and poorly immunogenic target antigen (Roose et al. 2013). Humoral and cellular immune responses are evoked both against HBc and the target antigen (Liang et al. 2018).

A disadvantage of HBc as the target antigen of a therapeutic vaccination might be the emergence of HBe-negative CHB. In periods of low-level viral replication after HBeAg

seroconversion, HBV core-specific CTLs might preferentially target hepatocytes which are infected by wt virus as they cannot distinguish HBe epitopes from identical HBc epitopes - HBe negative mutant strains might be selected because infected hepatocytes only express HBcAg and therefore might be less targeted by HBV core-specific CTLs (Hadziyannis und Vassilopoulos 2001). This issue should be kept in mind but in the first place, the direct and elemental objective of therapeutic vaccination is the seroconversion in CHB and the clearance of infection. And to achieve this, the best antigen formulation and probably a combination of different antigens will be necessary and will prevent the scenario which is described above (Barnes 2015).

The present study only targeted HBc. For a first evaluation of CD70 co-stimulation in this setting, cloning of the rMVA and evaluation of the immune response after protein-prime/MVA-boost vaccination was expected to be sufficient and more straightforward.

### **1.3. Co-stimulation of T cells via CD70/CD27 interaction**

#### **1.3.1. Characterization and biological function of CD27 and CD70**

CD27 and its ligand CD70 are members of the TNF/TNFR family, which are expressed by various cells of the immune systems. The interaction of membrane bound CD70 (mainly on dendritic cells) and membrane bound CD27 (on CD3+ cells) is important for efficient T-cell priming, T-cell survival and formation of effector and memory T cells (Jacobs et al. 2015; Schildknecht et al. 2007). Via the NF $\kappa$ B and c-Jun kinase pathways, signals are enhanced, that lead to proliferation, survival and differentiation, but CD27 engagement can also lead to apoptosis via SIVA interaction (Figure 10). Temporal limitation of interaction is important to prevent dysfunctional mechanisms and exhaustion of the naïve T-cell pool, that can occur under sustained CD70 expression (Tesselaar et al. 2003a).

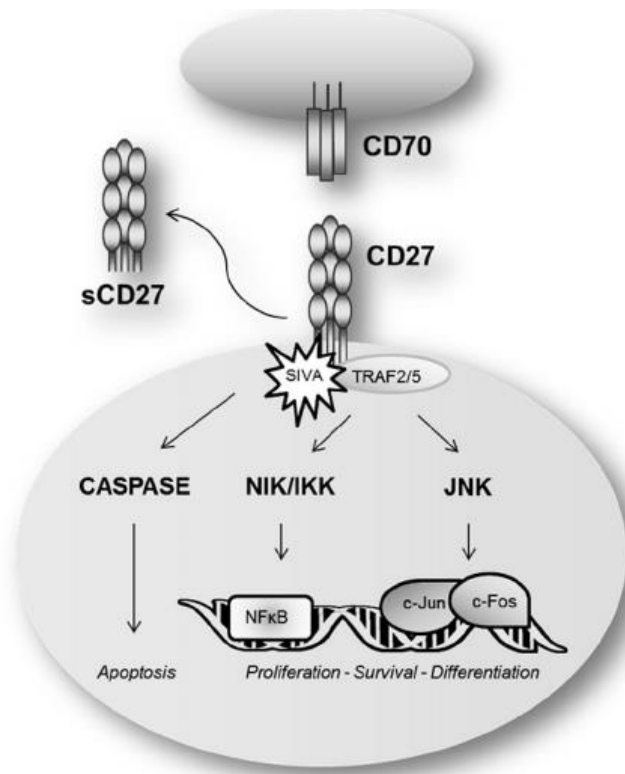


Figure 10 - **Stimulation of CD27 by CD70 (Jacobs et al. 2015)**. CD70 (for example presented by an antigen presenting cell) binds to its unique ligand CD27 (on T cells and B cells). The membrane-bound TNF-receptor CD27 interacts with TRAF2 which activates the NFκB pathway and TRAF5, which enters the c-Jun kinase pathway – both resulting in survival, proliferation and differentiation signals. By binding of CD27 to Siva, caspase-mediated apoptosis can be promoted. *NIK*: NFκB inducing kinase; *IKK*: IκB kinase; *JNK*: c-jun N-terminal kinase; *TRAF*: TNF receptor-associated factor.

### Structure and localization of CD27 and CD70

CD27 is a member of the TNFR family and is expressed as transmembrane homodimer of a size of 55 kDa per subunit (Denoeud und Moser 2011). It was identified in 1987 as an antigen that is upregulated during differentiation on anti-CD3-activated T cells (van Lier et al. 1987). CD27 is constitutively expressed on the surface of resting T cells and is further up-regulated after activation of unprimed T cells (CD45RA+) while expression diminishes in activated memory cells and effector T cells over time (Prasad et al. 1997; Grewal 2008). On B cells, CD27 is only expressed after B-cell receptor activation (Grewal 2008). In mice, CD27 is constitutively expressed on all thymocytes (Prasad et al. 1997).

The unique ligand of CD27 is CD70, which is a type II transmembrane glycoprotein that belongs to the TNF family. It has a molecular mass of 50 kDa and due to sequence homology with other members of the TNF superfamily it is predicted, that it is a

homotrimer, which probably binds to three CD27 homodimers (Jacobs et al. 2015). CD70 is transiently presented upon induction on the cell surface of mature DCs and B cells and in lower extent on T cells. (Jacobs et al. 2015; Flieswasser et al. 2022)

### **The effects of CD70/CD27 interaction**

Studies indicate, that triggering of CD27 is neither required nor sufficient to induce effector T-cell formation, but it is important for efficient priming of T cells and promotion of T-cell survival. This contributes to the formation of the effector and memory T-cell pool (Jacobs et al. 2015; Schildknecht et al. 2007). There is evidence, that CD27 has only a minor role in differentiation but is important for accumulation of cells and for their effector function - a lack of CD70 cannot be fully compensated by other co-stimulatory molecules (Denoeud und Moser 2011; Schildknecht et al. 2007; Roberts et al. 2010; Hendriks et al. 2003).

On naïve and unactivated cells in the mouse, CD70 is absent but transcription and localization at the plasma membrane (of mature DCs, B cells and in lower extent of T cells) can be induced by Toll like receptor and/or antigen receptor signaling (Tesselaar et al. 2003b; Denoeud und Moser 2011). The presentation of antigens by dendritic cells is required for the priming of CD8 T cells. Infections result in the upregulation of CD70 on activated, mature DCs, that contribute to the formation of the effector and memory T-cell pool (Schildknecht et al. 2007). It is likely, that restriction of CD70 expression is important to limit excessive effector cell formation after antigenic stimulation and to prevent dysfunctional mechanisms, that can occur under sustained CD70 expression (Tesselaar et al. 2003b; Denoeud und Moser 2011; Grewal 2008; Jacobs et al. 2015; Matter et al. 2006). Those adverse immunological effects are discussed in the following chapter.

### **Adverse immunological effects of CD70 stimulation are context-sensitive**

In contrast to the positive effects on effector and memory T-cell function, some studies indicate detrimental effects of CD27 stimulation in certain circumstances. In chronic viral infections, persistent immune activation and co-stimulation via CD27-CD70 interaction seem to result in the exhaustion of the naïve T-cell pool and B-cell depletion: Tesselaar et al. investigated the effects of HIV-like chronic immune activation in mice that constitutively expressed CD70 on B cells and found, that - dependent on CD27 and antigen stimulation - naïve T cells were depleted from

lymphoid organs by progressive conversion into effector-memory cells (Tesselaar et al. 2003a). Another study (Matter et al. 2006) analyzed the effects of CD27 signaling by CD4 T cells and found that this enhances the secretion of IFN $\gamma$  and TNF by CD8 T cells which led to destruction of splenic architecture and immunodeficiency with B-cell depletion and resulted in reduced and delayed virus-specific and unspecific neutralizing antibody response. They suggest blockade of CD27/CD70 signaling as a strategy to prevent chronic viral infection. They showed, that in mice, which are infected with a normally persistent LCMV strain, blocking of CD27 leads to elimination of the infection. Schildknecht et al. (Schildknecht et al. 2007) analyzed the role of CD70 co-stimulation in various infections in murine models and concluded, that the impact of the CD27/CD70 axis on CD8 T-cell priming may be determined by the persistence and duration of infection and antigen exposure (Denoeud und Moser 2011).

There is another field, in which CD70 might serve as a therapeutic target: CD70, which is not constitutively expressed by healthy cells, is upregulated and overexpressed in some malignant cells or tissues. It is presumed, that it may play a role in immune inhibition and immune escape of malignancies (Grewal 2008). In lymphomas, overexpression of CD70 is associated with an unfavorable prognosis, while CD70 deletion has no prognostic factor (Bertrand et al. 2013). In the respective murine model, targeted tumor therapy with anti-CD70 and complement factors lead to tumor growth inhibition (Israel et al. 2005; Grewal 2008). On the other hand, it was shown, that in a murine model in which tumor cells were transfected with co-stimulatory molecules as CD70 and CD80, tumor growth was suppressed in an IFN $\gamma$ - and CD8 T-cell dependent manner (Denoeud und Moser 2011).

### **1.3.2. CD70 as a promising co-stimulator in therapeutic vaccination**

Resting immature DCs are important for the regulation of T-cell tolerance. They maintain CD8 T-cell tolerance by synergistic stimulation of the proapoptotic molecules PD-1 and CTLA-4 on CD8 T cells (Probst et al. 2005). As it was described previously (see 1.1.4), immune tolerance is the basis for development of chronic HBV infection. In dysfunctional HBV-specific T cells of chronically infected patients upregulation of PD-1 (programmed cell death protein 1) was found (Boni et al. 2007).

In intrahepatic HBV-specific T cells, levels of PD-1 expression were even higher than in peripheral T cells (Fisicaro et al. 2010). Blocking of PD-1 was able to improve T-cell

function both in PBMC derived from chronically infected patients and in mouse models for chronic HBV infection (Boni et al. 2007; Tzeng et al. 2012; Fiscaro et al. 2010; Bunse et al. 2022). Another proapoptotic receptor, CTLA-4, was also found to be upregulated in HBV-specific CD8 T cells and also correlated positively with HBV-DNA levels. Levels were higher in HBV-tetramer positive cells (anergic cells) than in HBV-specific cells, that were capable of IFN $\gamma$  expression. Blocking of CTLA-4 led to T-cell expansion; and inhibition of both PD-1 and CTLA-4 had complementary and synergistic, nonredundant positive effects. (Schurich et al. 2011)

Stimulation of CD27 might be a promising approach to target tolerant HBV-specific CD8 T cells by various reasons. These reasons are defined by a number of preclinical studies: Stimulation of CD27 leads to increased accumulation and delayed contraction of effector T cells and contributes to a better CD8 T-cell memory response (Keller et al. 2009; Arens et al. 2004). In natural course of infection and artificial agonistic activation, CD27 activation stimulates and supports the maintenance of high numbers of specific CD8 T cells at the site of infection or in the tumor respectively (Roberts et al. 2010; Hendriks et al. 2003). CD8 T cells, which are stimulated by the CD70/CD27 axis were found to be not only better in quantity but also in effector function (IFN $\gamma$  secretion and cytopathic effects) (Keller et al. 2008; Roberts et al. 2010; Arens et al. 2004). Agonistic anti-CD27-Antibodies improve the effector function of NK and CD8 T cells and lower levels of PD-1 expression on CD8 T cells, whereas direct blocking of PD-1 was less efficient in doing so (Roberts et al. 2010). Moreover, already tolerized T cells (mediated by synergistic action of PD-1 and CTLA-4) were reactivated after antigen-presentation by resting CD70tgDCs (DCs with transgenic CD70) (Keller et al. 2008).

The potential to reactivate tolerant CD8 T cells and improve their effector cell function and especially their capability of IFN $\gamma$  secretion nominates CD70 as an appropriate element of therapeutic vaccination against chronic hepatitis B.

#### **1.4. Aim of the study**

An efficient therapeutic vaccination against HBV is a desirable treatment option in CHB. In a mouse model, Backes et al. (Backes et al. 2016) vaccinated wt and HBV1.3tg mice in order to break HBV-specific T- and B-cell tolerance and elicited effective virus-specific immune responses. They developed a heterologous vaccination regimen with a protein prime and a MVA-boost vaccination after three weeks, which broke tolerance even in high viremic mice. The viral vector for the boost vaccination was a recombinant MVA, that encoded HBcAg or HBsAg.

The scientific question of the present study was whether an additive effect on induction of HBV-specific immune responses in this protein-prime/MVA-boost therapeutic vaccination setting could be achieved by appropriate co-stimulation. CD70 was chosen as a promising candidate for co-stimulation of effector CD8 T-cell responses. To investigate the contribution of CD70 in induction of HBV-specific T-cell responses after vaccination, two MVA vectors were generated: one vector encoding the viral antigen HBc and CD70 (=rMVA-HBc-CD70) and an equivalent control vector without CD70 (=rMVA-HBc). Immune responses were analyzed in vaccinated C57Bl/6 mice and in HBV1.3tg mice.

Parts of the results of this study are published in (Stephan et al. 2023).

## 2. Materials and Methods

### 2.1. Materials

#### 2.1.1. Reagents and Enzymes

##### Reagent systems (KITs) or Standards

Kit or Standard	Name	Manufacturer
Protein Ladder	Page ruler plus® prestained protein Ladder	Thermo Fisher Scientific
TOPO blunt End cloning Kit	Zero Blunt® TOPO® PCR cloning Kit	Invitrogen, Life Technologies GmbH, Darmstadt, Germany
PCR kits	KOD Hot start DNA polymerase	Merck Millipore, Darmstadt, Germany
	Kapa Hifi HotStart PCR Kit	Kapa Biosystems, Wilmington, Massachusetts, USA
Kit for spin purification	QIAquick Gel Extraction Kit	Quiagen, Venlo, Netherlands

##### other Reagents and Enzymes

Name	Manufacturer
Trypsin	Life Technologies, Carlsbad, USA
Proteinase K	Roth, Karlsruhe, Germany
RNase A	Machery-Nagel, Düren, Germany
T4 DNA Ligase	Roche, Basel, Switzerland
Lipofectamin 2000	Thermo Fisher Scientific
CIAP (calf intestine alkaline phosphatase)	Thermo Fisher Scientific
Bam HI, Bcl I, Bgl II, Eco RI, Hind III, Nhe I, Sac II, Sal I-HF (Restriction enzymes)	New England Biolabs, Ipswich, UK

#### 2.1.2. Buffers and solutions

Name	Manufacturer or recipe
10x PBS pH 7,4	Gibco, Life Technologies GmbH, Darmstadt, Germany
TAE buffer (1x)	40 mM Tris, 20 mM acetic acid, 1mM EDTA
FACS	500 ml PBS, 5 g BSA, 500 µl Sodium-Azide
T4 ligase buffer	10x concentrated: Tris/HCl, 660 mmol/L, MgCl <sub>2</sub> , 50 mmol/L, DTT, 50 mmol/L, ATP, 10 mmol/L, pH 7.5 at 20 °C
Tris (pH9; 10 mM)	500 ml Milli-Q, 0,61 g Tris, to pH 9 with HCl
TAC for erythrocyte lysis	9 parts NH <sub>4</sub> Cl, 1 part Tris pH 7,65
Tris (pH 7,65; 0,17 M)	500 ml Milli-Q, 10,3 g Tris; adjust to pH 7,65 with HCl/NaOH
NH <sub>4</sub> Cl (0,16 M)	500 ml Milli-Q, 4,28 g NH <sub>4</sub> Cl

Tuerk solution	Sigma-Aldrich, Chemie GmbH, Munich, Germany
<i>Buffers for restriction enzymes:</i> NEBuffers (1.1; 2.1;3.1; CutSmart; EcoRI)	New England Biolabs, Ipswich, UK
QG buffer	from QIAquick Gel Extraction Kit (Quiagen, Venlo, Netherlands)
<i>for western blot (buffers kindly provided by F. Wilsch, Institute of Virology, Munich)</i>	
RIPA Lysis buffer	150 mM sodium chloride, 1.0% NP-40 or Triton X-100, 0.5% sodium deoxycholate, 0.1% SDS (sodium dodecyl sulfate), 50 mM Tris; pH 8.0
6x SDS sample buffer	0.375 M Tris pH 6.8, 60% (v/v) glycerol, 0.12 g/ml SDS, 0.093 g/ml DTT, 0.6 mg/ml bromophenol blue; Storage at - 20 °C
10x SDS running buffer	30.3 g/l Tris [250 mM], 145 g/l Glycine [1,93 M], 1% (v/v) SDS (1% Stock solution)
Western Blot transfer buffer pH 9.2	48 mM Tris, 39 mM Glycine, 20% (v/v) MeOH; pH is adjusted automatically
TBS-Tween (TBST)	100 ml 10x TBS pH 7,4, 1 ml Tween 20; to 1 l with dH <sub>2</sub> O
5 % blocking buffer	TBST + 5% milk powder (storage at -20 °C)
Amersham ECL Prime Western Blotting Detection Reagent	GE Healthcare
<i>for phenol/chlorophorm DNA extraction</i>	
TE buffer	10 mM Tris (to pH 8.0 with HCl), 1 mM EDTA
TEN buffer	10 mM Tris (to pH 7,5 with HCl), 10 mM NaCl, 1 mM EDTA
Phenol/chlorophorm/isoamylalcohol	Roth, Karlsruhe, Germany
EB buffer	10 mM Tris (to pH 8.5 with HCl)
<i>for Miniprep (reagents kindly provided by M. Mück-Häusl)</i>	
P1 - Resuspension Buffer	50 mM Tris-Cl, 10 mM EDTA; pH 8.0 – storage at 4 °C freshly add 100 µg/mL RNase A before use
P2 - Lysis Buffer	200 mM NaOH, 1% SDS – storage at RT
P3 - Neutralization Buffer	3.0 potassium acetat; pH 5.5 – storage at 4 °C or RT

### 2.1.3. Chemicals

Name	Manufacturer
Ethidium bromide (EtBr)	Serva, Heidelberg, Germany
Ethanol (EtOH)	Merck, Darmstadt, Germany
Ethylenediaminetetraacetic acid (EDTA)	Sigma, Munich, Germany
Methanol	Merck, Darmstadt, Germany
SDS	Serva, Heidelberg, Germany
Dimethyl sulfoxide (DMSO)	Merck, Darmstadt, Germany

Ethidium monoacid bromide (EMA)	Invitrogen, Carlsbad, USA
Brefeldin A (BFA)	Sigma-Aldrich, Chemie GmbH, Munich, Germany

#### 2.1.4. Primers for PCR

Lyophilized oligonucleotides (primers) were designed in Serial Cloner or ApE and purchased from Eurofins Genomics, Ebersberg, Germany. Stock solutions with 100 pmol/μl were prepared in sterile ddH<sub>2</sub>O according to the manufacturer's advice and stored at -20 °C. For a working solution, the stock solution was diluted 1:10 with 9 parts ddH<sub>2</sub>O.

No.	Associated genes	Application	Sequence 5' → 3'
1	CD70-5' end	fwd. primer	AGGAGCCCCGGGAGGGGGCTGCAGT
2	CD70-3' end	rev. primer	GGCCACCCGGGGTTGGGGTGGGAGT
3	BglII_Zeo-5'	fwd. primer	ATCCGCTAGCGCTACCGGACTCAGATCTGCGGAACCCCTATTTGTTTATT
4	CD70-3' SacII	rev. primer	AGAGGGGCGGATCCCGGGCCGCGGGTCAATCAGGGGCGCACCCACTGCA
5	NheI_CMV-Pr.-5'	fwd. primer	GCGCCCGTCAGATCCGCTAGCACAGATCTTCAATATTGGCCATTAGCCAT
6	HBc-3'_P2A-5'	rev. primer	CAGGGAGAAGTTGGTGGCTCCGGAGCCACATTGAGATTCCCGAGATTGAG
7	P2A	rev. primer	GTTCTCCTCCACGTCGCCGGCCTGCTTCAGCAGGGAGAAGTTGGTGGCTC
8	P2A-3'_EcoRI	rev. primer	CGATAAGGGCGAATTCAGCAAGGGCCGGGGTTCTCCTCCACGTCGCCGG
9	HBc-3'_BamHI	rev. primer	GGAGGGAGAGGGGCGGATCCGAATACTAACATTGAGATTCCCGAGATTGA
10	BclI_HBc-5'	fwd. primer	TTCGTGATCAACCATGGACATCGACCCTTATAAAGAATTTGGAGC
11	polyA-3'_Sall	rev. primer	GATGGTCGACGACAAACCACAACCTAGAATGCAGTG

#### 2.1.5. Cell lines and Bacteria

Organism Name	Description	Source
<i>Cell lines</i>		
HEK293 cells	Human embryonic kidney cells	Institute of Virology (kindly provided by M. Mück-Häusl)
DF1 cells	Continuous cell line of chicken embryo fibroblasts	Institute of Virology (kindly provided by A. Muschaweckh)
<i>Bacteria</i>		
<i>E. coli</i>	One shot TOP 10 chemically competent <i>E. coli</i>	Invitrogen, Life Technologies GmbH, Darmstadt, Germany

#### 2.1.6. Mouse strains

Name	Specification	Source
C57BL/6 wildtype (wt)	haplotype H-2b/b	Charles River Laboratories

		(Schulzfeld, Germany)
HBV1.3tg mice	HBV-transgenic mice (StrainHBV1.3.32 [5] (HBV genotype D, subtype ayw))	Original strain: F. Chisari, The Scripps Institute, La Jolla, CA, USA; inhouse breeding
DNGR1 deficient mice	The gene clec9a (coding for DNGR1) is replaced by eGFP	Original strain: C. Reis e Sousa, The Francis Crick Institute, London, GB; obtained from A. Verschoor, TU Munich; inhouse breeding

### 2.1.7. Plasmids, viruses and DNA material

Name	Specification	Source
<i>Plasmids</i>		
B 2-1	Plasmid carrying CMV-Promoter and HBc (see Appendix 1)	Institute of Virology
pIRES-eGFP	Plasmid carrying IRES and eGFP (see Appendix 1)	Institute of Virology, Helmholtz Center Munich (kindly provided by A. Muschaweckh)
pShuttle-empty	pLWA-73; plasmid carrying MVA flank regions and mH5 promoter (see Appendix 1) description: (Wyatt et al. 2009)	Institute of Virology, Helmholtz Center Munich (kindly provided by A. Muschaweckh)
<i>DNA</i>		
CD70 DNA	amplified from cDNA, derived from Epstein-Barr Virus (EBV)-immortalized human B-cell line	Institute of Virology, Helmholtz Center Munich (kindly provided by C. Dembek)
<i>Viruses</i>		
MVAwt	MVA wt virus (non-recombinant MVA-F6)	Institute of Virology, Helmholtz Center Munich
rMVA-core	Recombinant MVA encoding HBV core	Institute of Virology, Helmholtz Center Munich (Published in: (Backes et al. 2016))

### 2.1.8. Material for cell culture

#### Media for bacterial and cell culture

Name	Ingredients / Manufacturer
LB medium	5 g/l yeast extract, 10 g/l Bacto-tryptone, 10 g/l NaCl in dH <sub>2</sub> O, pH 7 (autoclaved)
low salt LB medium	5 g/l yeast extract, 10 g/l Bacto-tryptone, 5 g/l NaCl in dH <sub>2</sub> O, to pH 8 with NaOH (autoclaved)
LB agar	(low salt) LB medium supplemented with Agar (15 g/l)
RPMI-10	RPMI 1640 medium (Life Technologies GmbH, Gibco; Darmstadt, Germany) supplemented with 10% heat-inactivated FCS, 1% Penicillin/Streptomycin
RPMI-2 RPMI-1	as RPMI-10 but with 1% or 2% heat-inactivated FCS respectively

DMEM	Gibco, Life Technologies GmbH, Darmstadt, Germany
DMEM (+)	DMEM supplemented with 10%
optiMEM	Gibco, Life Technologies GmbH, Darmstadt, Germany
S.O.C. medium	Invitrogen, Life Technologies GmbH, Darmstadt, Germany

## Supplements for cell culture

Name	Lab name	Manufacturer / Concentration for bacterial selection
<i>Antibiotics</i>		
Ampicillin	A	100 µg/ml in LB medium or LB agar
Kanamycin	K	50 µg/ml LB medium or LB agar
Penicillin/Streptomycin	P/S	PAA Laboratories GmbH (Cölbe, Germany)
Zeocin	Z	25 µg/ml in low-salt LB medium or low-salt LB agar
<i>others</i>		
Agarose		Peqlab, Erlangen, Deutschland
Agar		Carl Roth GmbH + Co. KG, Karlsruhe, Germany
Fetal calf serum, heat-inactivated	FCS	Life Technologies GmbH, Gibco (Darmstadt, Germany)
Trypsin		Life technologies, Carlsbad, USA
Versene		Life technologies, Carlsbad, USA

### 2.1.9. Antigens and Adjuvants

Name	Source / Specification
HBcAg	APP Latvijas Biomedicinas (Riga, Latvia)
PCEP	Institute of Virology, Helmholtz Center Munich (originally by Dr. George Mutwiri, University of Saskatchewan)
CpG	CpG Oligodesoxynucleotide, ODN 1668, InvivoGen, San Diego, CA

### 2.1.10. Peptides, Antibodies and staining dyes

#### Synthetic peptides

Name	MHC restriction	Amino acid sequence		Origin	Source
B8R (B8R <sub>20</sub> )	H2-Kb	TSYKFESV		MVA	Kindly provided by Ingo Drexler
C93	H2-Kb	MGLKFRQL		HBV	JPT (Berlin)
Core pool 3	H2-Kb	Peptides 31-43		HBV	Thinkpeptides (Oxford, UK)

## Antibodies for Immunoblotting and Immunohistology

Name	Concentration	Specification	Manufacturer
<i>Antibodies for Immunoblotting</i>			
Anti-HBcAg	1:10 000	Polyclonal rabbit antiserum	DAKO Carpinteria, USA
Anti-GFP	1:5 000	Polyclonal rabbit antiserum	Sigma-Aldrich
Goat-anti-rabbit	1:10 000	Polyclonal, affinity isolated antibody, Horseradish peroxidase conjugated	Sigma-Aldrich
<i>Antibodies for Immunhistology</i>			
Anti-HBcAg	1:50	HBcAg primary antibody	Diagnostic Biosystems, Pleasanton, CA
Horseradish peroxide coupled secondary antibody			
Anti-CD3	ready to use	host: rabbit	IR503 Dako
Anti-Ki67	1:200		SP6, NeoMarkers/ Lab Vision Corporation

## Dyes for stainings

Name	Concentration for staining	Manufacturer
<i>Dyes for flow cytometry</i>		
LIVE/DEAD Fixable Near-IR Dead Cell Stain Kit	(according to user manual)	Life Technologies GmbH, Invitrogen (Darmstadt, Germany)
Ethidium monoazide bromide (EMA)	0,1 µl/well (in 100 µl FACS)	Invitrogen (Carlsbad, USA)

## Fluorochrome-labeled antibodies, Tetramer

Name	Concentration/well	manufacturer
CD70-PE	1 µl	BioLegend, San Diego, CA, USA
C93 Tetramer	0,4 µl	Institute for Microbiology, TU Munich
Strep-Tactin-PE	1 µl	IBA-lifesciences
CD8α-PacB	0,5 µl	eBioscience, San Diego, USA
CD4-PE	0,5 µl	eBioscience, San Diego, USA
IFN-γ-FITC	0,17 µl	eBioscience, San Diego, USA
TNF-α-PeCy7	0,25 µl	eBioscience, San Diego, USA
IL2-APC	0,25 µl	eBioscience, San Diego, USA
CD8α-PerCPCy5.5	1 µl	BioLegend, San Diego, CA, USA
CD4-PacB	1 µl	BD Biosciences
IFN-γ-APC	0,5 µl	BioLegend, San Diego, CA, USA
TNF-α-PECy7	1 µl	BD Biosciences
IL2-PE	1 µl	BioLegend, San Diego, CA, USA

### 2.1.11. Laboratory equipment / Devices

Besides the mentioned equipment, standard laboratory equipment was used, which was not restricted to a specific provider.

Name	manufacturer
Thermo cycler (for PCR): GeneAmp PCR System 2700	Applied Biosystems, Foster City, USA
Horizontal Electrophoresis System (A1 Gator, A2 Gator)	Owl Scientific, Portsmouth, USA
pH-Meter: InoLab pH Level 1	WTW GmbH, Weilheim
Thermoshaker: Thermomixer 5436 Comfort	Eppendorf, Hamburg
PAGE Equipment	PEQLAB
Trans-Blot® semi-dry Western Blot transfer unit	Biorad, München, Germany
C-DiGit® Blot Scanner	Li-Cor Biosciences GmbH, Lincoln, USA
Ultra sound needle (UW 200)	Bandelin electronic, Berlin
Centrifuges e.g. 5417C 4K15	Eppendorf, Hamburg Sigma Life Science, Hamburg
Ultra centrifuge: Optima™ L-90K ultracentrifuge SW32 rotor and buckets SW41 rotor and buckets	Beckmann, Munich
VI-CELL counter	Beckman Coulter
Nanodrop	Thermo Fisher scientific
Flow cytometer: LSR Fortessa	Becton Dickinson, Heidelberg
Reflovet (reflectance photometer for serum analysis)	Scil animal care company GmbH
AxSYM, immunochemical automated analyzer	Abbott Laboratories

### 2.1.12. Consumables

Besides the mentioned consumables, standard laboratory material was used for all experiments, which was not restricted to a specific provider.

Name	Manufacturer/Tradename
Cell culture flasks (25-175 cm <sup>2</sup> )	Sarstedt AG & Co, Nümbrecht, Germany
Cell culture flasks 225 cm <sup>2</sup>	Nunc Thermo Scientific
Whatman blotting paper	GE
PCR reaction tubes	Eppendorf, Hamburg
Hemocytometer (cell counting chamber)	Brand, Wertheim
Cell strainer 100 µm	BD Pharmingen, Hamburg, Germany

Cell culture plates, 6-, 12-, 96-well	SA Corning, New York, USA
Falcon tubes (15 ml, 50 ml)	BD Pharmingen, Hamburg, Germany
FACS tubes	Bio-Rad, Munich, Germany
Microtiter plates (96-well)	Roche, Basel, Switzerland
Ultracentrifuge tubes (UltraClear tubes)	Beckman, Munich, Germany
Reaction tubes (0.5 ml, 1.5 ml, 2 ml)	Eppendorf, Hamburg, Germany
Cryo tubes	Nunc Thermo Scientific
Petri dishes	Nunc Thermo Scientific

### 2.1.13. Software

Product	Version	Source
FacsDIVA	6.2	Becton Dickinson, Heidelberg, Germany
FlowJo	9.9	Treestar, Ashland, USA
GraphPadPrism	5.00	Graph Pad Software, San Diego, USA
Microsoft Office 365	1609	Microsoft, Redmond, USA
ApE – A plasmid Editor	v.2.0.47	M. Wayne Davis
Serial Cloner	2.5	Serial Basics
OligoCalc – Oligonucleotide properties calculator	3.27	Northwestern University, Chicago, USA

## 2.2. Methods

### 2.2.1. Cloning

Applied molecular cloning techniques and controls are depicted in Figure 11.

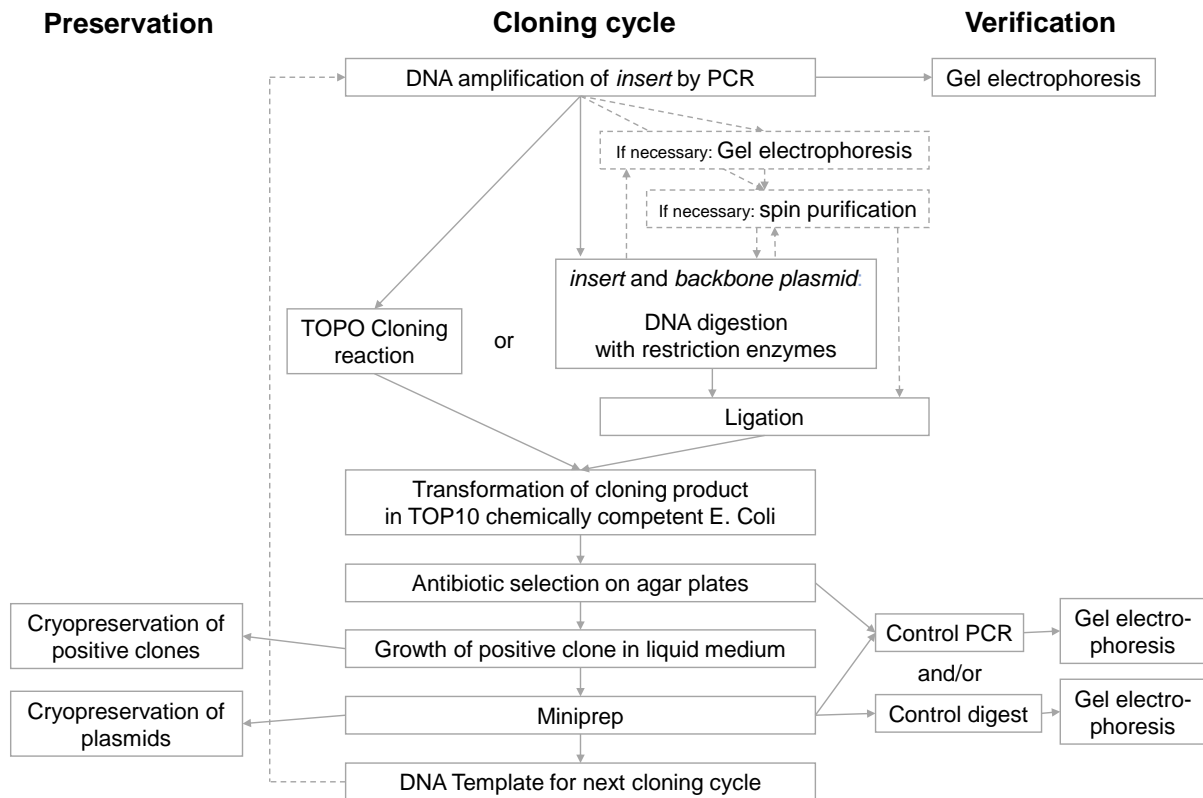


Figure 11 - **Cloning methods schematically.** To perform the cloning steps successfully, different paths had to be followed during cloning. The generation of a cloning product was either completed by a TOPO cloning reaction or by digestion and ligation of insert and backbone. The selection of clones (=transformed *E. coli* that had formed single colonies on an agar plate) was possible due to inserted antibiotic resistance genes and control PCRs and/or digests that verified the presence of the desired insert. When one cloning cycle was completed successfully, the products were preserved and the next cloning step was approached.

#### 2.2.1.1. Vector design and cloning strategy

ApE Software was used for vector design, visualization and sequence analysis.

Most cloning steps were performed by digestion and ligation. Therefore, the primer design required particular considerations: at the position, where another sequence ("insert") should be inserted into the backbone, unique restriction sites were identified. Primers were designed, that introduced appropriate restriction sites upstream and

downstream of the sequence, which was intended to be inserted into the backbone (=insert) (see chapter 2.2.1.11).

### 2.2.1.2. Polymerase chain reaction (PCR)

For the first cloning steps the KOD hot start Kit was used. Due to availability later the Kapa HiFi hot start Kit was used. Both polymerases are proofreading and comparable in the quality of the PCR products.

#### PCR for DNA amplification

For the amplification of DNA segments for cloning reactions the PCR reaction mix was set up according to the user instruction of the manufacturer in a total volume of 50  $\mu$ l per template DNA. The PCR program was set up according to the manual by choosing 30 cycles, adjusting the elongation time to the size of the estimated PCR product and by setting the annealing temperature to the calculated annealing temperature for the less stable primer (calculation performed with OligoCalc). If unspecific bands appeared after running 5  $\mu$ l of the PCR product mix on an agarose gel, a gradient PCR was performed to find an optimal annealing temperature for the primer pair (Figure 12).

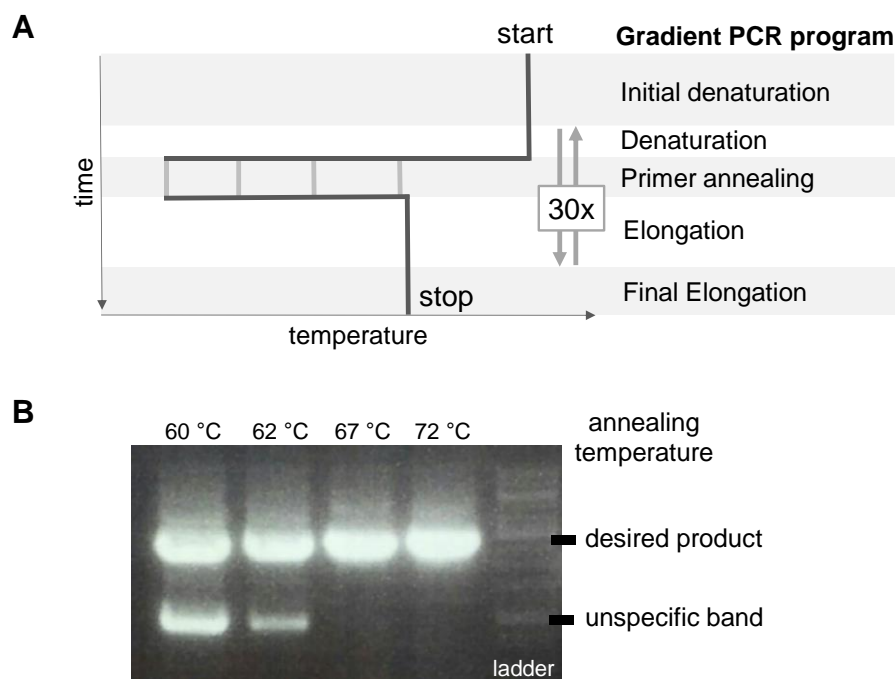


Figure 12 – **Illustration of a gradient PCR.** (A) The gradient PCR program is set up to use different annealing temperatures for multiple samples. (B) After agarose gel electrophoresis, the optimal

annealing temperature is visible. For this exemplary PCR it is 67 °C with an unspecific band at lower temperatures.

## Overhang PCR

The P2A cleavage site that consists of few base pairs was appended to the HBV core gene by an overhang PCR (Figure 13).

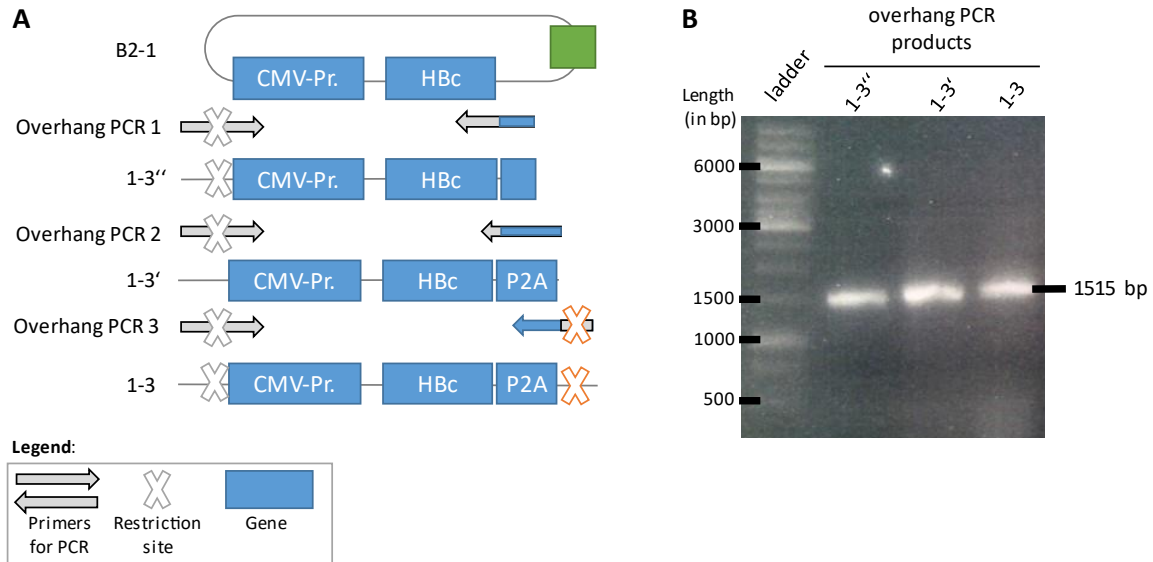


Figure 13 - **Overhang PCR of plasmid B2-1 for introduction of the P2A site.** (A) During 3 polymerase chain reactions, the sequence of the P2A gene was appended to the HBV core (HBc) gene. In Overhang PCR3, the second restriction site for the subsequent restriction enzyme digest was inserted. CMV-Pr.=CMV promoter. (B) Agarose gel electrophoresis of the PCR products (indicated in A). The elongation of about 20-30 base pairs per PCR is visible. The length of the last PCR product is 1515 base pairs.

## Control PCR

For a control PCR, only half the final concentration of polymerase and dNTPs (compared to the PCR protocol above) were used in a total volume of 10 µl per DNA template. The identification and verification of *E. coli* clones that carry the desired insert is depicted in Figure 14.

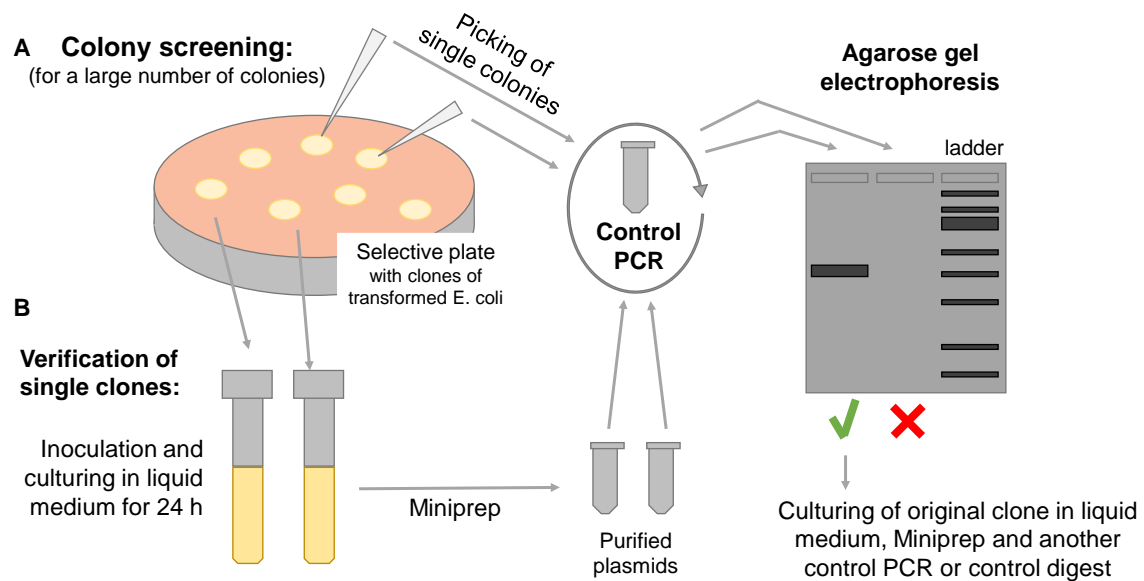


Figure 14 – **Identification of *E. coli* clones (colonies), that carry a specific insert.** The DNA template for the PCR reaction mix was either derived from a Miniprep (B) or by direct picking of single colonies with sterile pipette tips (A). The clones that were confirmed to be positive for the insert were cultured separately in liquid culture for 24 h and processed: Miniprep for DNA purification, a second control PCR or control digest and cryopreservation.

### 2.2.1.3. DNA digestion with restriction enzymes

#### Digestion in the course of a cloning reaction

For cloning by digestion and ligation, the insert and the backbone were digested with the respective restriction enzyme(s). The digest was performed following the recommendations of the manufacturer (concerning buffer and temperature) in a total volume of 50-80  $\mu\text{l}$  for 2-3 h. If not already included in the buffer, 1% BSA was added. 7000-10 000 Units of enzyme were used per  $\mu\text{g}$  of DNA.

If a double digest (2 enzymes) was necessary, the procedure depended on the requirements of the involved enzymes: if both restriction enzymes were at least 75% active in the same buffer and at the same temperature the digest was performed simultaneously in one reaction mix. If the enzymes digested best at different temperatures or needed different buffers, a sequential digest was done. This was performed either by DNA purification after the first digest or by setting up the first digest with the less concentrated buffer in a smaller volume (e.g. 20  $\mu\text{l}$ ), digesting for 1 h and then heat-inactivating the reaction at 65 °C for 20 min. Thereafter, the second enzyme

was added in a total volume of 50-80  $\mu\text{l}$  that has been filled up with  $\text{dH}_2\text{O}$ , BSA and a well calculated volume of the optimal buffer to reach the required salt concentrations.

After the digest, the DNA was purified for ligation either by spin purification (see 2.2.1.5) or by gel purification (see 2.2.1.4).

### Control digest

A control digest was performed to verify and identify the plasmids. The expected band pattern was estimated with the ApE Software and compared to the band pattern on the agarose gel. For the reaction mix, 2  $\mu\text{l}$  of purified plasmids (see 2.2.1.10) and 10 000 Units of restriction enzyme were set up in a total volume of 20  $\mu\text{l}$  of the respective digestion buffer. After 2 h of incubation at the optimal temperature, the whole reaction was loaded on an agarose gel for visualization of the band pattern.

#### 2.2.1.4. Agarose gel electrophoresis

Agarose gel electrophoresis (see Figure 15) was used to determine the length of PCR products and restriction digest products, to purify DNA fragments of a distinct length and to quantify DNA concentrations.

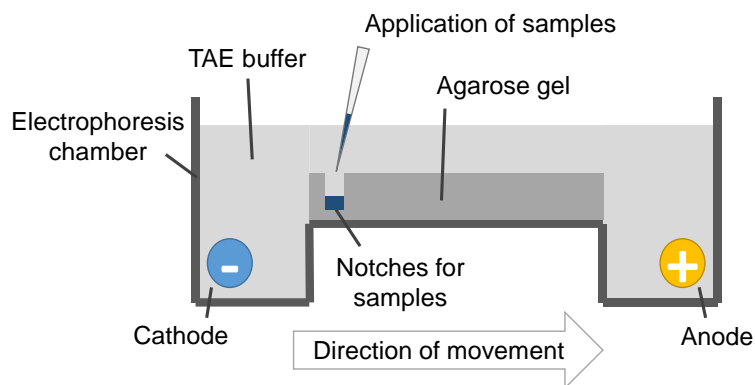


Figure 15 – **Schematic setup of an agarose gel in the electrophoresis chamber.** The sample and the ladder are applied in notches of the agarose gel. When voltage is applied, DNA particles move towards the anode and separate dependent on their size.

For preparation, a gel chamber was filled with a layer of 1 cm 1% agarose gel (1% agarose in TAE buffer, 60 °C + 3-10  $\mu\text{l}$  EtBr). A comb was applied to form the notches for sample application. The solidified gel was placed in an electrophoresis chamber and the comb was removed. For quantification and length determination, an aliquot of 5  $\mu\text{l}$  of the PCR product (+ 5  $\mu\text{l}$  loading dye) was applied. 5  $\mu\text{l}$  of DNA ladder were

applied in an extra notch. 120 V were applied for 20-30 min and DNA samples separated for size. Afterwards the DNA bands were visualized under UV light (wavelength of 312 nm).

## Gel purification

When it was necessary to extract DNA of a distinct size (e.g. in case of unspecific bands after a PCR or to eliminate DNA fragments after a digest and prior to ligation), a gel purification was performed (Figure 16). DNA particles of a distinct size were cut out from an agarose gel and afterwards purified by spin purification (see 2.2.1.5).

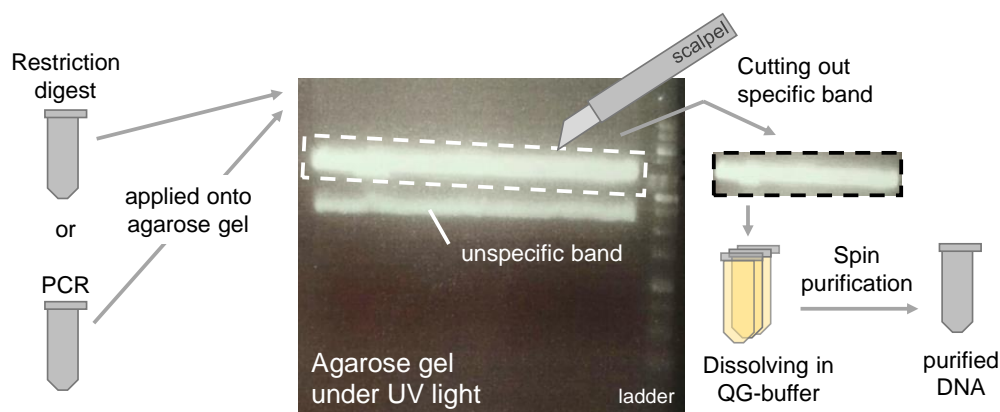


Figure 16 - **Gel purification of DNA samples (from restriction digest mix or PCR product)**. The whole reaction was loaded onto an agarose gel. 90 V were applied to the chamber for 30-45 min and the desired resulting band was cut out with a scalpel under UV light (dashed box). Then this slice was dissolved in the double amount of QG buffer by shaking it for 10 min at 55 °C. The purification was completed by a spin purification.

### 2.2.1.5. Purification of DNA (“spin purification”)

Spin purification of DNA (from a PCR or digest) was performed using the QIAquick Gel Extraction Kit and according to its manual. The PCR product or restriction digest product was loaded onto the spin columns in 500 µl QG buffer. The elution of the DNA from the spin column was completed by loading 20-35 µl of dH<sub>2</sub>O onto the column and spinning it at 14 000 rpm for 2 min.

### 2.2.1.6. Cloning by digestion and ligation

Cloning by digestion and ligation is based on the principle that two DNA fragments with compatible overlapping ends are connected by ligation to a circular DNA. A schematical overview on the protocol is depicted in Figure 17.

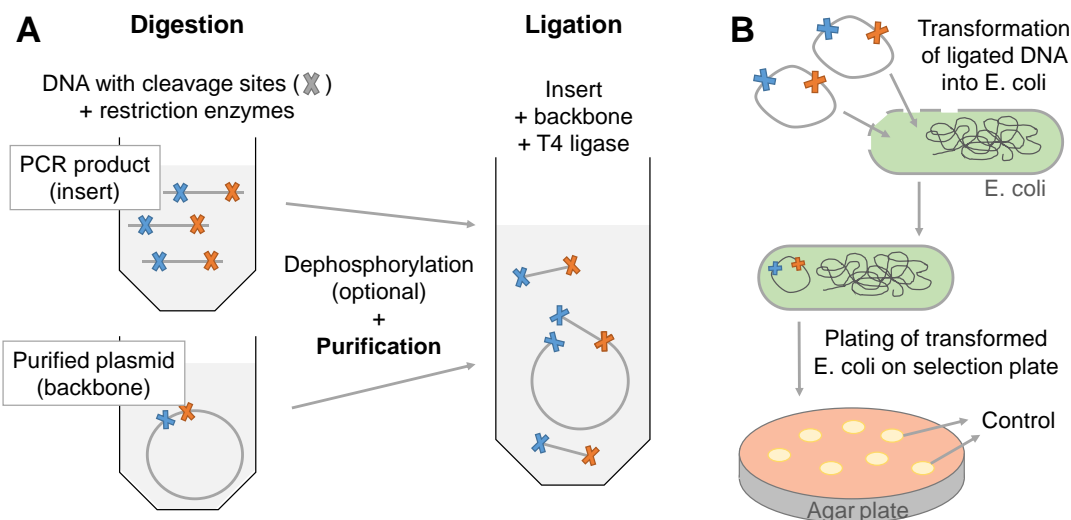


Figure 17 - **Cloning by digestion and ligation.** (A) A digest with restriction enzymes resulted in DNA with compatible overlapping ends (*crosses*). Insert and backbone with overlapping ends were purified and connected by a T4 ligase in a ligation reaction. If too many re-ligations of backbone occurred, the overlapping ends of the backbone were dephosphorylated to avoid re-ligation. (B) After ligation, the resulting circular DNA was transformed into TOP10 chemically competent cells. The resulting colonies (“clones”) were analyzed by control PCR and/or control digest.

## Dephosphorylation

Dephosphorylation prior to ligation was performed to avoid re-ligation of the backbone. The digested and purified DNA fragments were incubated following the recommendations of the manufacturer. The reaction was stopped by spin purification of the whole reaction mix.

## Digestion

See chapter 2.2.1.3.

## Ligation

For ligation, 100 ng total DNA were incubated with 2  $\mu$ l ligation buffer, 1  $\mu$ l T4 ligase and dH<sub>2</sub>O in a total volume of 20  $\mu$ l. Reaction conditions varied from 30 min at RT to OVN ligation at 6-16 °C. The ratio of insert to backbone was calculated to a proportion of 3 inserts to 1 backbone. If ligation was unsuccessful at the beginning, the ratio was varied from 1:2 to 1:5 or 1:10.

### 2.2.1.7. Blunt-end cloning (TOPO cloning reaction)

The TOPO cloning reaction was performed following the user instructions of the TOPO cloning kit: the insert was amplified by PCR as a Blunt End PCR Product. Then it was

incubated with the pCR II-Blunt-TOPO backbone for 30 min at RT. 2 µl of the reaction mix was then transformed into TOP10 chemically competent cells.

### 2.2.1.8. Transformation in TOP10 chemically competent cells

According to the manufacturers protocol, 1,5-2 µl of the cloning reaction (TOPO cloning or ligation) were transformed into 25 µl of competent cells. Then, the cell vials were filled up with 200 µl S.O.C. medium and incubated at 37 °C for 1 h (shaking). Afterwards, 10-50 µl of this cell suspension were plated onto 2 selection agar plates containing the respective antibiotic (Ampicillin, Kanamycin or Zeocin, for concentrations see Materials 2.1.8, supplements for cell culture). After OVN incubation at 37 °C, the resulting colonies were analyzed for the desired plasmid.

### 2.2.1.9. Culturing and preservation of *E. coli*

For amplification, *E. coli* colonies that contained a plasmid were cultured OVN (37 °C, shaking) in 3 ml LB medium containing the respective antibiotic (see 2.2.1.8).

## Cryopreservation of *E. coli* clones

After each cloning step, an *E. coli* clone that had been verified to carry the insert on a plasmid was cryopreserved in 25% glycerol, 25 % water and 50% LB medium. After the glycerol had been added the cells were directly stored at -80 °C.

To recover a colony, a sterile pipet tip was scratched over the frozen cells and then placed into a culture tube with 3 ml LB medium and incubated OVN (37°C, shaking).

### 2.2.1.10. Plasmid extraction by Miniprep

For the protocol of plasmid extraction from a liquid culture of *E. coli* see Figure 18.

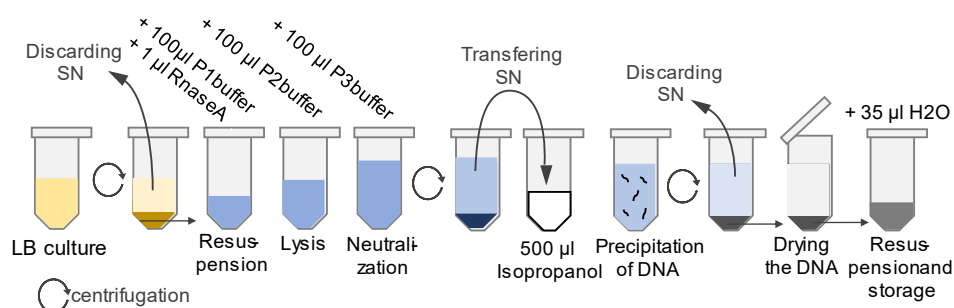


Figure 18 – **Schematic illustration of the Miniprep protocol (Plasmid extraction from *E. coli* in liquid culture).** 1.5 ml of the OVN culture (*LB culture*) was centrifuged at 14 000 rpm for 1 min. The SN was discarded and the pellet was resuspended in 100 µl *P1* resuspension buffer (+1 µl RNase A). After

adding 100 µl *P2* lysis buffer, the tubes were inverted several times for a gently mixing and incubated at room temperature for 5 min. Then, 100 µl *P3* neutralization buffer were added and the tubes were centrifuged (14 000 rpm, 5 min). After this centrifugation step, the plasmid holding supernatant was transferred to a new labelled 1,5 ml tube containing 500 µl isopropanol (-20 °C) for precipitation. The tubes were again centrifuged (14 000 rpm, 5 min). Then, the supernatant was discarded and 500 µl 70% ethanol (in dH<sub>2</sub>O) were added. After centrifugation (14 000 rpm, 3 min), the supernatant was discarded and the pellet in the tubes was dried for at least 15 min. The final resuspension was done by adding 35 µl PCR-grade water and shaking at 37 °C for 5-10 min.

The DNA concentration and purity of the Miniprep product was measured with Nanodrop and the integrity of the plasmid was visualized and quantified by running 1 µl on an agarose gel. The plasmids were stored either at 4 °C for several days or at -20 °C for long-term storage.

### 2.2.1.11. Specification of individual cloning steps

The individual cloning steps (see chapter 3.2.1) required application and combination of different cloning methods. The individual specifications are given below in Table 1.

Table 1 - **Specification of individual cloning steps for cloning of pShuttle-HBc and pShuttle-HBc-CD70.** Besides of the DNA components (templates for PCR of insert, backbone plasmid and product) the chart shows the letter of the reaction (according to the cloning scheme in Figure 30), the applied primers (the primer numbers and sequences are listed in 2.1.4) and the cloning method.

<b>Reaction</b>	<b>Amplification of insert: Primers (fwd./rev.)* Template for PCR</b>	<b>Backbone plasmid</b>	<b>Product (plasmid)</b>	<b>Applied Method</b>
<b>A</b>	Primers: 1 / 2 Template: cDNA (CD70)	pCR®-Blunt II- TOPO® Vector	p1-1	TOPO cloning
<b>B</b>	Primers: 3 / 4 Template: p1-1	pIRES_eGFP	p1-2	Cloning by digestion and ligation
<b>C</b>	Primers: 4 / 6,7,8 (sequentially) Template: B 2-1	-	1-3	Overhang PCR
<b>D</b>	- (1-3 served as insert)	p1-2	p1-4	Cloning by digestion and ligation
<b>E</b>	Primers: 10 / 11 Template: p1-4	pShuttle-empty	pShuttle- HBc-CD70	Cloning by digestion and ligation
<b>F</b>	Primers: 5 / 9 Template: B 2-1	pIRES_eGFP	p2-1	Cloning by digestion and ligation
<b>G</b>	Primers: 10 / 11 Template: p2-1	pShuttle-empty	pShuttle- HBc	Cloning by digestion and ligation

## 2.2.2. Cell culture methods

### 2.2.2.1. Culturing of eukaryotic cell lines

The handling of eukaryotic cells was always performed under sterile conditions. The cell lines were cultured in their appropriate medium: RPMI-10 for DF1 cells and DMEM (+) for HEK293 cells. They were constantly incubated at 37 °C, 5% CO<sub>2</sub>. The cells were split 2-3 times per week. The viability and confluency of the cells was assessed under the light microscope prior to splitting. If cells were healthy and >90% confluent, the old medium was removed using an appropriate sterile pipette and the cells were washed one time with DPBS. Cells were detached with 1.5, 3 or 5 ml Trypsin (for 25 cm<sup>2</sup>, 75 cm<sup>2</sup> or 175 cm<sup>2</sup> cell culture flasks) during an incubation time of 5 min. The detached cells were re-suspended in fresh medium and 2/3 – 9/10 of the suspension was discarded or transferred to fresh cell flasks (proportion depended on the growth of the cells – a 100% confluency 3 days after splitting was desired). Finally, the flask was filled up with medium to 5 ml, 12 ml, 20 ml or 25 ml (for 25 cm<sup>2</sup>, 75 cm<sup>2</sup>, 175 cm<sup>2</sup> or 225 cm<sup>2</sup> cell culture flask).

### 2.2.2.2. Transfection of eukaryotic cells

Cells were transfected using Lipofectamin2000 transfection reagent and according to its manual. The reagents listed in Table 2 were prepared, gently mixed and incubated (30 min, RT) to form DNA-Lipofectamin2000 reagent complexes. Then, the solution was given onto 50-80% confluent cells. One day later, the transfection efficiency (GFP expression) was checked under the fluorescence microscope.

Table 2 – **Protocol for the transfection of eukaryotic cells.** The table gives information on the transfection protocols for the transfection of HEK 293 (control of transgene expression) and for the transfection of DF1 cells (generation of recombinant MVA). \*plasmid DNA extracted from *E. coli* by Miniprep. DNA concentration was measured with Nanodrop.

	<b>Gene expression control</b>	<b>Generation of recombinant MVA</b>
<b>Cells to transfect</b>	HEK 293	DF1 cells
<b>Cell culture plates</b>	24 well cell culture plate	6 well cell culture plate
<b>Amount of DNA* in optiMEM (per well)</b>	800 ng DNA 50 µl optiMEM	1 µg DNA 250 µl optiMEM
<b>Amount of Lipofectamin in optiMEM (per well)</b>	2 µl Lipofectamin2000 50 µl optiMEM	15 µl Lipofectamin2000 250 µl optiMEM

### 2.2.3. Verification of gene transcription in eukaryotic cells

The plasmids p1-4 and p-1 (described in chapter 3.2.1) were transfected into HEK293 cells (chapter 2.2.2.2). The CMV promoter initiated the transcription of CD70, HBc and GFP which were detected as described below (Figure 19).

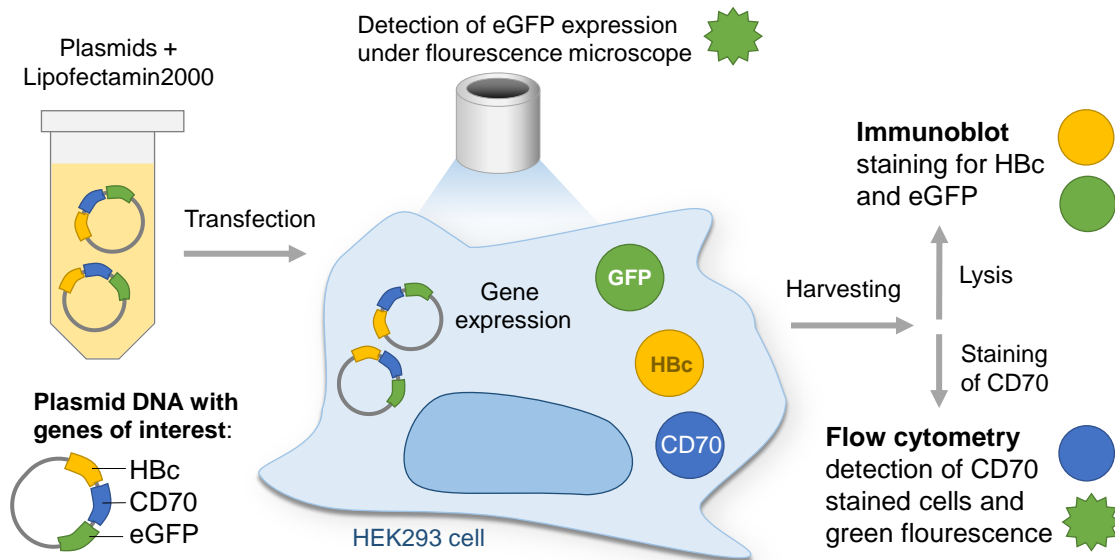


Figure 19 - **Transfection and analysis of HEK293 cells.** After transfection with plasmid DNA, HEK293 cells or cell lysates were analyzed threefold: green fluorescence was detected under the microscope and by flow cytometry. Furthermore, encoded genes were stained and verified by immunoblotting and by acquisition with the flow cytometer.

#### Harvest and preparation of cells for analysis

The transfected cells were incubated for 1 day for flow cytometry analysis and 2 days for immunoblotting. To harvest cells, the medium was removed and cells were incubated with 1 drop Versene (10 min, 37 °C). For flow cytometry analysis the detached cells were given in FACS buffer (+ 3 mM EDTA) and transferred to a 15 ml tube. After centrifugation (1600 rpm, 5 min), the SN was discarded and the cells were resuspended in FACS buffer (+EDTA) and transferred to a 96 well U-bottom plate for staining. For the analysis by western blot the cells were collected in 800 µl PBS, washed once with PBS, resuspended in 100 µl RIPA lysis buffer and stored at -80 °C.

##### 2.2.3.1. Flow cytometry analysis of transfected cells

For general description of staining procedure see chapter 2.2.6.5.

For the staining of transfected HEK293 cells and untransfected controls, FACS buffer +3 mM EDTA was used and the following steps were performed:

- Distribution of 200 µl of cell suspension to each well (U-bottom 96 well plate)
- LIVE/DEAD staining (Near-IR Dead cell Stain Kit in a volume of 50 µl, 30 min)
- three washing steps
- staining with CD70-PE (in 80 µl, 30 min)
- three washing steps
- transfer to FACS tubes in a total volume of 300 µl
- acquisition with flow cytometer (see chapter 2.2.6.5)

### 2.2.3.2. Immunoblotting of proteins

The full procedure of western blotting is depicted schematically in Figure 20.

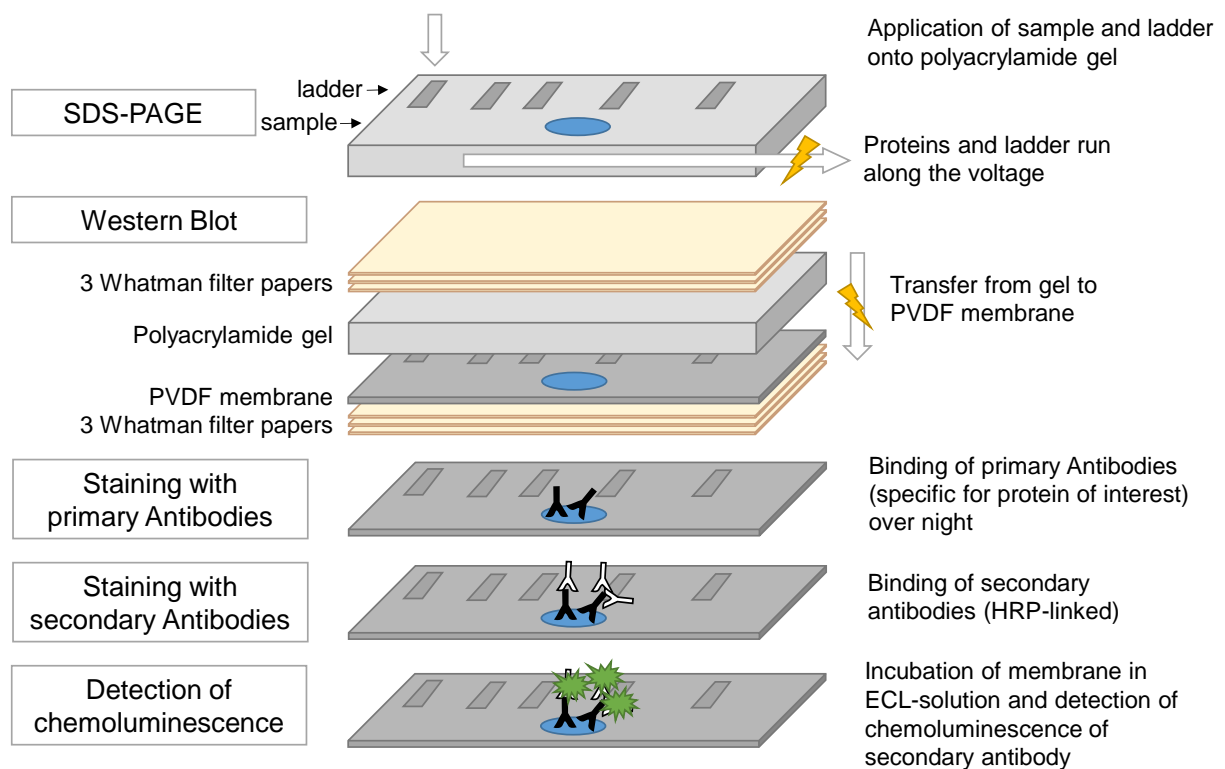


Figure 20 – **Schematic illustration of a western blot protocol.** The proteins were first separated by size in an SDS-PAGE and subsequently transferred to a PVDF membrane by western blot. The proteins were finally stained with primary antibodies (specific for the target protein) and secondary antibodies (specific for primary antibodies and linked to HRP). HRP-linked antibodies were detected after activation in an ECL-solution. *SDS-PAGE*: sodium dodecyl sulfate polyacrylamide gel electrophoresis, *PVDF*: polyvinylidene difluoride, *HRP*: horseradish peroxidase, *ECL*: enhanced chemoluminescence.

## **SDS-PAGE (sodium dodecyl sulfate Polyacrylamide-gel-electrophoresis)**

20 µl of the lysed samples (see chapter 2.2.3) were supplemented with 1/3 of loading buffer (4x concentrated) and heated to 98 °C for 5 min to denature the proteins. Then, the samples were shortly centrifuged and loaded on the polyacrylamide gel that was kindly provided by Florian Wilsch. The running chamber was set up and filled with 1x SDS running buffer before the pre-treated samples and 5 µl of SDS sample buffer were added to the notches of the gel. Each sample and a ladder were applied once for each primary antibody (anti-HBcAg and anti-GFP). The proteins run at 60 V through the stacking gel and at 120 V through the separating gel (two proportions of the polyacrylamide gel). The gel was run until the dye band had reached the bottom after 2,5 h.

## **Western Blot**

Whatmann filter papers were calibrated in western buffer for 15 min. The polyacrylamide gel was carefully eased from the glass plate and washed in water. The PVDF membrane was activated in MeOH for 3 min, rinsed with dH<sub>2</sub>O and calibrated in western buffer for >10 min. The western blot was set up as in Figure 20. 15-20 V were applied for 1 h. After the protein transfer, the PVDF membrane was washed in TBST buffer 3 times for 5 min each.

## **Staining**

The proteins on the PVDF membrane were blocked in blocking buffer for 1 h at RT in a 50 ml tube rolling constantly. Then, the membrane was cut in two for the individual incubation in the primary antibodies rabbit anti-GFP (dilution of 1:5 000 in 5% blocking buffer) and rabbit anti-HBcAg (dilution: 1:10 000). Incubation in primary antibodies was performed in a 50 ml tube filled with 10 ml of the antibody solution and constantly rolling at 4 °C OVN. The next day, the PVDF membranes were washed in TBST buffer 3 times for 5 min.

Then, the PVDF membranes were incubated in the secondary antibody goat anti rabbit (dilution: 1: 10 000) (binding the primary antibody) as above but for only 1 h at RT. Afterwards they were washed in TBST buffer 3 times for 10 min.

Finally, the membranes were incubated in the dark in 2 ml enhanced chemo-luminescence (ECL) solution (1:1) for 3 min to visualize the antibody-protein

complexes by measuring the chemo luminescence of HRP-linked secondary antibodies in an imaging system. Afterwards, the ladder was recorded under normal light without changing the position of the PVDF membrane.

## 2.2.4. Generation of recombinant MVA

### General information and conditions

All work with viruses was performed under sterile conditions (under laminar flow, with sterile pipet tips, ultra sound needle thoroughly disinfected). The respective viruses (rMVA-HBc and rMVA-HBc-CD70) were utilized sequentially and the working space was cleaned according to the Institute's regulations and disinfected using UV light for 20 min before and after every virus to avoid cross-contamination. For general information of cell culturing methods see chapter 2.2.2.

### Production of recombinant MVA

Recombinant MVA was generated by infection of a producer cell line (DF1 cells) with MVAwt (wildtype virus) and simultaneous transfection with a shuttle plasmid (with transgene construct). By homologous recombination the insertion cassette of the shuttle plasmid was integrated into the MVAwt genome (see Figure 21).

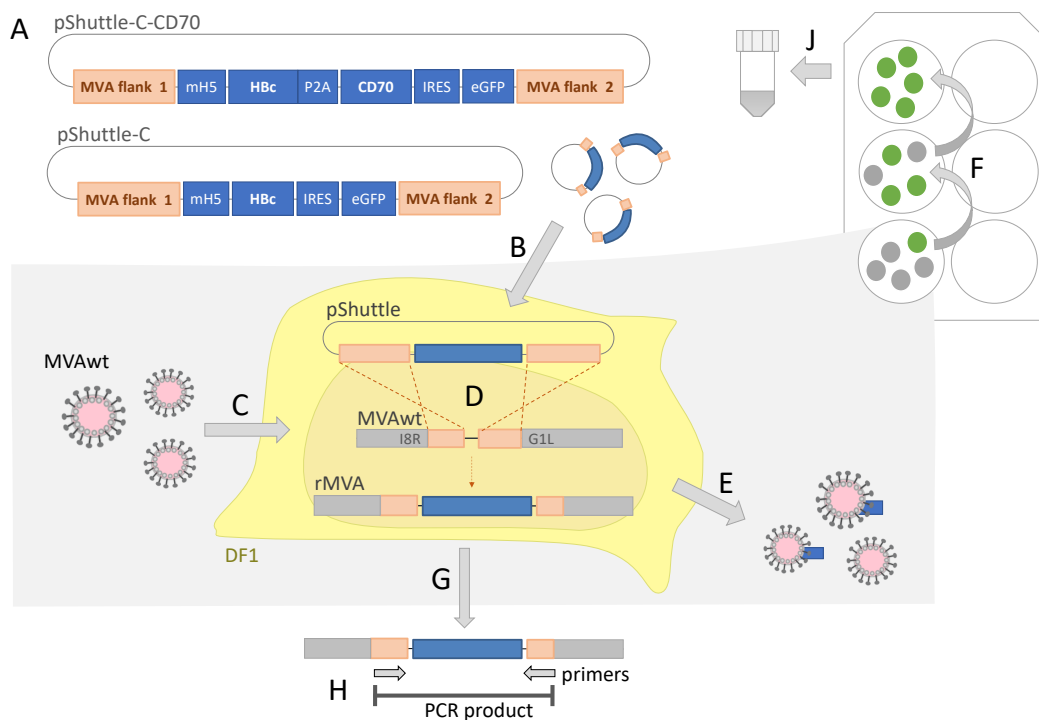


Figure 21 - **Production of rMVA – schematic illustration.** DF1 cells (B), that had been infected with MVAwt viruses (C) were transfected with shuttle vector plasmids (A) in a 6-well plate. Homologous

recombination **(D)** took place in the cells, which thus produced and released rMVA and MVAwt **(E)**. To eliminate the undesired presence of wt virus, several passages in DF1 cells **(F)** were necessary. To prove the purity of rMVA, DNA was extracted from cell samples **(G)** and the insertion cassette was amplified by PCR **(H)** with primers binding in the MVAflank regions (*MVA flank 1 and 2*). As soon as the rMVA was free of MVAwt, a vaccination stock was produced **(J)**. *I8R, G1L*: MVA genes flanking the transgene region.

To obtain a pure and high concentrated vaccination stock of recombinant MVA, remnants of MVAwt were eliminated by selection and dilution steps. If free of MVAwt contamination, the recombinant viruses were amplified and purified.

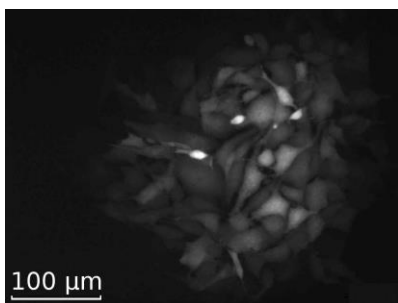
#### **2.2.4.1. From Shuttle plasmid to pure and high concentrated vaccination stock of recombinant MVA**

##### **Homologous recombination in DF1 cells**

On a 6 well plate, 90% confluent DF1 cells were infected with MVAwt: old medium was replaced by 0,5 ml of a virus solution (MOI of 0,01). After 1,5 h of incubation, the cells were transfected (2.2.2.2) with pShuttle-HBc and pShuttle-HBc-CD70, respectively. On the next day, GFP production of transfected cells was detected with the fluorescence microscope and proved the transfection efficiency.

##### **Elimination of MVAwt contamination**

2 days after infection and transfection, some DF1 cells were scraped off the plate with a pipet tip and transferred to a 1,5 ml tube with 30 µl of RPMI-10. The cell material was freeze-thawed 3 times (-80 °C/37 °C) to release the viruses from the cells. Prior to the infection of fresh DF1 cells, this virus solution was 3 times sonicated for 30 s to detach agglutinated viruses. Then, it was diluted 1:10 and 1:100. Fresh 90% confluent DF1 cells on a new 6 well plate were infected with 1 µl of each dilution.



On the next day, green fluorescent cells and cell plaques were visible under the microscope (Figure 22).

Figure 22 – **Plaque of DF1 cells which are infected with rMVA.** The green fluorescence (GFP) was recorded with a fluorescence microscope (Magnification: 20x). Each plaque originated from a single virus, that spread the infection to the neighboring cells.

In the well with the highest infection dilution one green plaque was picked: the plaque was marked on the exterior of the plate bottom under the fluorescence microscope

and carefully scratched off with a pipet tip. With this material, another passage of freeze-thawing, sonicating, diluting and infection was performed.

After about 8 passages, viral DNA was isolated from cell lysates by a phenol/chlorophorm extraction (see next paragraph). A control PCR was performed to exclude contamination with MVAwt. The gel electrophoresis resulted in a second characteristic band in case of the presence of MVAwt (see Figure 23). If so, a few more passages were performed prior to a further control PCR.

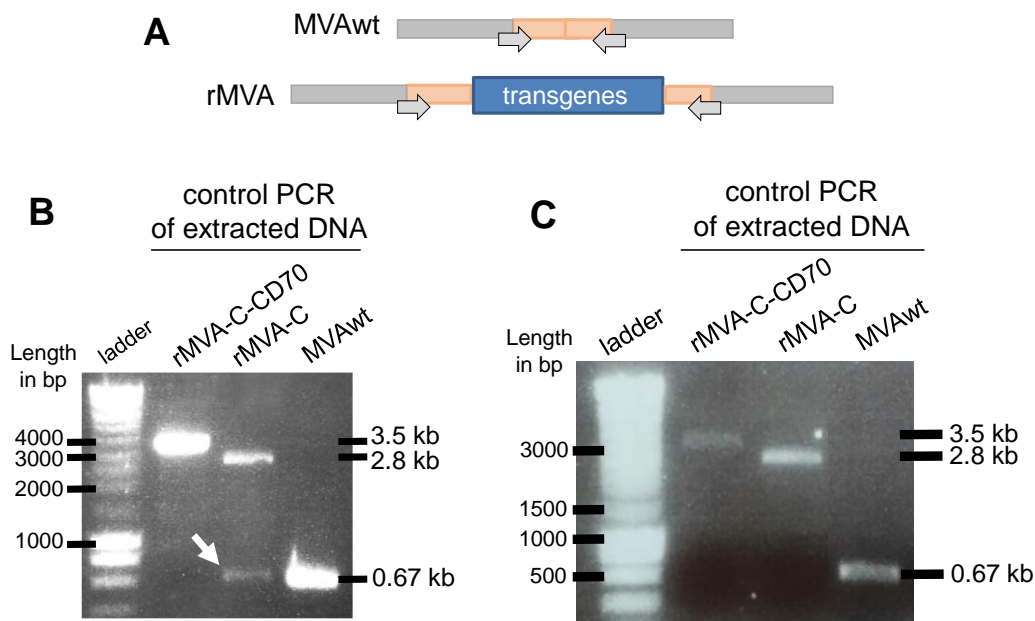


Figure 23 – **Control PCR for the exclusion of MVAwt contamination.** (A) Contamination with MVAwt was excluded by a PCR (primers: *grey arrows*), that amplified the region between the MVA flanks (red). rMVA with transgenes resulted in a longer PCR product. (B, C) Agarose gel electrophoresis of PCR products. (B) The sample of rMVA-HBc is still contaminated with a small amount of MVAwt (*white arrow*) while rMVA-HBc-CD70 is already free of contamination. (C) A few passages on DF1 cells later, there was only one band visible at the expected size for each sample: Both rMVA were free of wildtype contamination and ready for amplification.

### Phenol/chlorophorm Extraction prior to control PCR

Phenol/chlorophorm extraction was performed to isolate DNA from cultured DF1 cells. 50 µl of 3 times freeze-thawed cells were supplemented with: 400 µl TE buffer (pH 8,0), 50 µl TEN buffer (10x), 50 µg Proteinase K and 23 µl SDS to set free the DNA and to make the solution alkaline. Then it was incubated at 56 °C for 2-4 h shaking at 550 rpm. Afterwards 600 µl phenol/chlorophorm/isomyalalcohol was added and mixed in thoroughly. During a centrifugation at 1300 rpm, 10 min at RT the solution separated

into two phases. Proteins accumulated in the lower phase while DNA concentrated in the upper aqueous phase. This upper phase was pipetted in a fresh 1,5 ml tube and filled up with the 2-fold volume of EtOH to precipitate the DNA. After an incubation of 30 min at -80 °C the sample was centrifuged at 1300 rpm, 15 min, 4 °C. The SN was discarded and the pellet washed with 250 µl 75% EtOH. After repeated centrifugation the SN was discarded and the pellet was dried for several minutes. It was resuspended in 50 µl EB buffer and the DNA concentration and purity was measured by using Nanodrop.

### **Amplification of rMVA for vaccination stock**

After MVAwt contamination was excluded, a pure and high concentrated rMVA vaccination virus stock was produced. For information of cell culturing methods see chapter 2.2.2.

#### Pre-culture:

100% confluent DF1 cells were infected with 1 µl of viral solution (freeze-thawed infected DF1 cells) in a 175 cm<sup>2</sup> cell culture flask. When 90 % of the cells showed a cytopathic effect (CPE), the cells were harvested in their medium using a cell scraper. The medium and cells was freeze-thawed three times (-80 °C/37 °C) and RPMI-10 was added up to a total volume of 50 ml.

#### Culture for high scale amplification:

In 10 225 cm<sup>2</sup> cell culture flasks with DF1 cells at 90-100% confluency, the medium was replaced by 5 ml of the pre-culture. After 1 h of incubation 15 ml RPMI-10 were added. After no more than three days of incubation, when about 90% of the cells showed a CPE, the cells were harvested in their medium. After centrifugation, the pellets were resuspended and pooled in 30 ml Tris (pH9; 10 mM). The cell suspension was stored at -80 °C until purification.

### **Purification**

Tris (pH9; 10 mM) was used for the purification protocol, as illustrated in Figure 24.

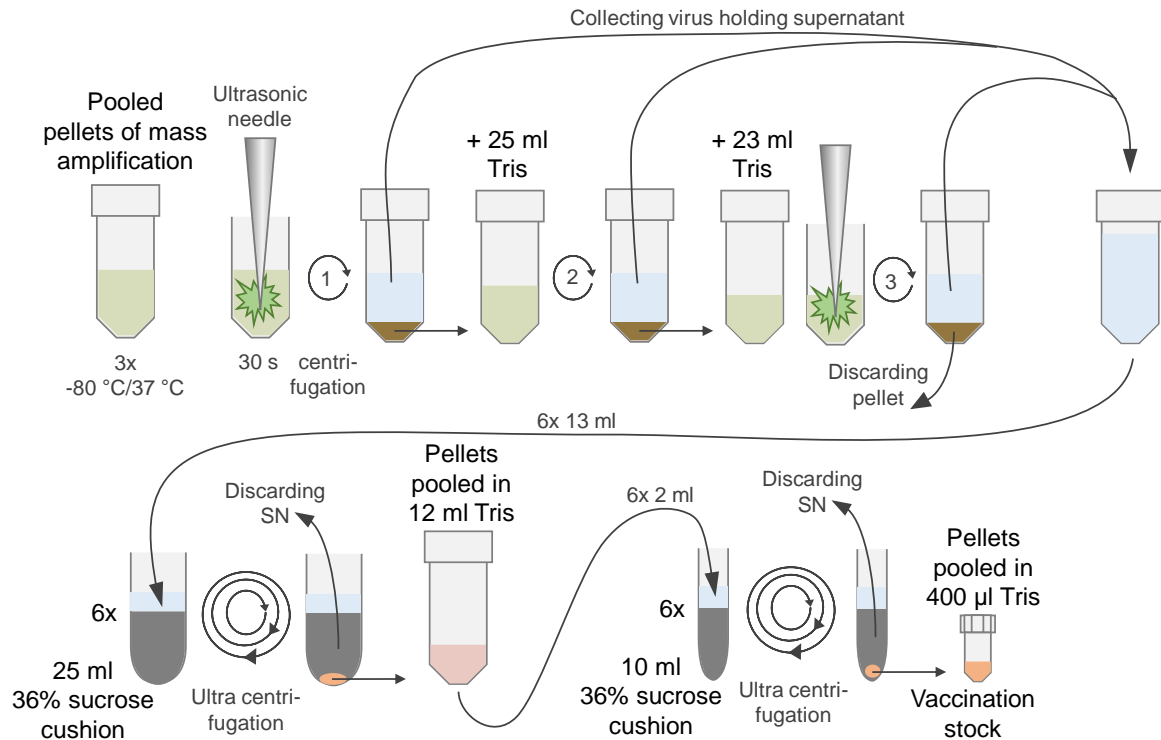


Figure 24 - **Purification of MVA virus.** Normal centrifugation was performed at 4000 rpm, 4°C for 5 min each, to separate the MVA particles from the pellets and collect them in the SNs. First ultra-centrifugation was performed at 13 500 rpm, 4° for 90 min on a 36% sucrose cushion (13 ml of MVA suspension on 25 ml of Sucrose (Tris (pH9; 10 mM) + 36% sucrose, autoclaved)) using UltraClear tubes and the Beckman SW32 rotor and buckets. MVA holding pellets were resuspended and pooled in 12 ml Tris (pH9; 10 mM). The second ultra-centrifugation was performed with 2 ml MVA suspension on 10 ml 36% sucrose using UltraClear tubes and the Beckman SW41 rotor and buckets. After last centrifugation, the SN was discarded and the pellets were drained off and dried upside down for 10 min and finally pooled in a total volume of 400 µl Tris (pH9; 10 mM) and stored in a cryo vial at -80 °C.

## Titer determination

The titer determination was carried out on confluent DF1 cells on a 96 well flat bottom plate in a total volume of 200 µl RPMI-2. From the respective MVA stocks, two independent dilution series from  $10^{-8}$  to  $10^{-13}$  were prepared after thawing the stocks on ice and sonicating them. 100 µl of the dilutions were added to eight wells each, plus eight wells negative control (only RPMI-2). After one week of incubation the cells were checked for CPE and GFP expression using the fluorescent microscope and light microscope. The titer of the MVA stock was calculated with the following equation:

$$y = \left( 10^{a-0,5-\left(\frac{xa}{16}\right)+\left(\frac{xb}{16}\right)+\left(\frac{xc}{16}\right)} \right) * 10$$

a represents the dilution factor that led to CPE/GFP expression in all wells (e.g.  $10^{-9}$ ; a=9) and xa, xb and xc stands for the number of infected wells in the next higher solutions (Mayr 1974).

## **Storage and handling of vaccination stock**

Storage conditions of purified vaccination stock was  $-80\text{ }^{\circ}\text{C}$  in a cyro vial. For the preparation of vaccination mixes it was thawed and kept on ice. Before opening it under the laminar flow the vial was carefully disinfected on the outside. Clotting of viral particles was prevented by sonicating (3 times 30 s) before pipetting.

## **2.2.5. Treatment of mice**

### **2.2.5.1. Mouse Strains**

In this study, C57BL6, DNNGR1 deficient and HBVtg mice were used for vaccination experiments with HBc protein and/or (recombinant) MVA.

C57BL/6 mice were female and at the age of 8 to 11 weeks at the time of vaccination.

Male and female DNNGR1-deficient mice were used at the age of 8 to 12 weeks at first vaccination. Clec9a codes for DNNGR1, a cell membrane bound receptor of CD8a+ DC. It recognizes intracellular proteins that are released by necrotic cells and its loss-of-function impairs cross-presentation and CD8 T-cell activation (Zelenay et al. 2012). By comparing immune responses to those of C57BL/6 mice after MVA immunization, the role of cross-presentation in MVA immunization was estimated.

HBVtg1.3 mice, which were used for vaccination experiments are a mouse model for chronic HBV infection (Guidotti et al. 1995): HBVtg1.3 mice carry a greater-than-genome length construct of the HBV genome that reaches from the Enhancer I gene 1.3 times around the circular genome until the polyadenylation signal. HBV is replicated in liver and kidney and infectious particles and antigens HBs and HBe are released into the blood while no liver disease nor immunity against HBV antigens can be observed. The mice were derived from in-house breeding under specific pathogen-free conditions following institutional guidelines. Female and male mice at the age of 9-22 weeks were used for vaccination experiments. Vaccination groups were matched for age, sex and primarily for HBeAg titers.

## Ethical statement

Animal experiments were conducted in strict accordance with the regulations of the German Society for Laboratory Animal Science (GV-SOLAS) and the health laws of the Federation of European Laboratory Animal Science Associations (FELASA). Experiments were approved by the local Animal Care and Use Committee of Upper Bavaria (Permit No. 55.2-1-54-2532-103-12). Mice were kept in a specific pathogen-free facility under appropriate biosafety level following institutional guidelines.

## Vaccination of mice

The vaccination was administered either intraperitoneally (for MVA vaccinations) or subcutaneously in the neck or gluteal region (for protein vaccinations). In both cases mice were manually immobilized and no anesthesia was used.

The composition of the protein prime is listed in Table 3. The MVA vaccine was administered in a volume of 250  $\mu$ l PBS with  $10^8$  IU of recombinant or wildtype MVA per vaccination dose.

Table 3 - **Composition of protein-prime vaccination.**

Protein-prime vaccination	per mouse
PCEP	25 $\mu$ g
CpG	32 $\mu$ g
HBcAg (not for control group)	30 $\mu$ g
sterile PBS	up to a volume of 50 $\mu$ l

## Blood sample collection from the facial vein

To estimate serum markers during the vaccination phase, blood samples were collected from the facial vein. A lancet was used to incise vessel and blood drops were collected in serum vials, that were used for isolation of blood serum.

### 2.2.6. Ex vivo immunological analysis

#### Preparation of mice

To investigate the antigen-specific immune response, mice were sacrificed by either using CO<sub>2</sub> or Isofluran. For analysis, blood serum, spleen, lymph nodes and liver were taken.

## **Collection of blood serum**

For isolation of blood serum, blood was taken from the vena cava and from the heart cavities and collected in serum vials. To isolate the serum, the vials were centrifuged at 12 000 rpm, RT for 15 min. Then, the sera were transferred to new Eppendorf vials, Alanin aminotransferase (ALT) was measured (next chapter) and the remaining serum was stored at -20 °C for later analysis.

### **2.2.6.1. Serological analysis**

ALT was measured from fresh, unfrozen serum. 32 µl of a dilution (1:3; serum:PBS) were applied to the appropriate test strip and measured with Reflovet. HBc-Ag, HBsAg anti-HBs and anti-HBc were quantified by Natalie Röder using AxSYM assays after thawing.

### **2.2.6.2. Preparation of Splenocytes**

Spleens were pushed through a 100 µm cell strainer, which was rinsed with RPMI-1 afterwards. After centrifugation (1500 rpm, 4 °C, 5 min), the pellets were resuspended in 3 ml TAC medium for lysis of erythrocytes (2 min, 37 °C, shaking). Straight afterwards, the cells were put on ice and washed with 40 ml cold RPMI-1 and centrifuged as above. The pellets were resuspended in 20 ml of RPMI-10 for counting. Cells were kept on ice until analysis.

### **2.2.6.3. Preparation of liver associated lymphocytes (LAL)**

Livers were perfused with cold PBS. With a plunger, the tissue was pushed through a 100 µm cellstrainer, which was carefully washed with ice cold RPMI-1 afterwards to collect all liver cells. In a total volume of 40 ml, the cells were centrifuged (1500 rpm, 4 °C, 10 min). The pellet was resuspended in 10 ml RPMI-10 + 0,05 collagenase and incubated at 37 °C for 30 min (vortexing every 5-10 min). After centrifugation (1500 rpm, RT, 10 min), the SN was pipetted off carefully and discarded. The separation of LAL, erythrocytes and hepatocytes from the slimy pellet was obtained through a Percoll gradient (Figure 25). Then, the cells were supplemented to 40 ml with RPMI-1, and centrifuged (1500 rpm, RT, 10 min). The pellet was resuspended in 5 ml RPMI-10 for counting. Cells were kept on ice until analysis.

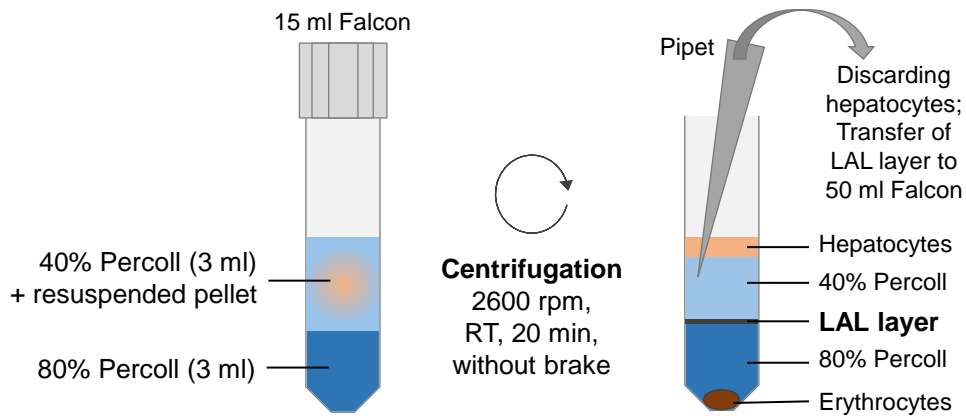


Figure 25 – **Isolation of liver associated lymphocytes (LAL) with a Percoll gradient separation.** The cell pellet was resuspended in 3 ml of 40% Percoll and layered on a 80% Percoll layer. After centrifugation, the hepatocytes were carefully pipetted off and the LAL layer was completely transferred to a new 50 ml Falcon.

#### 2.2.6.4. Counting cells

To count cells manually, they were usually diluted 1:10 with 90  $\mu$ l Tuerks solution. The cells were counted under a microscope using a hemocytometer. Three quadrats were counted and the number of cells/ml calculated like this:

$$\frac{\text{cells}}{\text{ml}} = (\text{counted cells} \times \text{dilution factor (e.g. 10)} \times 10^4) / 3$$

For counting with the VI-CELL counter the samples were diluted 1:10 with 9 parts PBS and automatically counted according to the user manual.

#### 2.2.6.5. Analysis of cells by flow cytometry

The specificity and functionality of T-cells was estimated by staining and analysis of isolated cells from the spleen and liver of mice. For detection of HBV core-specific cells, splenocytes or LAL (liver associated lymphocytes) were stained with C93 tetramer. To assess the functionality of antigen-specific T cells, the cells were stimulated with peptides (e.g. the CD8 T-cell epitopes C<sub>93</sub> and B8R) and cytokine production was detected by intracellular staining.

### General information on staining protocols

Except for the EMA staining the whole staining and storage of cells was performed on ice and in the dark. Samples for a single stain (live/dead staining plus respective

fluorescent markers attached to surface protein) of every dye have been included for compensation.

Elements of one washing step:

- (re)suspension of pellet in 200 µl FACS buffer
- centrifugation (1400 rpm, 4 °C, 2 min)
- removal of the SN
- resuspension of cell pellets (in FACS buffer or according to the protocol)

### Stimulation of isolated splenocytes and LAL

On the day of isolation,  $4 \times 10^6$  cells/well were distributed to a U-bottom 96 well plate and incubated (16 h, 37 °C, 5% CO<sub>2</sub>) in the respective peptide stimulation mix (Table 4). One sample per mouse and cell type was left either unstimulated (only BFA) or was stimulated with OVA (ovalbumin antigen) as negative control. Stimulation was terminated by cooling the cells to 4 °C.

Table 4 - Composition of peptide stimulation mix.

Component		Concentration
Peptide (only one of the following)	B8R	0,25 µg/well
	C <sub>93</sub>	0,25 µg/well
	HBc 15mer peptide pool	0,36 µg/well
Brefeldin A		10 µg/ml
RPMI-10		-
= total volume: 210 µl/well		

### Intracellular Staining (ICS)

After stimulation with peptides, cells were stained with an intracellular cytokine staining. First, dead cells were stained with EMA (see Table 5). After two washing steps, cells were stained for surface markers CD8 and CD4. After three washing steps, cells were permeabilized for 20 min using 100 µl/well Cytofix/Cytoperm Kit. After two washing steps with Perm/Wash solution instead of FACS buffer and centrifugation at 1600 rpm, the cells were stained for intracellular cytokines (IFN $\gamma$ , TNF, IL-2; see Table 5). After three washing steps with Perm/Wash, the cells were transferred to FACS

tubes in a total volume of 300  $\mu$ l FACS buffer for acquisition. Concentration of the staining dyes are given in chapter 2.1.10.

Table 5 - **ICS staining panels A and B**. The table gives information on the three staining steps: LIVE/DEAD staining, surface staining and intracellular staining. \*IL2 was not included in staining of BL6-r1-experiment.

Staining panels	A (for DNGR1 -/- experiment chapter 3.1)	B	Volume/well, incubation buffer	Incubation conditions
<b>Target proteins</b>				
<i>LIVE/DEAD staining</i>			100 $\mu$ l, FACS buffer	20 min on ice in bright light
	EMA	EMA		
<i>Surface staining</i>			50 $\mu$ l, FACS buffer	30 min on ice in the dark
CD8	CD8- PerCPCy5.5	CD8-PacB		
CD4	CD4-PacB	CD4-PE		
<i>Intracellular staining</i>			50 $\mu$ l, FACS buffer or P/W buffer	30 min on ice in the dark
IFN $\gamma$	IFN- $\gamma$ -APC	IFN- $\gamma$ -FITC		
TNF	TNF- $\alpha$ -PECy7	TNF- $\alpha$ -PeCy7		
IL-2	IL2-PE	IL2-APC*		

### Tetramer staining

Splenocytes and LAL were stained with C<sub>93</sub> tetramer to detect HBV core-specific CD8 T cells. The tetramer binds specifically to C<sub>93</sub>-specific CD8 T cells and is equipped with a strep-tag that can be bound by Streptactin-PE for detection by flow cytometry.

The staining was performed on a U-bottom 96 well plate with 4x10<sup>6</sup> fresh, unstimulated cells/well. For each mouse, one sample was dyed with C<sub>93</sub> tetramer and streptactin-PE and one control sample with streptactin-PE only. Except for the samples for compensation, all samples were dyed with CD8-PB and a live/dead stain.

### Staining procedure:

- LIVE/DEAD stain with either EMA (see ICS protocol above) or Near-IR Dead Cell Stain Kit (in 50  $\mu$ l/well in FACS buffer for 30 min)
- Two washing steps
- Staining with C<sub>93</sub> tetramer and/or Streptactin-PE (in 50  $\mu$ l/well in FACS buffer for 30 min)
- Three washing steps
- Staining with CD8-PB in 50  $\mu$ l/well in FACS buffer for 30 min
- Three washing steps
- Transfer to FACS tubes in 300  $\mu$ l FACS buffer for acquisition

### Flow cytometry data acquisition

Samples were acquired within few hours after staining with a flow cytometer using the FACSDiva software. PMT voltages were adjusted for all parameters by setting the mean autofluorescence values of live/dead stained cells to approximately  $10^2$  for all fluorochrome channels that were used.

### Analysis of flow cytometry data

Flow cytometry data was analyzed using Flow Jo software. Gating was performed on compensated samples and gates were identical for individual mice and cell types (synchronal group gates). Representative gating strategies for tetramer staining and intracellular staining are shown in Figure 25 and Figure 27. For the evaluation of reacting CD4<sup>+</sup> T cells, gating was performed analogue to Figure 27 with gating for CD4<sup>+</sup> cells instead of CD8<sup>+</sup> cells.

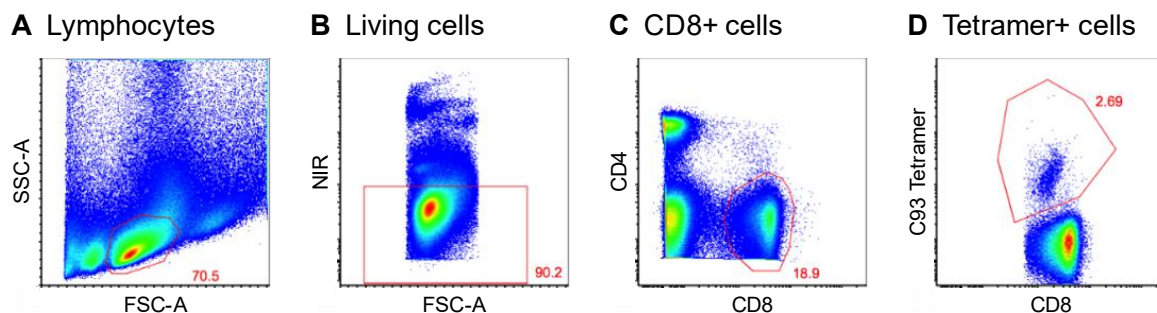


Figure 26 - **Representative gating strategy for C<sub>93</sub> tetramer staining assay.** Lymphocytes were gated on compensated samples based on FSC versus SSC plot (**A**). Dead cells were excluded by NIR staining (**B**) and living cells were gated for CD8<sup>+</sup> cells (**C**) and finally for tetramer<sup>+</sup> cells (**D**).

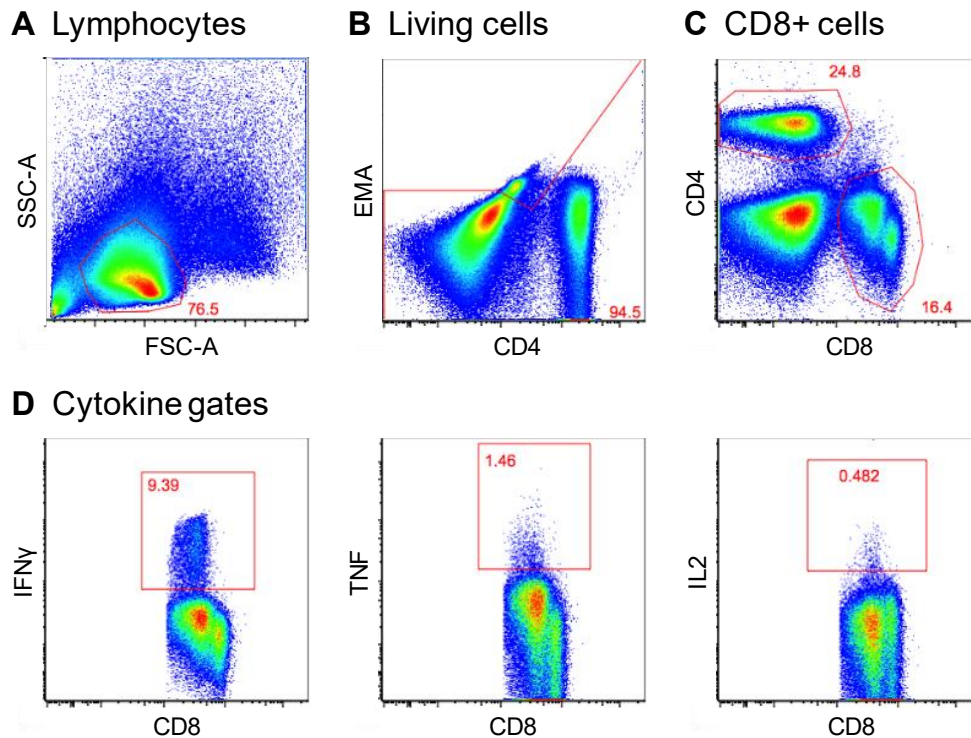


Figure 27 - **Representative gating strategy for Intracellular Cytokine Staining assay.** After compensation, cells were gated for lymphocytes based on FSC versus SSC plot (A). After gating for living cells (B) CD8+ cells were included (C) to gate for the individual cytokines (D). For the detection of single cells that expressed more than one cytokine, Boolean gates (combination of gates) were created.

## 2.2.7. Immunohistochemistry

One slice of perfused liver tissue was given into 4% formalin solution for immunohistochemistry. Fixation of samples and histological staining was performed by members of the group of Mathias Heikenwalder (Institute of Virology, Helmholtz Zentrum Munchen). Histological analysis with 2  $\mu$ m formalin-fixed, paraffin-embedded (FFPE) sections was performed with Bond Polymer Refine Detection Kit (Leica) on BondMax immunohistochemical staining system (Leica). Sections were stained for HBcAg, CD3 and CD3+Ki67, nuclei were stained with hematoxylin.

### Analysis of liver histology

For quantification of stainings, whole slides were scanned using a SCN400 slide scanner (Leica) and scored manually: in 6-10 randomly chosen areas of 0.5 mm<sup>2</sup> on CD3-stained paraffin sections, cells (CD3+ or HBc+) were counted and merged for further statistical analysis. For estimation of T-cell proliferation within the liver, cell

accumulations of  $\geq 3$  CD3+ cells (or  $\geq 6$  CD3+ cells) were counted in the whole liver section and normalized to the size of the individual section (=cell accumulations/mm<sup>2</sup>).

### **2.2.8. Statistical analysis and visualization**

Graphs were created using Graph Pad Prism (with background (=unstimulated or unstained cells respectively) subtracted samples). All statistical analyses were performed using Graph Pad Prism software. Results are pictured as mean (SD).

To compare 3 groups, a one-way ANOVA was used with – if significant – a student's t-test as post hoc test. Differences between two groups (if >2 mice/group) were analyzed for statistical significance using two-tailed student's t-test. The confidence level was 95%. p-values < 0.05 were considered significant.

## 3. Results

### 3.1. Immune response to rMVA-mediated antigens is not exclusively dependent on cross-presentation

MVA induces apoptosis in infected cells and immune responses to MVA antigens and transgenes of recombinant MVA are partly dependent on direct presentation and in parts on cross presentation (Gasteiger et al. 2007). The extent of either presentation way depends on various factors and is not well predictable as ambivalent findings exist in the available literature. CD70 can only perform its co-stimulation function if it is processed by the direct presentation pathway and thus is presented intactly on the cell's surfaces (see Figure 9).

DNGR1 was identified as a receptor which specifically mediates cross-priming of T cells during vaccinia virus infection in mice (Iborra et al. 2012). In DNGR1 deficient mice, cross-presentation and cross-priming are impaired (Durant et al. 2014). To assess the role of cross-presentation in MVA vaccination, immune responses of DNGR1 deficient mice were compared to those of C57/Bl6 mice (C57Bl/6 mice).

#### Immunization of DNGR1 knockout and C57Bl/6 mice with rMVA-core

DNGR1 deficient mice and C57Bl/6 mice were vaccinated with rMVA-core. MVA-specific and HBV core-specific CD8 T-cell responses were analyzed after 1 and 2 vaccinations with MVA-core (Figure 28).

After two immunizations, the proportion of MVA<sub>B8R</sub>-specific IFN $\gamma$ -producing CD8<sup>+</sup> splenocytes was equal in wt and in DNGR1 knockout mice, indicating that cross-presentation has a minor impact in the present setting. Unexpectedly after one immunization, the proportion of MVA<sub>B8R</sub>-specific IFN $\gamma$ -producing CD8 T cells was significantly higher in DNGR1 deficient mice than in C57Bl/6 mice (3,5 $\pm$ 0.3% in DNGR1 deficient mice versus 1,3 $\pm$ 0.1% in C57Bl/6 mice). The unvaccinated mice had no Hbc- or MVA-specific T-cell response as expected.

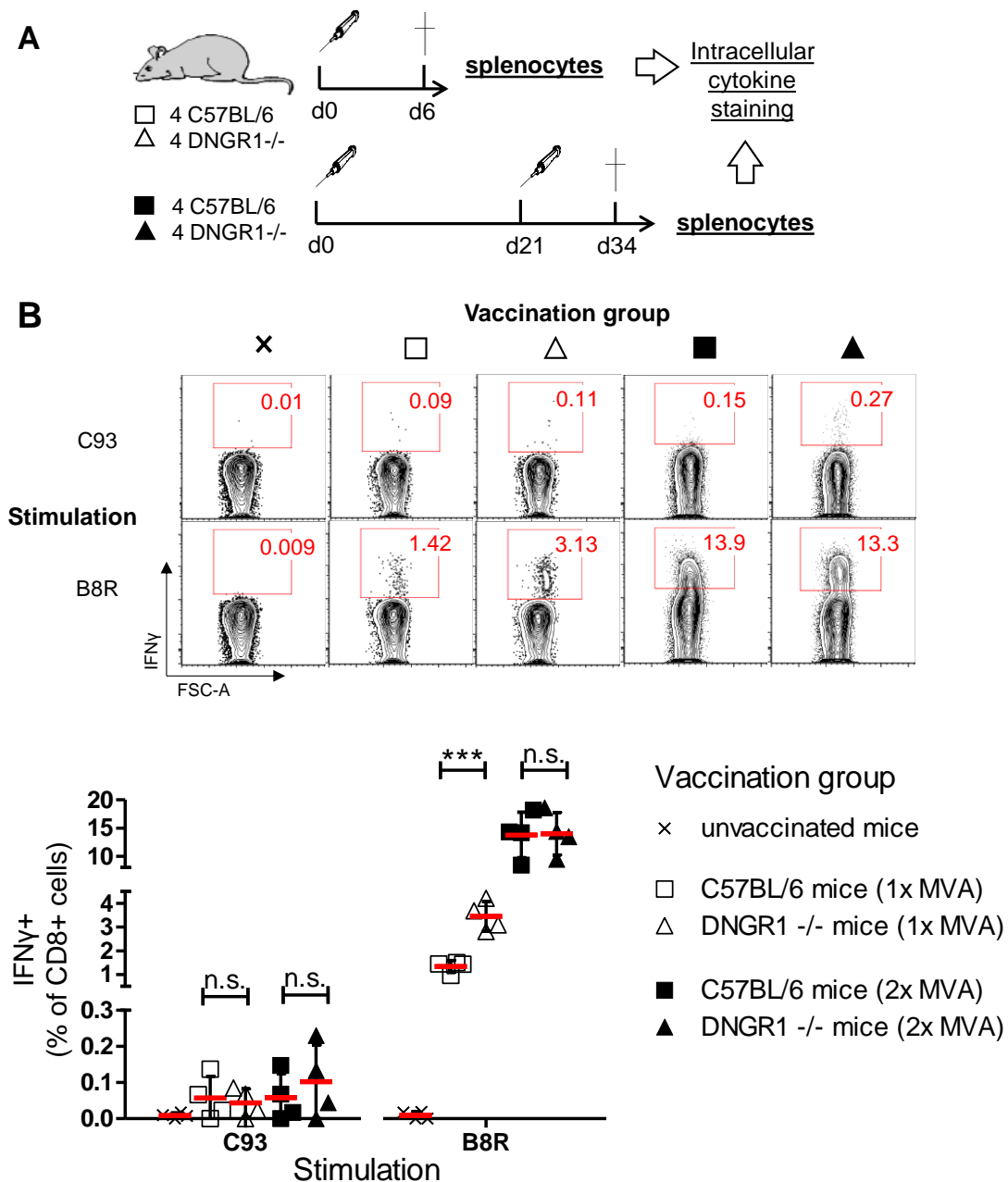


Figure 28 – MVA-specific and HBV core-specific CD8 T-cell responses of DNDR1 deficient and C57BL/6 mice after vaccination with rMVA-core. (A) DNDR1 deficient mice and C57BL/6 mice were vaccinated 1 or 2 times with rMVA-core (single vaccination dose:  $10^8$  IU rMVA-core i.p.). As negative control, 4 DNDR1 deficient mice remained unvaccinated. 6 days (if once vaccinated) or 12 days (if twice vaccinated) after last immunization, splenocytes were isolated and stimulated with HBC- (C<sub>93</sub>) and MVA-derived (B8R) epitopes and analyzed for IFN $\gamma$ -expression of CD8 T cells by intracellular staining (n=4 mice/group). (B) IFN $\gamma$ -positive cells of total CD8 T cells isolated from the spleen after stimulation with C<sub>93</sub> (HBc) or B8R (MVA). Contour plots show representative data of mice that were vaccinated twice. Diagram shows all mice of both vaccination schemes. Statistical analysis: one-way ANOVA and subsequent student's t-test. Red bars: mean.

In general, the HBV core-specific CD8 T-cell response was weaker in comparison to the response to the high immunogenic MVA<sub>B8R</sub> epitope in all vaccinated mice, which was expected. With a maximum of 0.23% of HBV core-specific CD8 T cells, the proportions of HBV core-specific T cells was very low in all vaccination groups in comparison to the values which were observed after protein-prime/MVA-boost vaccinations. This was expected, as it was shown previously, that HBc-protein-prime/MVA-boost vaccination with MVA-core is far more effective in eliciting HBV core-specific CD8 T-cell responses than one or two vaccinations with MVA-core alone (Backes et al. 2016). Between wt and DNGR1 deficient mice, no significant difference of the HBV core-specific CD8 T-cell responses was observed after one or after two immunizations supporting the finding that cross presentation has a minor impact.

The results show that DNGR1 deficient mice vaccinated with rMVA-core are not impaired in the generation of MVA- and HBV core-specific T-cell responses. This observation suggests that the transgenes (including CD70) are presented intactly on the cell surface and justifies the approach to co-stimulate and re-activate the HBc-transgene-specific immune response by CD70 through vaccination with rMVA-HBc-CD70.

### 3.2. Generation of recombinant MVA vectors

To estimate the effect of CD70 co-expression on induction of HBV core-specific T-cell responses after protein prime and MVA-boost vaccination of mice, two recombinant MVA vectors (rMVA) were designed and generated: MVA containing the transgene HBc only (MVA-HBc) and MVA containing the transgenes HBc and human CD70 (MVA-HBc-CD70) (Figure 29).

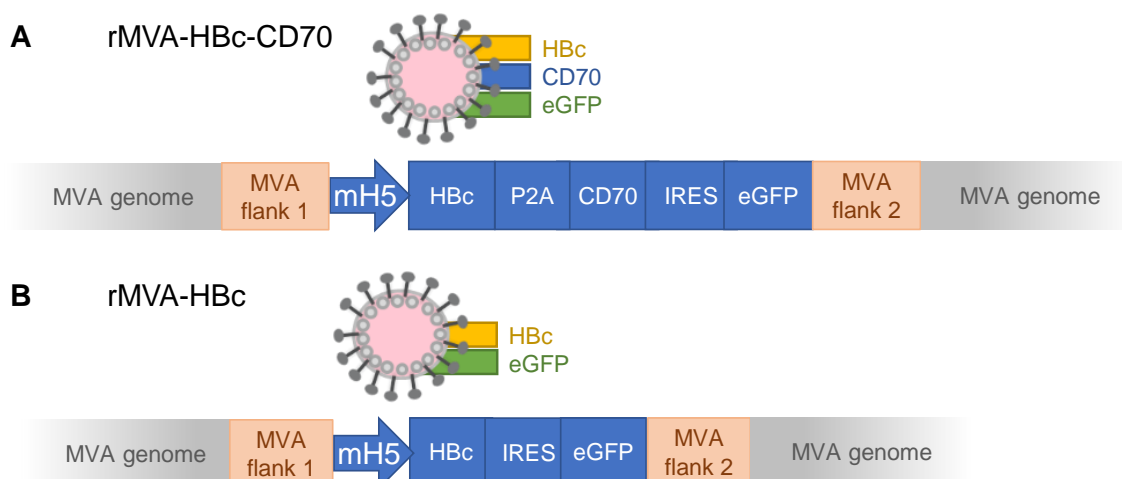


Figure 29 – **Gene expression cassettes of rMVA-HBc-CD70 and rMVA-HBc.** rMVA-HBc-CD70 **(A)** and rMVA-HBc **(B)** constructs. *MVA flank 1* and *flank 2*: MVA-DNA sequences to target insertion of transgenes between the essential I8R and G1L gene sites. *mH5*: mH5 promoter. *IRES*: internal ribosomal entry site. *P2A*: cleavage site. *eGFP*: sequence for enhanced green fluorescing protein.

eGFP was inserted as reporter transgene in both vectors. The mH5 promoter was used for strong and predominantly early transcription of transgenes (Wang et al. 2010). In addition the following components were used: the cleavage site P2A allowing equal expression levels of HBc and CD70 and the internal ribosomal entry site (IRES) in order to attach eGFP to the construct.

Finally, the transgene constructs were cloned into shuttle plasmids and inserted into MVAwT by homologous recombination resulting in rMVA.

### **3.2.1. Cloning of rMVA-HBc-CD70 and rMVA-HBc**

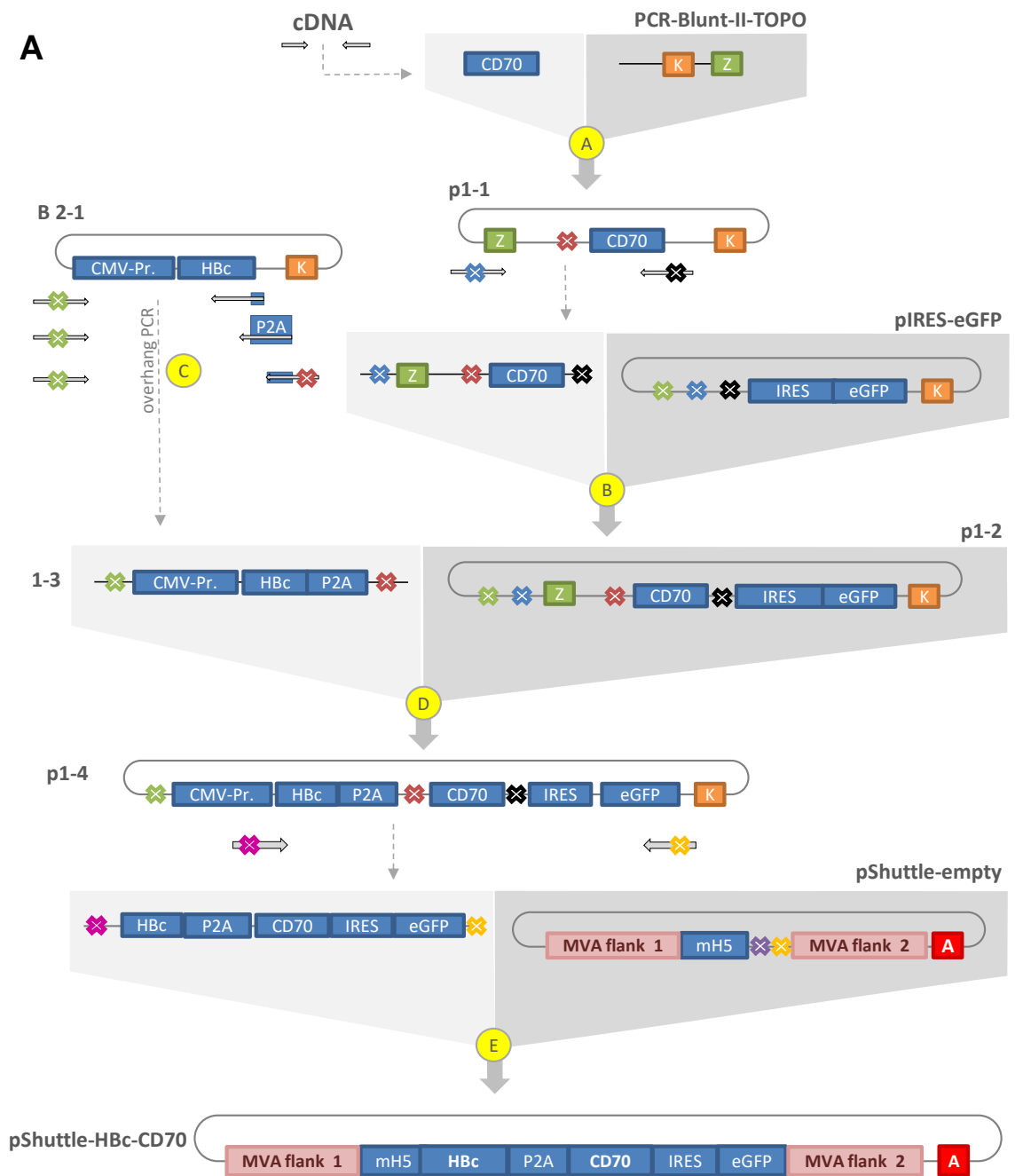
The single cloning steps for the generation of the shuttle plasmids pShuttle-HBc-CD70 and pShuttle-HBc were performed as described in the cloning strategy (Figure 30). For technical details of the cloning reactions (indicated by yellow letters in Figure 30) please refer to Table 1.

Both constructs HBc-CD70-eGFP (plasmid p1-4) and HBc-eGFP (plasmid p2-1) were proofed for correctness prior to the transfer into the shuttle plasmids:

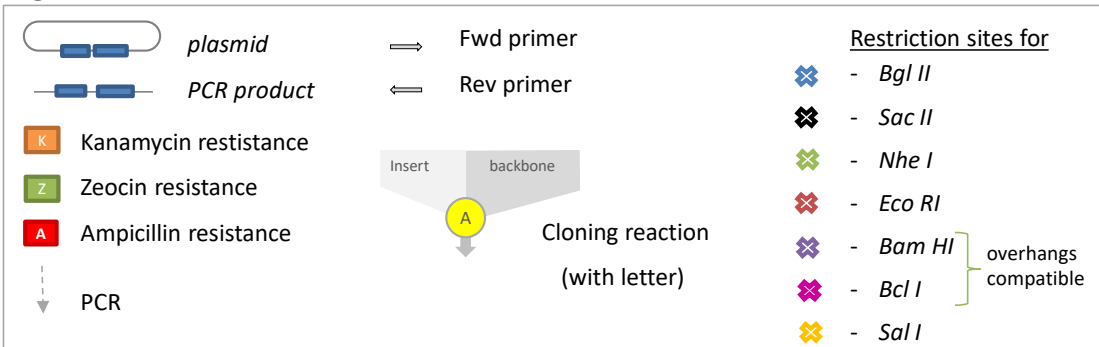
- Control PCRs of plasmids p1-4 and p2-1 were performed to verify the presence of the insert of the expected size (Figure 31 A and B).
- Integrity of HBc and CD70 genes was confirmed by sequence analysis performed by GATC-biotech (refer to Appendices 3-5 for aligned sequences)
- The plasmids p1-4 and p2-1 were transfected into eukaryotic cells to verify the correct expression of the transgenes HBc, CD70 and eGFP genes by FACS analysis (refer to section 3.2.2).

Then, the constructs were cloned into empty shuttle plasmids (pShuttle-empty) to obtain the plasmids pShuttle-HBc-CD70 and pShuttle-HBc. A control digest was performed for both shuttle plasmids (Figure 31 C and D).

The shuttle plasmids pShuttle-HBc-CD70 and pShuttle-HBc were then used for insertion of the transgenes into MVAwT by homologous recombination.



**Legend**



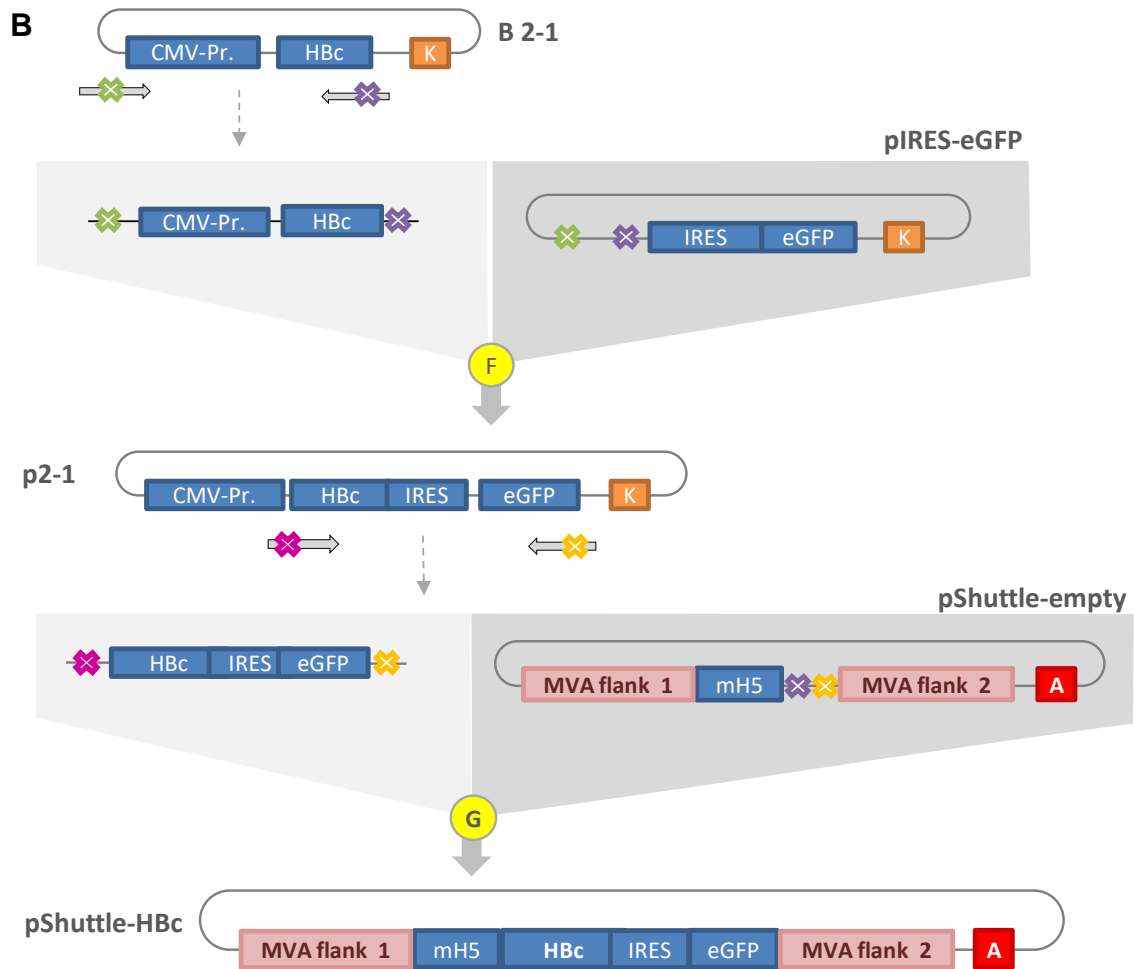


Figure 30 – **Cloning strategy for pShuttle-HBc-CD70 (A) and pShuttle-HBc (B)**. Both plasmids were generated in several cloning steps (cloning reactions indicated by yellow letters with technical details in Table 1). Cloning was performed either by blunt-end-cloning or by cloning by digestion and ligation. *cDNA*: complementary DNA; *HBc*: HBV core DNA sequence; *CMV-Pr.*: CMV-Promoter; *IRES*: DNA sequence of internal ribosomal entry site; *eGFP*: DNA sequence of enhanced fluorescent protein;  *fwd.*: forward;  *rev.*: reverse; *P2A*: sequence of P2A cleavage site; *MVA flank 1 and 2*: MVA sequences.

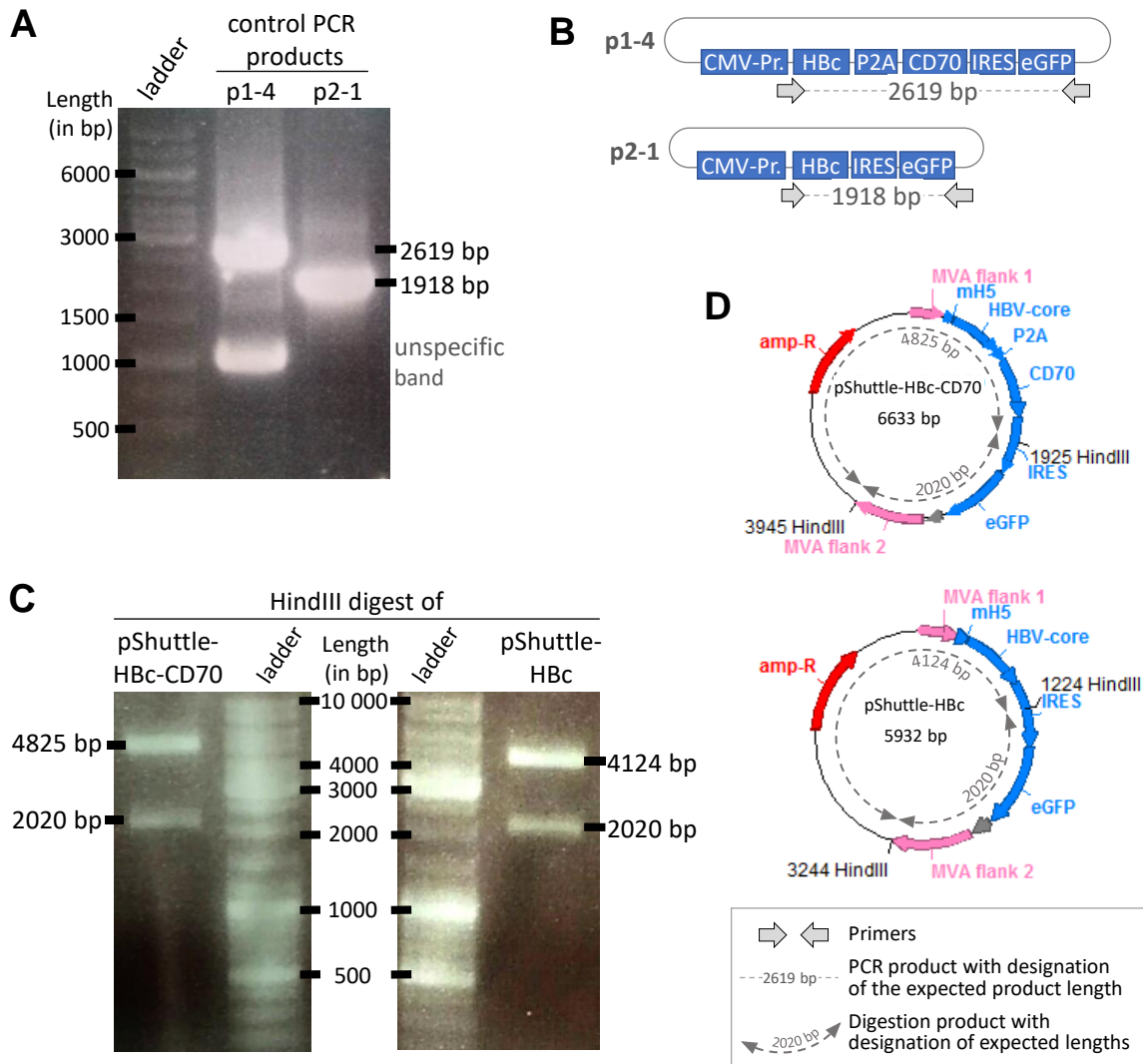


Figure 31 – **Agarose gel electrophoresis of DNA products from key cloning steps.** (A) Control PCRs of p1-4 and p2-1. After gel electrophoresis of PCR products, bands are visible at the expected lengths. The PCR of p1-4 resulted in an additional unspecific band at about 1000 bp. The schematic presentation of the resulting PCR products is illustrated in (B). (C) HindIII digest of pShuttle-HBc and pShuttle-HBc-CD70 resulted in the expected and correct restriction digest products. The schematic presentation of the digests and its products is given in (D). *bp*: basepair; *HindIII*: HindIII digestion site with number of position within the plasmid; *MVAflank 1 and 2*: MVA sequences; *mH5*: mH5 promoter gene; *P2A*: P2A cleaving site; *IRES*: internal ribosomal entry site; *eGFP*: enhanced green fluorescence protein; *amp-R*: Ampicillin resistance gene.

### 3.2.2. Verification of correct transgene transcription in eukaryotic cells

The plasmids p1-4 and p2-1 comprise the final transgene constructs HBC-(CD70)-eGFP under the control of a CMV-promoter, that enables expression in eukaryotic cells. To examine the expression of the transgenes in eukaryotic cells prior to construction of recombinant MVA, HEK293 cells were transfected with plasmids p1-4

and p2-1 and analyzed for correct gene expression of transgenes (HBc, CD70 and eGFP). A schematic overview of the experiment is given in Figure 19. The correct gene expression was evaluated by flow cytometry for CD70 and eGFP and by Western Blot for HBc and eGFP.

### Flow cytometry analysis of CD70 and eGFP expression

To analyze CD70 and GFP expression, transfected HEK293 cells were stained for CD70 and analyzed by flow cytometry (Figure 32). The untransfected control shows neither green fluorescence nor CD70 expression whereas both transfected samples show eGFP expression. In all stained samples, the main cell bulk shifted towards PE, compared to the unstained control, indicating background fluorescence of the CD70-PE antibody. However nearly all cells transfected with p1-4 prominently presented CD70 on their surfaces. eGFP however, was only detectable in a third of the cells transfected with p1-4 or p2-1. This is explained by the function of IRES, which appends eGFP to the construct: translation of downstream mRNA is lower than upstream mRNA and the positive correlation of translation levels is visible in the diagonal accumulation of cells in the sample p1-4. Of note, a compensation error is not constituted in this sample, as visible by the well positioned single cells expressing GFP and no or less CD70. The lower expression of eGFP due to IRES has no relevance for the properties of the vaccination vector as it only serves as a reporter protein.

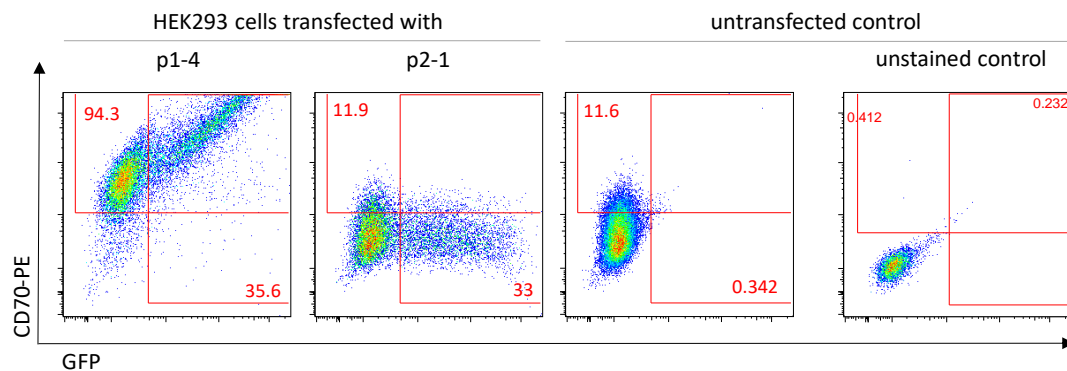


Figure 32 - **Flow cytometry analysis of eGFP and CD70 expression in HEK293 cells transfected with plasmids p1-4 and p2-1.** HEK293 cells were transfected with plasmids p1-4, p2-1 or remained untransfected and harvested after one day. Samples were stained with live/dead staining (NIR) and CD70-PE and gated for living cells prior to analysis of CD70 and eGFP expression. Gates for CD70 and GFP positive cells were set on the unstained control. Numbers indicate the percentage of positive cells. *p1-4*: plasmid encoding the HBc-CD70 transgene; *p2-1*: plasmid encoding the HBc transgene.

## Western Blot analysis of HBc and eGFP expression

Expression of HBc and eGFP was detected by immunoblotting of cell lysates of HEK293 cells transfected with the plasmids p1-4 (HBc-CD70 construct), p2-1 (HBc construct) or the untransfected control

Figure 33). During staining of HBc, unspecific background staining appeared at the sizes 28 kDa, 36 kDa, 72 kDa and 130 kDa in all samples including the untransfected control. The HBV core-specific bands were visible at their expected sizes (red circles in right column) with the HBV core-specific band of p1-4 transfected cells being slightly longer than the HBV core-specific band of p2-1 transfected cells. This is most likely due to remnants of the cleavage protein P2A, which is only integrated in the p1-4 construct and stays partly attached to the HBc protein. The eGFP protein was also detected at the expected size in both samples, p1-4 and p2-1.

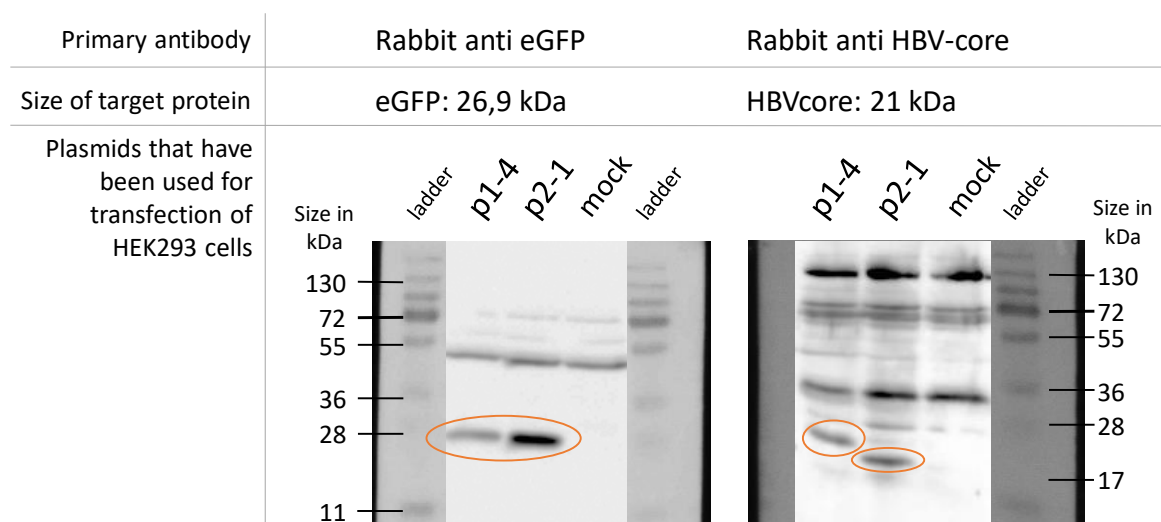


Figure 33 - **Detection of HBc and eGFP after immunoblotting.** HEK293 cells were transfected with plasmids p1-4, p2-1 or remained untransfected (mock) and were harvested after two days. After proceeding the lysed cells through a western blot protocol, they were stained with antibodies against HBcAg and eGFP. The HBc- and GFP-specific bands are visible at the expected sizes (red circles). *p1-4*: plasmid encoding the HBc-CD70 transgene; *p2-1*: plasmid encoding the HBc transgene; *eGFP*: enhanced green fluorescent protein.

In summary, the correct expression of the transgenes HBc, CD70 and eGFP was confirmed by FACS and/or Western Blot analysis of HEK293 cells transfected with the plasmids p1-4 or p2-1.

The plasmids p1-4 and p2-1 were used for the generation of rMVA-HBc-CD70 and rMVA-HBc (for technical details refer to chapter 2.2.4).

### **3.3. Comparison of rMVA-HBc and rMVA-HBc-CD70 in vivo**

To estimate the newly constructed vaccination vectors preclinically, C57Bl/6 mice and HBV1.3tg mice were vaccinated in a prime-boost regimen and immune responses and effects on serum markers and cellular responses in the liver were investigated.

In the first part of this work, C57Bl/6 mice were vaccinated and the antigen-specific responses of splenocytes were analyzed to assess the capacity of CD70 to boost an immune response. This setting corresponds to a prophylactic vaccination as those mice are naïve for the antigen HBc.

The second and more specific part of this work was the vaccination of HBV1.3tg mice. Besides its limitations this HBV transgenic mouse model often serves as a model for chronic HBV infection, where immune system is tolerant towards the antigen (Dembek und Protzer 2015). The viral antigens are predominantly expressed in the liver, the organ of natural infection in humans. Using this model, the effects of CD70 in therapeutic vaccination could be analyzed in manifold aspects.

#### **3.3.1. CD70 co-expression in vaccination against HBc improves the number and function of HBV core-specific T cells in C57Bl/6 mice**

To estimate the co-stimulatory effect of CD70 in vivo by comparison of the vectors rMVA-HBc-CD70 and rMVA-HBc C57Bl/6 mice (C57BL/6) were vaccinated with a HBc protein prime and a rMVA boost. As C57Bl/6 mice are naïve for all antigens that are delivered by the vaccine and immune response is not focused to any organ, splenocytes were isolated for analysis.

##### **3.3.1.1. Number of HBV core-specific CD8 T cells is increased after co-expression of CD70 in the MVA-boost vaccination**

The number of HBV core-specific CD8 T cells was determined by C<sub>93</sub> tetramer staining (Figure 34). A 2.5-fold increase of the number of HBV core-specific CD8 T cells was detected in C57Bl/6 mice that were vaccinated with rMVA-HBc-CD70 (16,77% of total CD8 T cells) compared to those vaccinated with rMVA-HBc (6,6% of total CD8 T cells). The difference between the two groups was significant ( $p=0.008$ ).

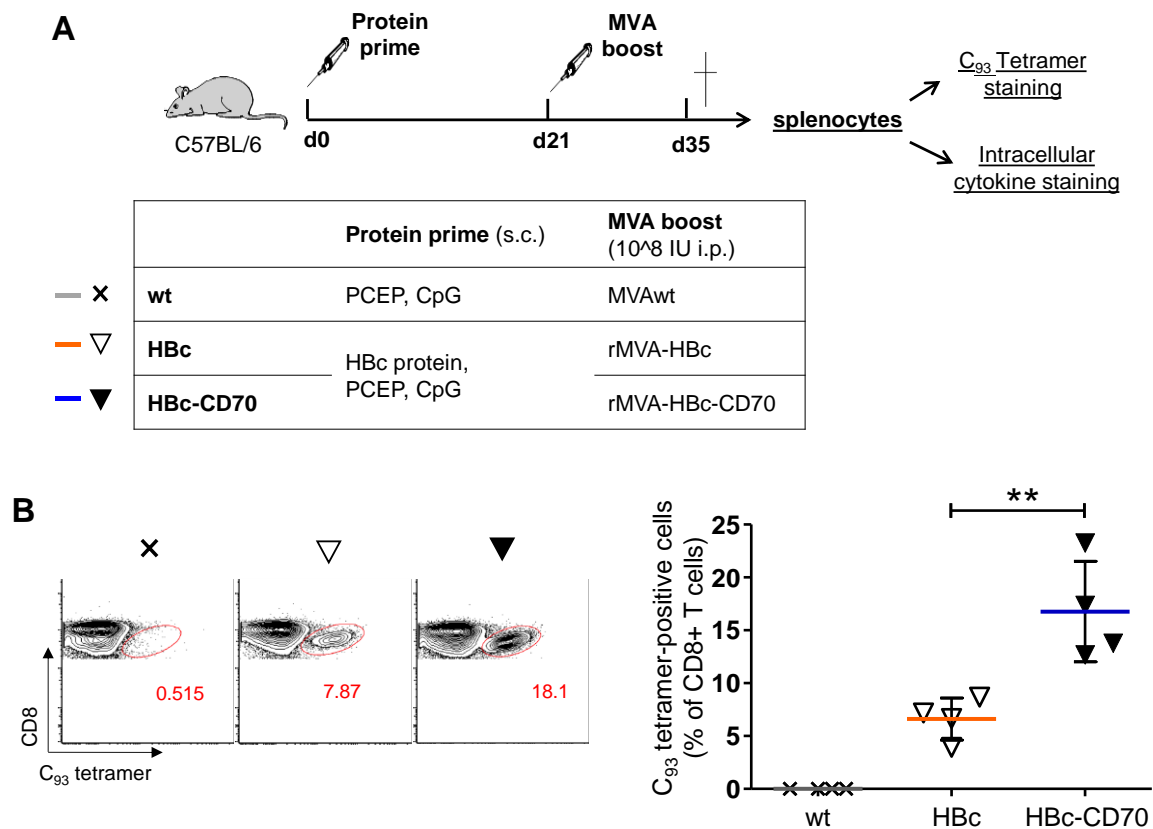


Figure 34 - HBV core-specific CD8 T-cell responses of C57Bl/6 mice after prime-boost vaccination with and without CD70. **(A)** Experimental setup: At day 0, C57Bl/6 mice were vaccinated s.c. with 25  $\mu$ g PCEP and 32  $\mu$ g CpG as adjuvants and 30  $\mu$ g HBc protein for groups HBc and HBc-CD70 (protein prime). 21 days later, the immune reaction was boosted with an i.p. injection of 10<sup>8</sup> IU of the respective MVA. 14 days after the MVA boost, splenocytes were isolated for analysis (ICS or tetramer staining). **(B)** Splenocytes were stained with a live/dead and CD8 dye and with C<sub>93</sub> Tetramers + streptactin (negative samples for background subtraction without C<sub>93</sub> tetramer). Gates were set on control group (wt). Plots show one representative mouse/group. Graph: background subtracted values; bars: mean (SD), statistical test: one-way ANOVA and subsequent unpaired t-test.

### 3.3.1.2. The functionality of HBV core-specific CD8 T cells is improved upon co-stimulation by CD70

Tetramer staining allows the detection of CD8 T cells with a specific T-cell receptor without providing information about their functional capacity. The functionality of antigen-specific T cells can be determined by ex vivo re-stimulation of cells with the antigen, blockage of cytokine release (resulting in intracellular accumulation of cytokines) and subsequent staining of intracellular cytokines (ICS).

ICS of splenocytes of vaccinated C57Bl/6 mice revealed, that not only the proportion of HBV core-specific CD8 T cells (Figure 34, B) but also the proportion of CD8 T cells

that produce cytokines upon antigenic stimulation (Figure 35) was increased in the vaccination group rMVA-HBc-CD70 compared to the vaccination group rMVA-HBc. After C<sub>93</sub> peptide stimulation, the proportion of CD8 T cells that produced IFN $\gamma$  was significantly higher when CD70 was contained in the MVA boost (12.2% vs. 5.6%; p=0.0086). In order to assess the MVA vector-specific CD8 T-cell response, cells were stimulated with B8R peptide, the immunodominant MVA-derived CD8 T-cell epitope in C57Bl/6 mice (Tscharke et al. 2005). The proportion of cells responding to peptide stimulation was not significantly altered by CD70 co-stimulation (3.7% for C-CD70 vs. 2.6% for vaccination group C). Expressed in x-fold standard deviations (mean SD of group HBc and HBc-CD70), the difference between the vaccination groups was 1.81x SD for the C<sub>93</sub> response but only 1.01xSD for the B8R response. This implies, that indeed the effect of CD70 co-stimulation was stronger for the C<sub>93</sub>-specific response than for the B8R-specific response.

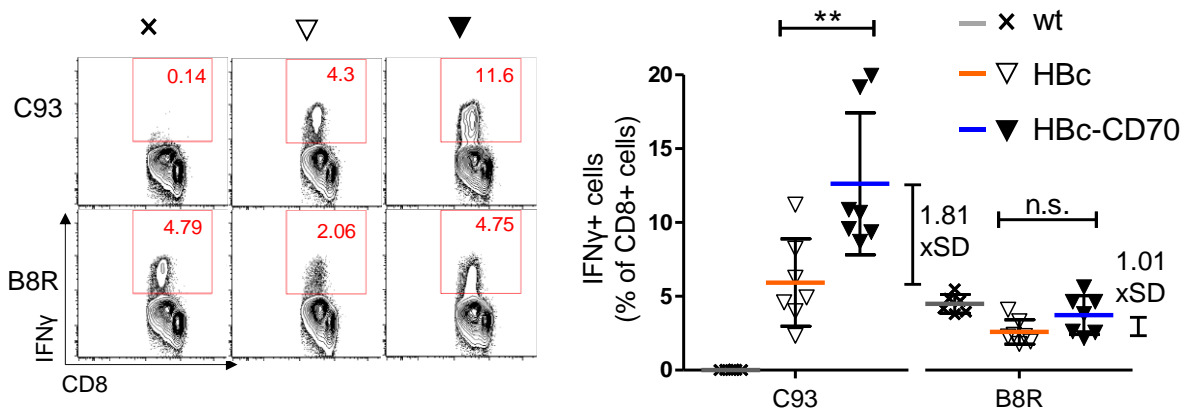


**Figure 35 – CD8 T cells, that produce IFN $\gamma$  after stimulation with HBc- and MVA-specific epitopes.** C57Bl/6 mice were vaccinated with a s.c. protein prime (30  $\mu$ g HBc protein for groups HBc and HBc-CD70 and 25  $\mu$ g PCEP + 32  $\mu$ g CpG as adjuvants for all groups) and a i.p. MVA boost 21 days later ( $10^8$  IU MVAwt or rMVA-HBc or rMVA-HBc-CD70 for respective vaccination groups). At day 35, splenocytes were isolated, stimulated with C<sub>93</sub> or B8R peptides, stained for surface markers and intracellular cytokines and measured with flow cytometry. Unstimulated samples were included for background subtraction. Gates were set on unstimulated samples. The contour plots (left) show one representative mouse per group. Graph: Bars: mean (SD); statistical test: one-way ANOVA and subsequent students t-test (results only shown for comparison of groups HBc and HBc-CD70); n.s.: not statistically significant. Calculation of difference in x-fold SD: mean SD of HBc and HBc-CD70 (calculated separately for data of C<sub>93</sub> and B8R). C<sub>93</sub>: HBc-derived dominant CD8 T-cell epitope; B8R: MVA-derived dominant CD8 T-cell epitope.

It was shown previously that CD70 co-stimulation not only leads to expansion of antigen-specific CD8 T cells but also to acquisition of effector functions (Keller et al. 2008; Roberts et al. 2010; Arens et al. 2004). This was also apparent in these vaccination experiments in C57Bl/6 mice when the proportion of CD8 T cells, that produced IFN $\gamma$  upon C<sub>93</sub> stimulation (effector function) was set in relation to C<sub>93</sub> tetramer-positive CD8 T cells (quantity). This “gain of function” ratio was computed with background subtracted values of each individual mouse (Figure 36, A). In vaccination group HBc, the ratio was 5.7 $\pm$ 0.03 (mean $\pm$ SD) while it was significantly higher after CD70 co-expression in vaccination group HBc-CD70 (6.8 $\pm$ 0.02 (mean $\pm$ SD)). This difference between the vaccination groups was significant (p=0.013).

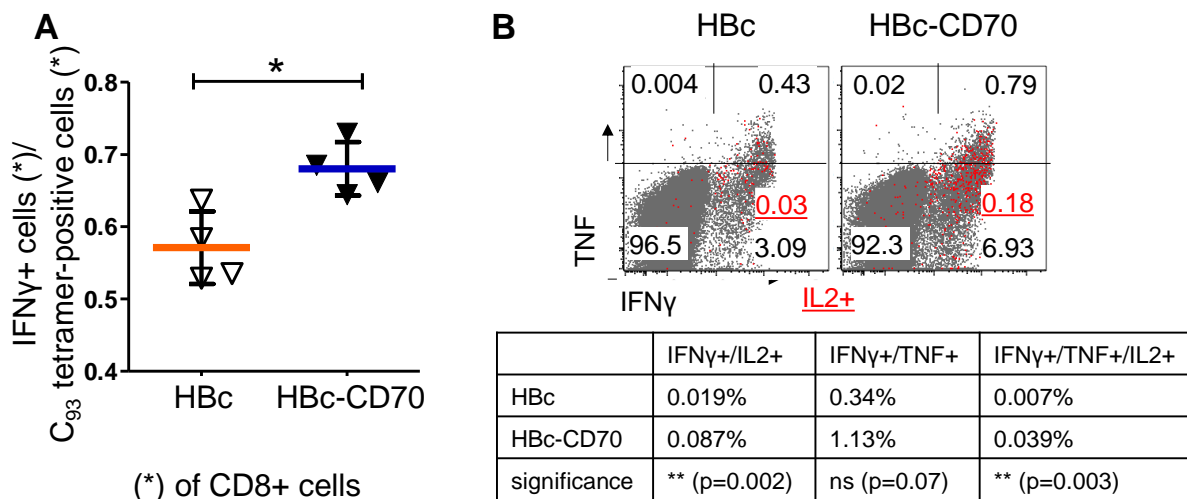


**Figure 36 - Gain of function of C<sub>93</sub>-specific CD8 T cells upon CD70 co-stimulation.** C57Bl/6 mice were vaccinated with a 30  $\mu$ g HBc protein prime (+ 25  $\mu$ g PCEP and 32  $\mu$ g CpG s.c.) and a MVA boost 21 days later (10<sup>8</sup>IU rMVA-HBc or rMVA-HBc-CD70 i.p. for vaccination groups HBc and HBc-CD70 respectively). At day 35, splenocytes were isolated, stimulated with C<sub>93</sub> peptide and stained with ICS or stained with C<sub>93</sub> tetramer without stimulation. Unstimulated samples were included for background subtraction. Gates were set on unstimulated samples. **(A)** IFN $\gamma$ + CD8 T cells after C<sub>93</sub> stimulation were set in relation to C<sub>93</sub> tetramer+ CD8 T cells (for each mouse individually). Graph shows mean $\pm$ SD (bar and whiskers) and significance (student's t-test). Data from one single experiment. **(B)** Evaluation of the capacity of CD8 T cells to produce the effector cytokines IFN $\gamma$ , TNF and IL-2 after C<sub>93</sub> stimulation. The contour plots show one representative mouse per group. The table shows the mean values (% of CD8+ T cells) of 4 mice/group.

Multifunctionality is the ability of CD8 T cells to produce several cytokines simultaneously and is thought to be very desirable in HBV infection: impaired cytokine production or cytokine release of HBV-specific CD8 T cells have been associated with

CHB while the simultaneous production of various cytokines was found to be important in the immunological control of HIV as another chronic infection or in vaccinations that led to protective immunity (Kosinska et al. 2012). Therefore, we assessed the simultaneous expression of the antiviral effector cytokines IFN $\gamma$ , TNF and IL-2 as another measure of the quality of the HBV core-specific CD8 T-cell response by ICS after stimulation with C<sub>93</sub> peptide (Figure 36, B). It was shown, that the multifunctionality of those CD8 T cells (simultaneous expression of 2 or 3 cytokines) was increased in group HBc-CD70 compared to group HBc.

These results suggest, that co-stimulation with CD70 not only increased the number of HBV core-specific CD8 T cells but also improved their effector function in terms of expression of IFN $\gamma$  upon antigenic stimulation and multifunctionality.

### 3.3.1.3. HBV core-specific CD4 T-cell response upon co-expression of CD70

It was already depicted that co-stimulation by CD70 improves the function of CD8 T cells, which are the crucial effector cells in the control and elimination of HBV infection. The CD4 T-cell response was determined by stimulation with a pool of HBc derived proteins. Co-expression of CD70 did not significantly improve the CD4 T-cell function of splenocytes, however in two out of four mice of the vaccination group HBc-CD70, IFN $\gamma$  production was considerably higher, which was not the case in vaccination group HBc (Figure 37).

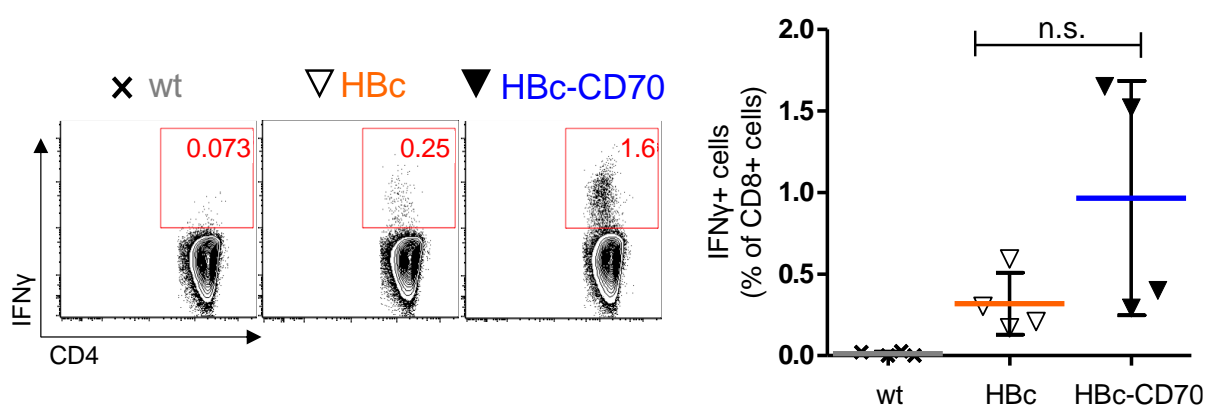


Figure 37 – HBV core-specific CD4 T-cell response upon CD70 co-stimulation. C57Bl/6 mice were vaccinated with a protein prime (30  $\mu$ g HBc protein for groups C and C-CD70 and 25  $\mu$ g PCEP + 32  $\mu$ g CpG as adjuvants for all groups s.c.) and a MVA boost 21 days later (10<sup>8</sup>IU MVAwt or rMVA-HBc or rMVA-HBc-CD70 i.p. for respective vaccination groups *wt*, *HBc* and *HBc-CD70*). At day 35, splenocytes

were isolated and stimulated with core pool 3 (CD4 and CD8 T-cell epitopes). Samples were stained for surface markers and intracellular cytokines and measured with flow cytometry. Unstimulated samples were included for background subtraction. Contour plots show one representative mouse per group. Graph: Bars: mean (SD); statistical test: one-way ANOVA and subsequent students t-test (results only shown for difference between the groups HBc and HBc-CD70); n.s.: not statistically significant. Data from one experiment.

### 3.3.2. Vaccination of HBV1.3tg mice

HBV1.3tg mice express and produce the HBV antigens and virions in the liver and their T cells are tolerant towards HBV antigens. They serve as a mouse model for (vertically transmitted) chronic HBV infection.

Figure 38 gives an overview on the vaccination scheme in HBV1.3tg mice (similar to prime/boost vaccination of C57Bl/6 mice) and the readout of the vaccination experiments in HBV1.3tg mice. A table summarizing the individual experiments with the corresponding data which was applicable for analysis can be found in Appendix 6.

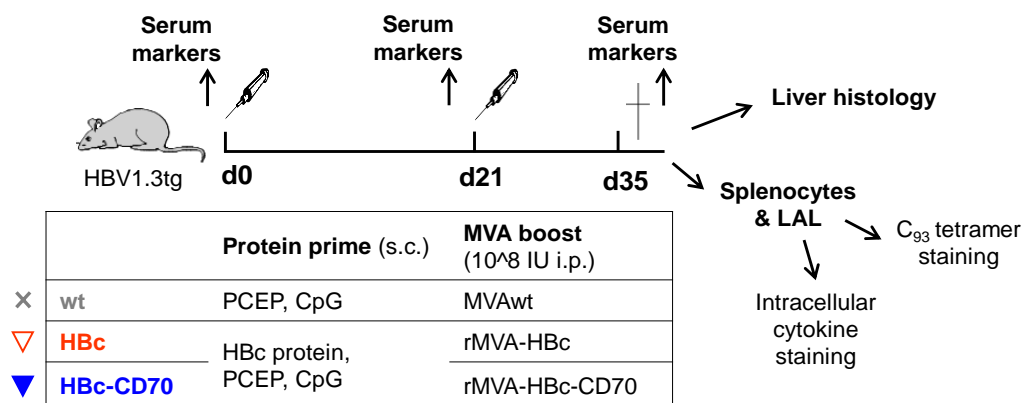


Figure 38 - **Experimental scheme for protein-prime/MVA±CD70-boost vaccination in HBV1.3tg mice.** At day 0, HBV1.3tg mice were vaccinated s.c. with 25 µg PCEP and 32 µg CpG as adjuvants and 30 µg HBc protein for groups HBc and HBc-CD70. 21 days later, the immune reaction was boosted with an i.p. injection of 10<sup>8</sup> IU of (r)MVA (see table). 14 days later, liver samples were taken for liver histology and splenocytes and LAL were isolated for analysis (ICS and tetramer staining). Blood samples were taken at all relevant time points for determination of serum markers.

#### 3.3.2.1. Co-expression of CD70 in protein-prime/MVA-boost vaccination increases the number of T-cell clusters in livers of HBV1.3tg mice

Histological liver samples of vaccinated mice were stained with CD3 and ki67 to assess the reaction of T cells in the liver. In the liver, antigen production takes place and homing of T cells is expected. To evaluate the effects of vaccination (+/- CD70)

on T cells in the liver, single T cells and T-cell clusters in the liver were counted (Figure 39, A and B).

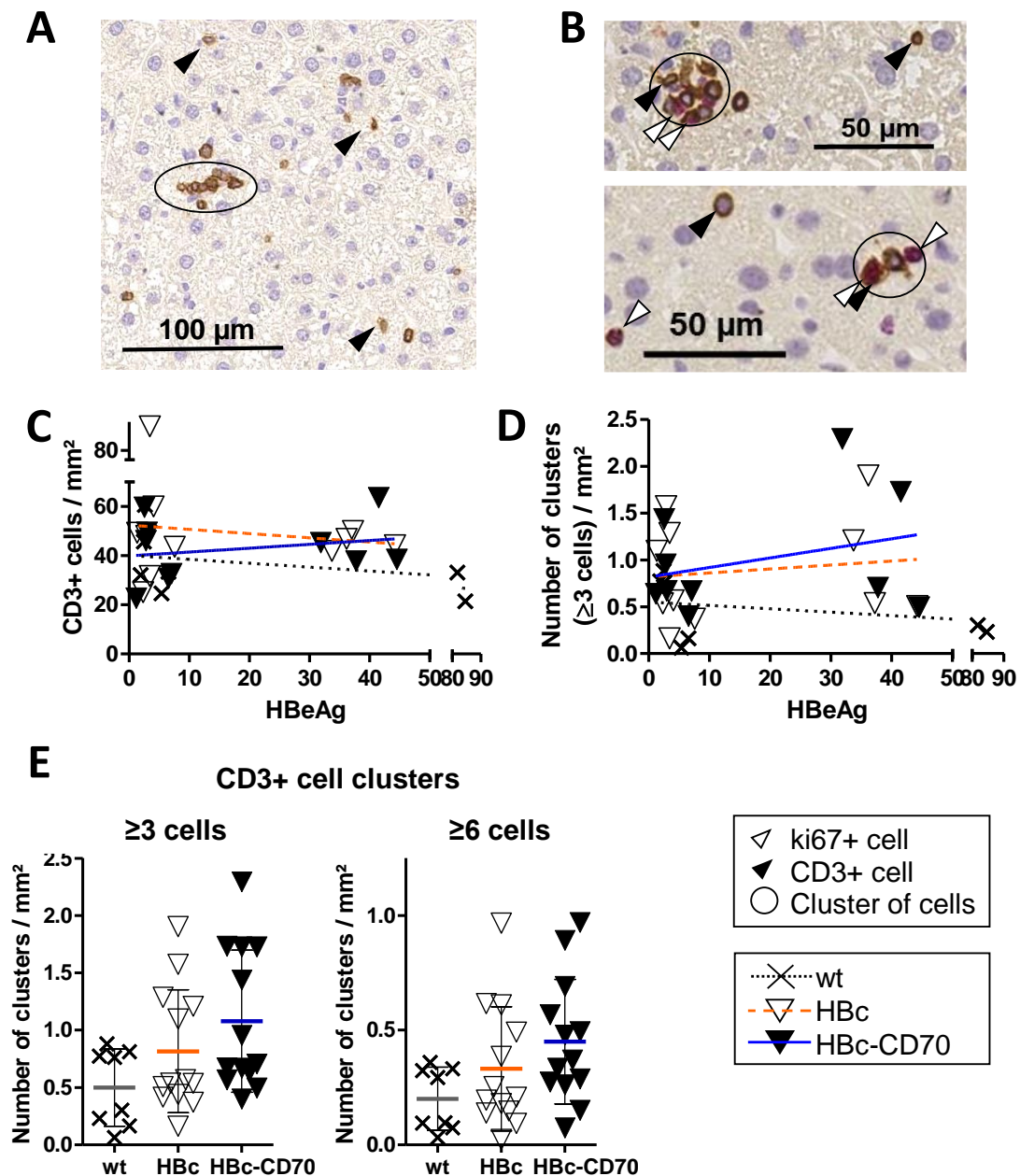


Figure 39 – **CD3+ cells in livers of vaccinated HBV1.3tg mice.** HBV1.3tg mice were primed with HBc protein and PCEP and CpG as adjuvants (adjuvants only for group wt). 21 days later, mice were boosted with (r)MVA: group wt: MVAwt; group HBc: rMVA-HBc; group HBc-CD70: rMVA-HBc-CD70. At day 35, livers were taken and histological cuts were stained for CD3+ (and ki67+) cells. **(A)** Representative liver section, which is stained for CD3+ cells. *black arrows*: single CD3+ cell; *circle*: cell clusters of ≥3 or ≥6 cells. **(B)** Double stainings (CD3 (*black arrows*) and ki67 (*white arrows*)) of liver sections. In clusters of CD3+ cells, double positive (CD3+ plus ki67+ = proliferating) cells are present. **(C)** CD3+ cells were in relation to the respective HBeAg titer (S/CO) prior to the protein prime. **(D)** Cell clusters of ≥3 CD3+ cells were set in relation to the HBeAg titer (S/CO) prior to the protein prime. **(E)** Number of cell clusters

of  $\geq 3$  or  $\geq 6$  CD3<sup>+</sup> cells. Data was not statistically significant (one-way ANOVA); graphs: bars indicate mean ( $\pm$  SD).

We found, that the absolute numbers of T cells and the numbers of T-cell clusters did not correlate with HBeAg titers of HBV1.3tg mice (Figure 39, C and D). The absolute number of T cells in the liver was in the same range in any vaccination group (Figure 39, B) but the number of T-cell clusters (accumulations of  $\geq 3$  or  $\geq 6$  cells in direct contact) was increased in vaccination groups HBc and HBc-CD70 (Figure 39, E). The improvement was highest in vaccination group HBc-CD70. Clusters of  $\geq 6$  cells were rarer than clusters of  $\geq 3$  cells but the relation between the vaccination groups was similar. The clusters of CD3<sup>+</sup> T cells were double-positive for CD3 and ki67 (Figure 39, B) and thus most probably spots of T-cell proliferation.

These results confirm, that vaccination against the HBV core antigen leads to T-cell proliferation in the liver of HBV1.3tg mice. This effect was even stronger in mice that were vaccinated with rMVA-HBc-CD70. But those proliferation spots only account for a small number of total CD3<sup>+</sup> T cells in liver samples. Most CD3<sup>+</sup> T cells are single cells and most likely not specific for HBc.

### **3.3.2.2. The induction of the HBV core-specific T-cell immune response is dependent of antigenemia**

According to the vaccination scheme (Figure 38), HBV1.3tg mice were vaccinated with HBc protein and MVAwt, rMVA-HBc or rMVA-HBc-CD70. Mice were sacrificed at day 35 and splenocytes and liver associated lymphocytes (LAL) were isolated and analyzed by flow cytometry after ICS or tetramer staining. The results are analyzed in subgroups of high and low HBeAg titers. HBV1.3tg mice express HBV and its antigens at different levels and HBV-specific immune responses correlate inversely, as described previously (Backes et al. 2016). The anti-vector immunity, monitored by B8R stimulation, was not affected by the HBe-antigen titer.

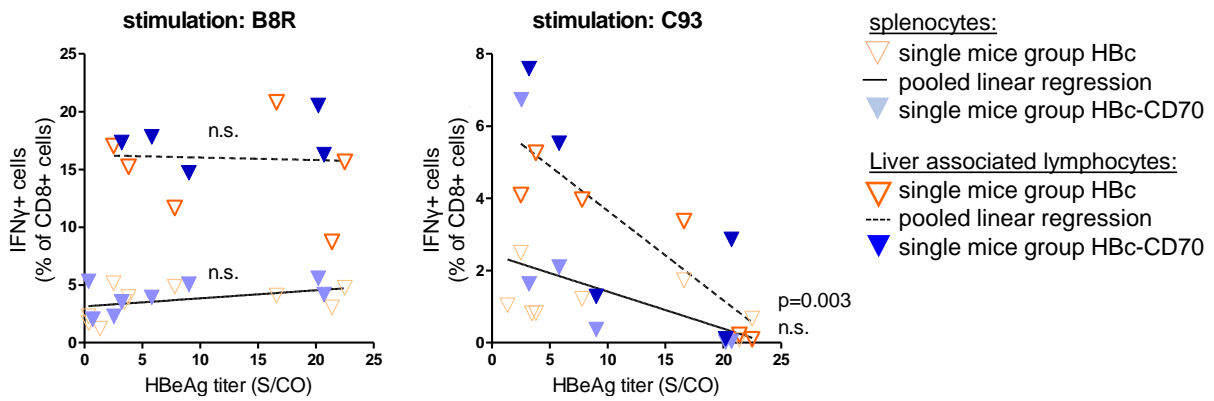


Figure 40 – **Correlation of HBeAg titer with HBC- and MVA-specific CD8 T-cell response.** HBV1.3tg mice were primed with HBc protein and PCEP and CpG as adjuvants (adjuvants only for group *wt*). 21 days later, mice were boosted with (r)MVA: group *wt*: MVAwt; group *HBc*: rMVA-HBc; group *HBc-CD70*: rMVA-HBc-CD70. At day 35, splenocytes and LAL were isolated and evaluated for the C<sub>93</sub>- and B8R-specific CD8 T-cell response. Unstimulated samples were included for background subtraction. The plots show the respective CD8 T-cell response in relation to the HBeAg titer (S/CO) prior to the protein prime. Due to a great range of HBeAg titers, the linear regression (showing a correlation) was performed in a pooled group of vaccination groups HBc and HBc-CD70. Single data points have a color code to distinguish the vaccination groups HBc and HBc-CD70. The group MVAwt is not shown in this analysis.

### 3.3.2.2.1. CD70 co-expression enhances the number of HBV core-specific T cells in a therapeutic vaccination setting using rMVA-HBc-CD70

To estimate the effect of CD70 co-expression on the number and functionality of CD8 T cells, we performed tetramer staining and intracellular staining of cells from livers and spleens of vaccinated HBV1.3tg mice. The HBeAg titers of mice ranged from 0.5 to 22.5 S/CO and data were analyzed in two groups (>/< 8 S/CO).

The results of the C<sub>93</sub> tetramer staining in Figure 41 suggest that CD70 co-stimulation has a positive influence on the number of HBV core-specific CD8 T cells. Especially in mice with low HBeAg titers (1-8 S/CO), the proportion of CD8 T cells specific for HBc were higher in both splenocytes and in LAL in vaccination group HBc-CD70 (results not statistically significant).

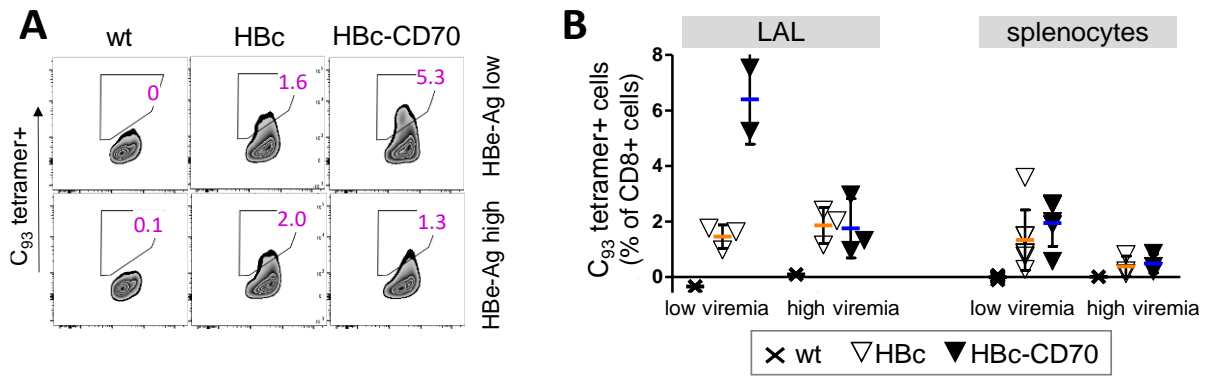


Figure 41 – **C<sub>93</sub>-specific CD8 T cells from spleens and livers of vaccinated HBV1.3tg mice.** HBV1.3tg mice were primed with HBc protein and PCEP and CpG as adjuvants (adjuvants only for group *wt*). 21 days later, mice were boosted with (r)MVA: group *wt*: MVAwt; group *HBc*: rMVA-HBc; group *HBc-CD70*: rMVA-HBc-CD70. At day 35, splenocytes and LAL were isolated and analyzed. Cells were stained with C<sub>93</sub> tetramer plus streptactin (negative samples for background subtraction without C<sub>93</sub> tetramer). Gates were set on control group (*wt*). **(A)** Contour plots show one representative mouse per group (CD8+ LAL). **(B)** C<sub>93</sub>-specific LAL and splenocytes (% of CD8 T cells). Graphs depict mice from two individual experiments. *HBeAg low* = HBeAg: 1-8 S/CO, *HBeAg high* = 8-23 S/CO. Differences between the vaccination groups (>2 mice/groups) were not statistically significant (one-way ANOVA).

HBV core-specific CD8 T cells were also analyzed in respect to their functionality: Splenocytes and LAL from vaccinated HBV1.3tg mice were stimulated with C<sub>93</sub> and B8R and the production of effector cytokines upon stimulation was evaluated.

The HBV core-specific response is presented in subgroups of low and high HBeAg titers (>/< 8 S/CO) (Figure 42, A and B). Due to the limited number of mice paired with a wide spectrum of HBeAg titers, it was not possible to distinguish more precisely by antigenemia and the results are not very conclusive. It was expected, that CD70 leads to an increased HBV core-specific CD8 T-cell response. Nevertheless, we see that there is indeed a tendency towards a higher proportion of HBV core-specific CD8 T cells in mice of group HBc-CD70 in comparison to mice of group HBc. This was particularly evident in low viremic mice (Figure 42, B).

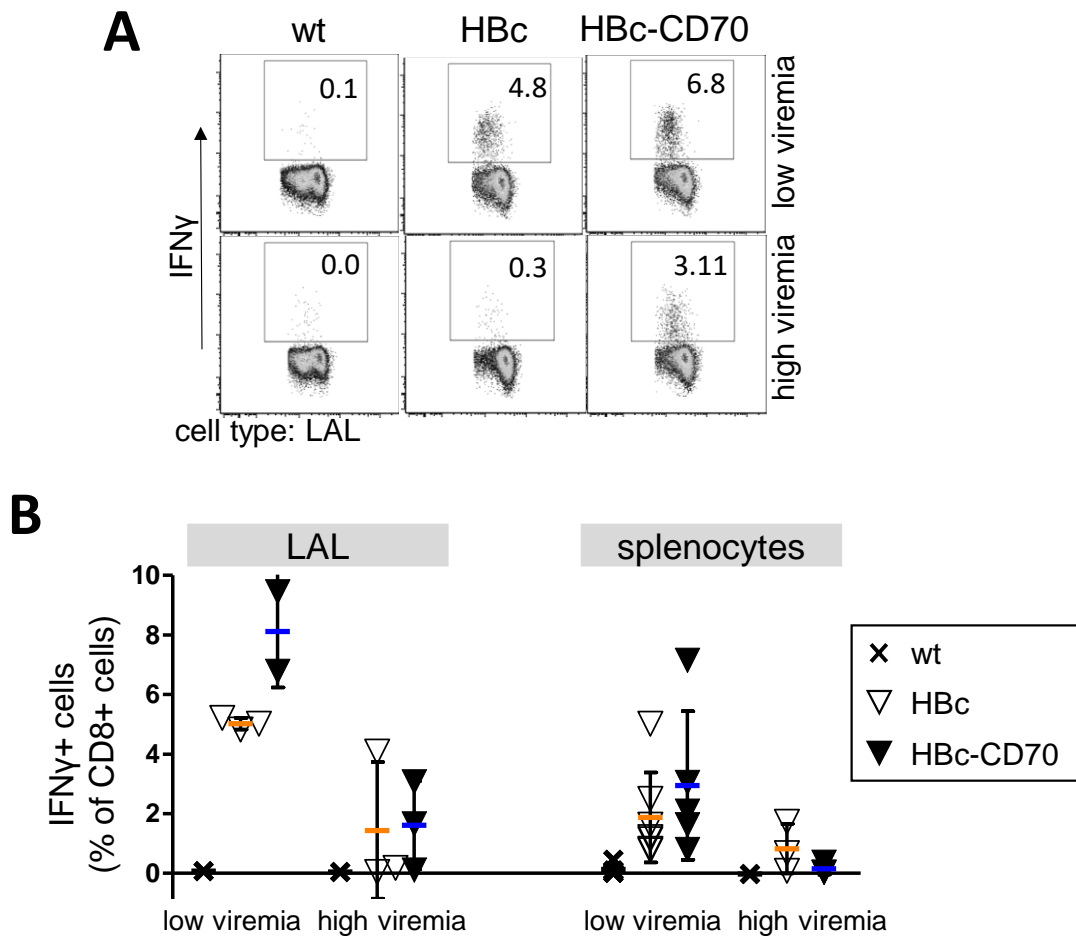


Figure 42 - **C<sub>93</sub>-specific CD8 T cells from spleens and livers of vaccinated HBV1.3tg mice.** HBV1.3tg mice were primed with HBc protein and PCEP and CpG as adjuvants (adjuvants only for group *wt*). 21 days later, mice were boosted with (r)MVA: group *wt*: MVAwt; group *HBc*: rMVA-HBc; group *HBc-CD70*: rMVA-HBc-CD70. At day 35, splenocytes and LAL were isolated and stimulated with C<sub>93</sub> or B8R peptides prior to ICS. Unstimulated samples were used for background subtraction and gating. **(A)** Representative data for the C<sub>93</sub>-specific response (LAL of high and low viremic mice). **(B)** Reactive splenocytes and liver associated lymphocytes after C<sub>93</sub> stimulation. Differences between the vaccination groups were not statistically significant (one-way ANOVA). *HBeAg low* = HBeAg: 1-8 S/CO, *HBeAg high* = 8-23 S/CO.

The MVA vector-specific CD8 T-cell response was similar in all vaccination groups (*wt*, *HBc* and *HBc-CD70*) (Figure 43, A and B). The MVA-specific response was not altered after CD70 co-expression during vaccination which is in correspondence with the effects that were found in C57Bl/6 mice (Figure 35).

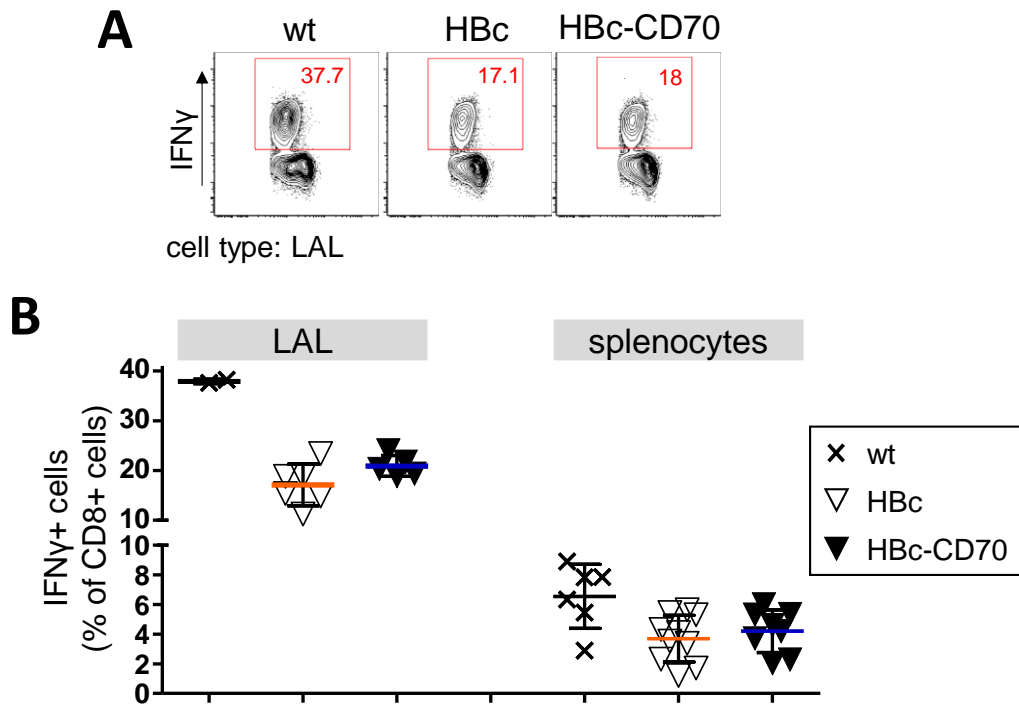


Figure 43 - **B8R-specific CD8 T cells from spleens and livers of vaccinated HBV1.3tg mice.** HBV1.3tg mice were primed with HBc protein and PCEP and CpG as adjuvants (adjuvants only for group *wt*). 21 days later, mice were boosted with (r)MVA: group *wt*: MVAwt; group *HBc*: rMVA-HBc; group *HBc-CD70*: rMVA-HBc-CD70. At day 35, splenocytes and LAL were isolated and stimulated with C<sub>93</sub> or B8R peptides prior to ICS. Unstimulated samples were used for background subtraction and gating. **(A)** Contour plots show LAL of one representative mouse per group after stimulation with B8R peptide (= MVA vector specific CD8 T-cell response). **(B)** Proportion of reactive CD8 T cells after B8R stimulation (splenocytes and LAL). Differences between the vaccination groups were not statistically significant (one-way ANOVA).

### 3.3.2.2.2. CD4 T-cell response of vaccinated HBV1.3tg mice

The CD4 T-cell response of HBV1.3tg mice also was analyzed after vaccination with MVA-HBc or MVA-HBc-CD70 (control group: vaccination with MVAwt). As only one experimental experiment was performed with CD4 T-cell stimulation (round 4, see Appendix 6), only very weak data were available that did not lead to a conclusion (Figure 44). Overall, CD4 T-cell responses after stimulation with HBV core-derived peptides were hardly detectable. However, the highest percentage of IFN $\gamma$ + CD4 T cells after stimulation with HBV core-derived peptides was detected in vaccination group HBc-CD70 in each group respectively.

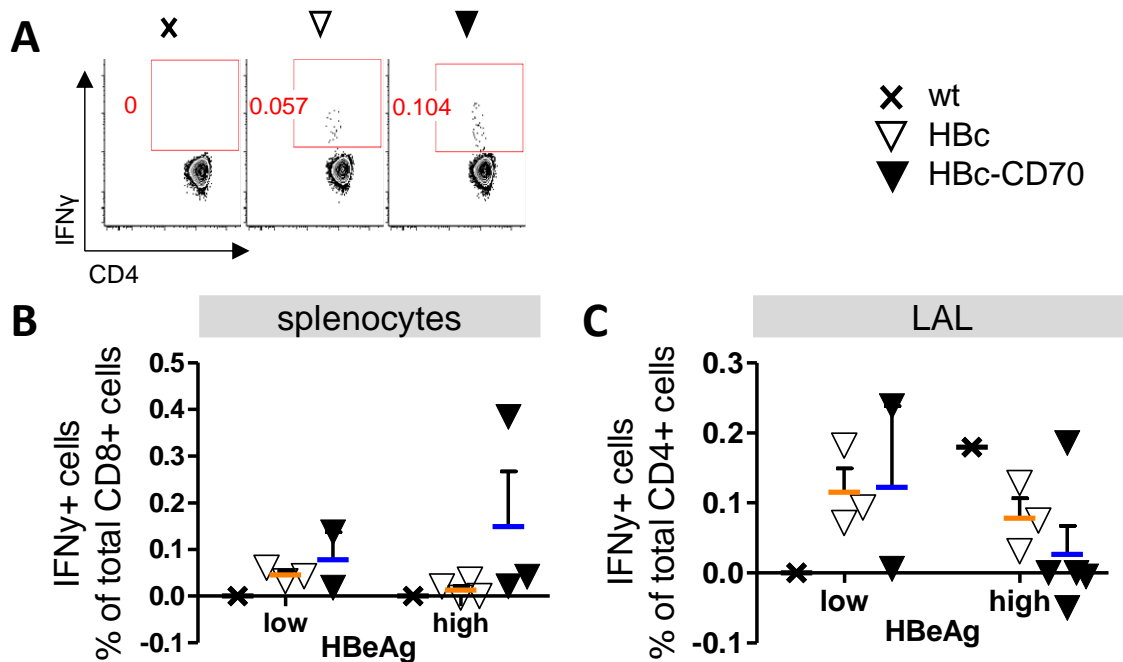


Figure 44 – **HBV core-specific CD4 T cells of HBV1.3tg mice.** HBV1.3tg mice were primed with HBc protein and PCEP and CpG as adjuvants (adjuvants only for group *wt*). 21 days later, mice were boosted with (r)MVA: group *wt*: MVAw<sub>t</sub>; group *HBc*: rMVA-HBc; group *HBc-CD70*: rMVA-HBc-CD70. At day 35, splenocytes were isolated and stimulated with core pool 2 prior to ICS. Unstimulated samples were included for background subtraction and gating. **(A)** Contour plots show one representative mouse per group (splenocytes of mice with low HBeAg titers). The graphs show the summarized results of IFN $\gamma$  secretion of splenic **(B)** and liver associated **(C)** CD4 T cells after HBV core-peptide stimulation. Data from one experiment. Differences between the vaccination groups were not statistically significant (student's t-test). Graph: bars indicate mean (+/- SD). *HBeAg low* = HBeAg: 1-8 S/CO, *HBeAg high* = 8-23 S/CO.

### 3.3.2.3. CD70 co-expression during boost vaccination does not affect HBV-related serum markers in HBV1.3tg mice

The serum markers of vaccinated HBV1.3tg mice were analyzed at days 0, 21 and 35 of the vaccination experiments (see Figure 38). HBeAg and HBsAg serve as markers for HBV replication.

As expected, anti-HBc antibodies already raised after the protein prime in both vaccination groups HBc and HBc-CD70 independently of CD70 co-expression (Figure 45, A, also described by (Backes et al. 2016)). As also expected, no anti-HBs antibody production was observed in any mouse as HBs was not included in prime or boost vaccination (Figure 45, B).

HBeAg reduction was observed in both vaccination groups HBc and HBc-CD70 (Figure 45, C). In low viremic mice, HBeAg levels dropped to low or undetectable levels, while in high viremic mice HBeAg levels were significantly decreased similarly in both vaccination groups HBc and HBc-CD70. HBsAg, a second measure for HBV replication also was decreased in both vaccination groups after vaccination of high viremic mice. In low viremic mice, HBsAg was hardly detectable prior to vaccination, which has been previously described (Backes et al. 2016) and didn't allow the observation of a reducing effect upon vaccination in low viremic mice (Figure 45, D).

In order to have a more detailed look at the effect of the prime/boost vaccination on viral replication, the reduction of HBeAg levels was visualized for both vaccination elements (protein prime and MVA boost) separately (Figure 45, E). The reducing effect on the HBeAg levels was highest after the protein prime in both vaccination groups HBc and HBc-CD70 (first panel), but the MVA boost had a slight additional reducing effect on HBeAg levels (second panel). Further, it could be observed, that the protein prime had a greater effect in mice with low HBeAg titers whereas the MVA boost caused a reduction of HBeAg levels in mice with higher HBeAg titers. The effect seemed to be independently of CD70 co-expression.

In summary, vaccination against HBV core (groups HBc and HBc-CD70) led to the formation of anti-HBcAb and to a reduction of HBV replication markers in low and in high viremic mice.

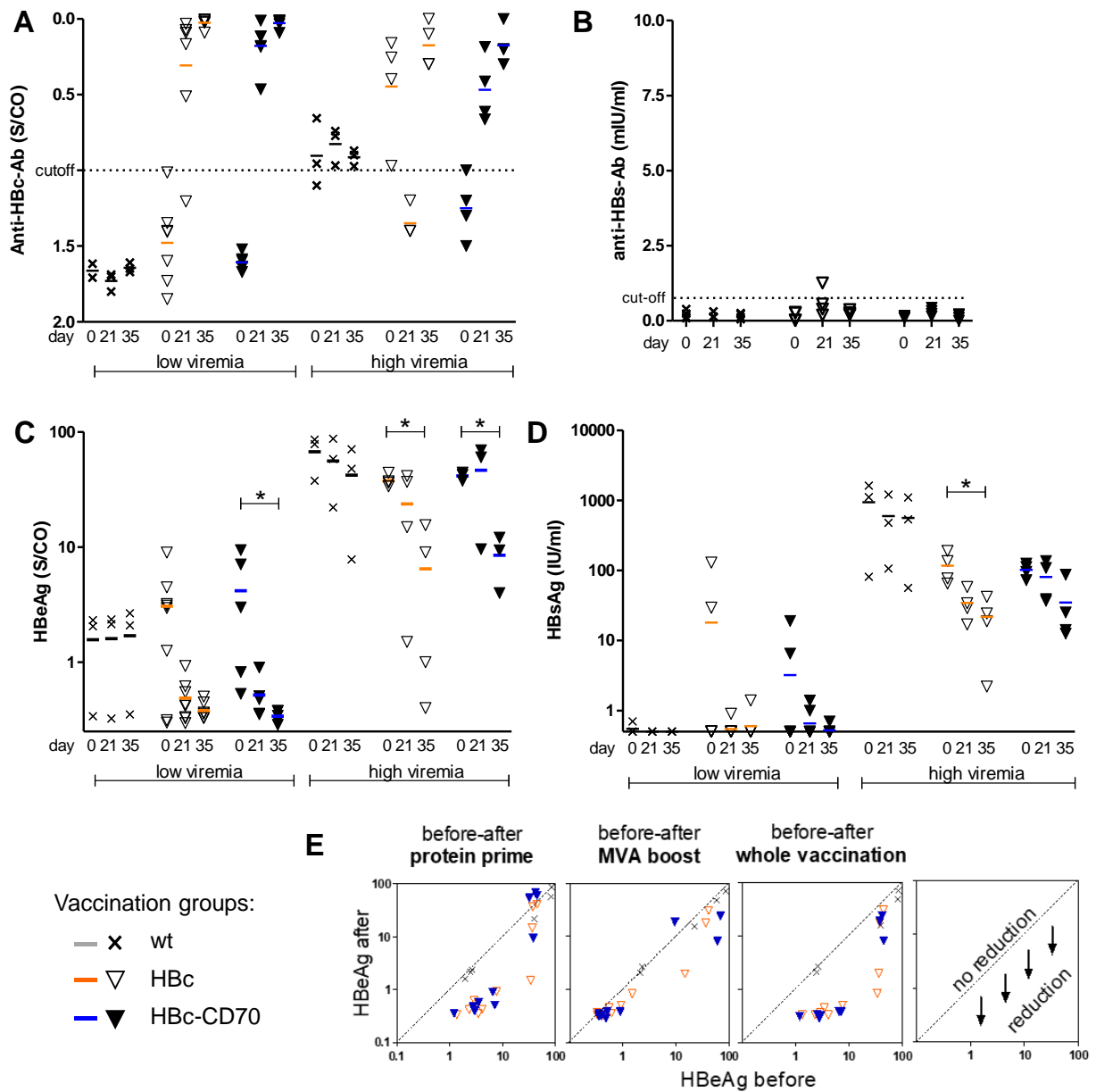


Figure 45 - **Development of HBeAg-related serum markers in HBV1.3tg mice during vaccination.** HBV1.3tg mice were primed with HBeAg protein and PCEP and CpG as adjuvants (adjuvants only for group wt). 21 days later, mice were boosted with (r)MVA: group wt: MVAwt; group HBc: rMVA-HBc; group HBc-CD70: rMVA-HBc-CD70. Blood serum was taken at day 0, 21 and 35 for analysis of serum markers. **(A)** Anti-HBc-Antibodies in the sera of low and high viremic mice. **(B)** Anti-HBs-Antibodies in the sera of low viremic mice. HBeAg **(C)** and HBsAg **(D)** levels of low and high viremic mice. **(E)** Values of the HBeAg levels in the sera of individual mice were plotted in pairs of different vaccination steps. First panel shows the reduction from day 0 to day 21 (=effect after protein prime), second panel shows the reduction from day 21 to day 35 (=effect after MVA boost) and third panel shows the summarized reduction from day 0 to day 35. *Low viremic mice*: HBeAg prior to vaccination < 8 S/CO, *high viremic mice*: HBeAg prior to vaccination >8 S/CO. Graphs: bars indicate mean. Statistics in A, C and D were performed with one-way ANOVA. \**p*-value <0.05.

### 3.3.2.4. CD70 does not promote long-lasting immunopathology in the liver

To investigate if co-expression of CD70 promotes liver damage due to an increased T-cell activity, alanine aminotransferase (ALT) was measured as a marker for liver damage. A mild elevation of ALT was observed 14 days after the MVA boost in all vaccination groups - even in the control group, which was vaccinated with adjuvants and MVAwt only (Figure 46). The elevation of ALT was not dependent on the viremia of the vaccinated mice (HBeAg titer prior to the experiment). Thus, the observed elevation of ALT most likely is no effect of any anti-HBc-activity (humoral or cellular immune response) but rather an effect that is caused by the vector itself or by immune activity against or caused by the vector.

However, it might be that ALT levels are higher only one week after the MVA boost (personal conversation with Anna Kosinska).

Overall, the available data suggest, that this vaccination and particularly CD70 co-expression by MVA does not lead to severe or long-lasting immunopathology.

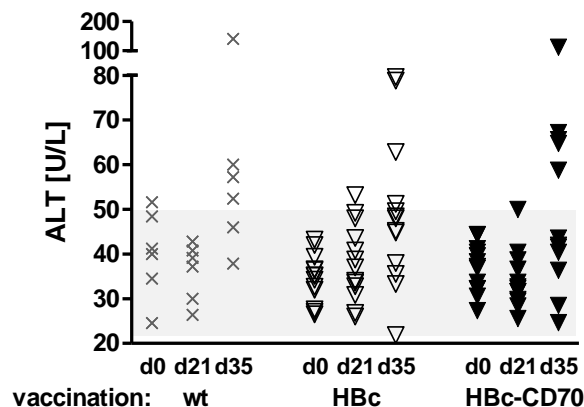


Figure 46 - ALT elevation in HBV1.3tg mice after MVA vaccination. HBV1.3tg mice were primed with HBc protein and PCEP and CpG as adjuvants (adjuvants only for group wt). 21 days later, mice were boosted with (r)MVA: group wt: MVAwt; group C: rMVA-HBc; group C-CD70: rMVA-HBc-CD70. At days 0, 21 and 35 (14 days after MVA boost), ALT was measured in the blood serum. HBeAg titers of depicted mice were 1-45 S/CO. Light grey: normal range of ALT in mice.

### 3.3.2.5. Tendency to reduced HBcAg expression in hepatocytes of HBV1.3tg mice after CD70 co-expression

Having shown, that vaccination itself and CD70 co-stimulation in particular has a positive effect on induction of an HBV core-specific CD8 T-cell response in the livers

of HBV1.3tg mice, we next questioned whether vaccination led to a reduction of HBcAg in the liver.

According to Chu et. al. the viral protein HBcAg is present both in the nucleoli and the cytoplasm of infected hepatocytes of patients (Chu et al. 1997; Chu et al. 1995). The levels of HBcAg expression in nucleoli, but not in the cytoplasm, was shown to correlate strongly with HBV-DNA levels in the serum. The distribution characteristics were shown to correlate with the state of disease and hepatitis as well as cellular factors of the hepatocytes: in states of low inflammation and in quiescent hepatocytes, HBcAg more likely locates in the nucleus. During hepatitis and in proliferating (regenerating) hepatocytes, HBcAg is more likely located in the cytoplasm. (Chu et al. 1997; Chu et al. 1995)

In HBV1.3tg mice, HBcAg is present in nucleoli and cytoplasm of hepatocytes and kidney cells: complexes of HBc proteins are built de novo in the nucleus and are not transported via the nuclear membrane (Guidotti et al. 1994). Following cell division and in cells where HBV 3.5 mRNA (pgRNA) is more abundant (predominantly in centrilobular region of livers of HBV1.3tg mice), HBcAg particles are also found in the cytoplasm (Guidotti et al. 1995).

Liver sections of vaccinated HBV1.3tg mice (groups see Figure 38) were stained for HBc protein and HBc+ cells were counted (Figure 47). In the control group (wt) the expected correlation between HBcAg+ cells in liver section and the HBeAg level pre-boost was clearly evident, as it was for the group HBc. Of all groups, the vaccination group HBc-CD70 showed the lowest numbers of HBcAg+ cells in livers – especially in mice with high HBeAg levels in the serum. Due to small numbers of animals in combination with widely scattered HBeAg levels in the serum pre-boost, a significant trend was not observed.

In conclusion, 14 days after the MVA-boost immunization, a significant reduction of HBc protein was not observed in hepatocytes of vaccinated mice.



## 4. Discussion

Over 290 million people in the world are estimated to be chronically infected with HBV of whom hundreds of thousand die each year by complications like liver cirrhosis or hepatocellular carcinoma (WHO 2022). By now, there is no treatment available that reliably and effectively cures chronic HBV infection.

In CHB, HBV-specific T cells are immune tolerant towards HBV and do not effectively eliminate the virus. It has been shown previously, that *TherVacB* (heterologous protein-prime/MVA-boost vaccination, see 1.1.5) is able to break HBV-specific immunological tolerance in HBV transgenic mice with low to moderate HBV antigen concentrations, but at high HBV antigen concentrations, the therapeutic vaccine failed to induce HBV-specific CD8 T-cell immunity (Backes et al. 2016). Therefore, the *TherVacB* strategy was successfully combined with additional treatments before, during, and after vaccination in preclinical studies, which significantly increased the therapeutic efficacy even in animals with a high antigen load up to the permanent elimination of the virus in the AAV-HBV mouse model (model for CHB by infecting mice with Adenovirus which carries transgenic HBV) (Michler et al. 2020; Bunse et al. 2022; Kosinska et al. 2019).

### 4.1. HBV core as target antigen in protein-prime/MVA-boost vaccination

*TherVacB* incorporates the HBsAg and HBcAg in the protein-prime/MVA-boost vaccination (Backes et al. 2016). In order to investigate the role of CD70 co-expression in vaccine-induced CD8 T-cell immunity, only one antigen – the HBV core protein, a strong inducer of HBV-specific CD8 T-cell responses – was chosen as model antigen. The HBV surface protein was omitted in order to firstly exclude interference across specific responses and secondly avoid a robust antibody response with significant effects on HBV parameters (Michler et al. 2020; Kosinska et al. 2019; Kosinska et al. 2021). The use of HBV core as target antigen therefore allowed the scientific question of whether CD70 co-expression during the MVA-boost vaccination would increase T-cell immunity to be addressed.

## **4.2. MVA is a suitable boost vector for therapeutic vaccination with a transgenic co-stimulatory component**

### **4.2.1. Recombinant MVA is preferably used as boost vector**

As vaccination vector, MVA has a lot of advantages (high package capacity, high immunogenicity and good safety profile) but is preferably combined with a (protein) prime vaccination to effectively enhance target antigen-specific CD8 T-cell responses. Kastenmuller et al. demonstrated, that specific T cells compete for viral or transgenic epitopes on MVA-infected host cells (Kastenmuller et al. 2007). While this cross-competition was not important during priming, they showed, that T-cell cross-competition forms the immunodominance hierarchy at recall in boost vaccination and is strongly dependent on the timing of antigen expression of infected APCs. It has been demonstrated that in MVA-boost vaccination antigen-experienced CD8 T cells responding to epitopes derived from early viral proteins have a competitive advantage over those responding to epitopes that originate from late viral proteins. (Kastenmuller et al. 2007)

After vaccination of C57Bl/6 mice with MVA-core only (without protein prime), we observed, that the MVA vector-specific response was 10-fold higher, than the transgene-specific response - after two MVA vaccinations, it was even 10<sup>2</sup>-fold higher than the transgene-specific response (Figure 28). In sharp contrast, we saw that after protein-prime/MVA-boost vaccination in C57Bl6 mice, the target antigen-specific CD8 T-cell response (HBV core-specific) was 2-4 fold greater than the response against the immunodominant MVA epitope B8R (Figure 35). This means, that in our experiments we also could see, that a recall-response against a transgene under an early promoter (mH5) competed successfully against vector-specific immunity (a primary response). Further, we saw, that the mutual expression of transgene and CD70 focused the co-stimulatory effect of CD70 on the transgene. This indicates, that exact timing of CD70 co-expression during boost vaccination in combination with a protein prime effectively boosts transgene-specific CD8 T-cell responses and reduces the risk of unwanted co-stimulation.

#### **4.2.2. rMVA infected cells present the transgene (HBV core) and the MVA-specific early antigen B8R mainly by direct presentation**

Prior to the generation of the MVA vector expressing CD70 next to our target gene, we investigated whether the MVA transgenes - namely CD70 - can be assumed to be presented intact on the cell surfaces of antigen-presenting cells - so that it can exert its co-stimulatory function - or whether it must be assumed that most of the CD70 transgene is presented via the cross-presentation pathways - i.e. fragmented into T-cell epitopes - and is therefore useless for our approach.

To estimate the effect of cross-presentation in MVA immunization, immune responses of C57Bl/6 mice were compared to those of DNNGR1 deficient mice after vaccination. DNNGR1 mice lack a receptor for the uptake of dead cells and hence cross-presentation is impaired in these animals (Iborra et al. 2012). Mice were vaccinated once or twice with a recombinant MVA encoding HBcAg (rMVA-core). MVA- and HBcAg-specific activity of CD8 T cells was analyzed.

Surprisingly, MVA-specific responses were similar or even higher in DNNGR1 deficient mice than in C57Bl/6 mmice. After one vaccination, the MVA-specific CD8 T-cell response was 2.3-fold higher in DNNGR1 deficient mice ( $p=0.0007$ ) than in C57Bl/6 mice and was equally high after two vaccinations (Figure 28). The CD8 T-cell response upon stimulation with C<sub>93</sub> peptide (HBV core-derived epitope) was similar in all vaccination groups but 10<sup>2</sup>-fold lower than the MVA-specific CD8 T-cell responses.

The results of this experiment confirm, that CD8 T-cell responses to transgenes and the early MVA antigen B8R depend mainly on direct presentation. The limited time of transgene expression and presentation on infected cells before MVA-infected cells undergo apoptosis is enough to elicit CD8 T-cell responses. Consequentially, it can be expected, that transgenic CD70 will be presented intactly on MVA-infected cells and can provide its co-stimulatory function.

Still, it should be considered, that the route of administration of vaccinia virus is crucial for the importance of direct vs. cross-presentation (Shen et al. 2002). In the present study, rMVA was always administered i.p., but it is possible, that the impact of cross-presentation could increase in other application routes (as i.m. or s.c. vaccination), which could result in an abolished effect of CD70 co-stimulation.

The highly limited life-time of MVA-infected cells was a concern for the suitability of MVA as vaccination vector. But exactly this property brings an advantage when it comes to the safety of co-stimulation, especially by CD70: when co-stimulation is only temporary, the risk of over-stimulation of the immune system is limited. With respect to the specific properties of CD70 that have been found in many studies (see 1.3.1), constant stimulation by CD70 might have detrimental attenuating effects on immune responses while the beneficial effects depend most probably on temporarily limited exposure (Tesselaar et al. 2003a; Matter et al. 2006; Schildknecht et al. 2007). Delivery by MVA serves this requirement very well.

It remains an interesting question, why MVA-specific immune responses are higher in DNGR1 deficient mice than in C57Bl/6 mice. The available literature regularly shows impaired immune responses in DNGR1 deficient mice. The readout after one vaccination was performed six days after the MVA immunizations, when T cells are in the effector phase. In this constellation, the MVA-specific CD8 T-cell response was much higher in DNGR1 deficient mice. When mice were vaccinated twice (with three weeks in between), splenocytes were isolated for analysis 13 days after the last immunization and the heights of immune responses were almost identical. It would be interesting if the time point of analysis or the number of vaccinations contributed more to the significant advantage of DNGR1 deficient mice. But since this was not part of the scientific question of this work, it was not investigated further.

#### **4.2.3. CD70 and MVA is a suitable combination of co-stimulatory transgene and vector**

Keller et. al. showed, that co-stimulation of CD8 T cells by CD70/CD27 worked best on a subset of DCs (CD8+ DC) but poorly on other cells (for example B cells) (Keller et al. 2008). MVA infects a broad range of hematolymphoid cells (Chahroudi et al. 2005). In line, this work confirms that rMVA infects cells that upon expression of transgenic CD70 bring the desired advantages: increased antigen-specific CD8 T-cell stimulation. Furthermore, this work suggests, that the time frame of interaction between infected cells and T cells is on the right time point and long enough for exploitation of the CD70/CD27 axis. Moreover, a restricted time frame (apoptosis of infected cells) could prevent both hyperactivation of the immune system and on the

other side dysfunctionality and exhaustion due to prolonged CD27 activation (Tesselaar et al. 2003b; Matter et al. 2006; Denoed und Moser 2011).

### **4.3. CD70 co-stimulation improves the HBV core-specific T-cell response of vaccinated mice**

The results of intracellular and tetramer stainings for HBV core-specific T cells in vaccinated C57Bl/6 and HBV1.3tg mice substantiated the assumption that CD70 improves the CD8 T-cell response in quantity and quality. In C57Bl/6 mice, that were vaccinated with rMVA-HBc-CD70, the proportion of HBV core-specific CD8 T cells was significantly higher than in mice that were vaccinated with rMVA-HBc (2.5-fold, Figure 34). Furthermore, CD70 co-expression was able to trigger IFN $\gamma$  production in a higher portion of HBV core-specific CD8 T cells after vaccination with rMVA-C-CD70 in comparison to mice receiving vaccination without CD70 resulting in increased levels of functional T cells (Figure 35, Figure 36). These results indicate, that the enhanced immune response after vaccination with CD70 was firstly due to an increased number of HBV core-specific CD8 T cells and secondly due to more effective cells, that actually produce IFN $\gamma$  upon HBc peptide stimulation. IFN $\gamma$  is an important antiviral cytokine which can induce HBV cccDNA degradation without lysis of cells (Xia et al. 2016). Thus, IFN $\gamma$  is supposed to be very important for the clearance of HBV. A gain-of-function in terms of IFN $\gamma$ -expression by specific CD8 T cells, which has been observed in this study upon CD70 co-stimulation is very favorable in CHB.

It was shown in chimpanzees, that for viral clearance in acute HBV infection, CD8 T cells are the main effector cells and responsible for viral clearance while CD4 T cells play a minor role (Thimme et al. 2003). In therapeutic vaccination though, CD4 T cells have been shown to play a crucial role during the protein-prime phase for the development of the cellular immune response using *TherVacB* in AAV-HBV infected mice (Su et al. 2023). On the other hand, co-stimulation by CD70 was shown to uncouple the development of CD8 T-cell responses from CD4 T-cell help (Keller et al. 2009). Hence the main focus of this work was not on CD4 T-cell responses. Still, CD70 co-stimulation also showed an influence on CD4 T-cell responses of vaccinated C57Bl/6 mice. In two out of 4 mice, IFN $\gamma$  secretion of CD4 T cells was clearly increased after vaccination with rMVA-HBc-CD70 and HBc-peptide stimulation of splenocytes (Figure 37).

The findings of the vaccination experiments in C57Bl/6 mice were at least partly confirmed in HBV1.3tg mice. Unfortunately, the results lacked significance due to small numbers of animals. Most values of immune response evaluation correlate inversely with viremia of transgenic mice. The necessity of subgroup analysis left each subgroup with 2-5 animals. Though, a tendency, which confirms the beneficial effect of CD70 co-stimulation on HBV core-specific CD8 T-cell responses was apparent in the analysis of LAL and splenocytes (see Figure 41 and Figure 42).

In HBV1.3tg mice, LAL were isolated and analyzed in addition to splenocytes. This allows a distinction between peripheral and local immune response. In the vaccination experiments, CD8 T-cell responses were generally higher in LAL but also the beneficial effect of CD70 co-stimulation seemed to be greater in LAL in comparison to splenocytes (see Figure 41 and Figure 42). This was in accordance with Hendriks et al. (Hendriks et al. 2003), who found in a mouse model of influenza infection that effects of CD27 stimulation predominantly contribute to T-cell responses at the site of infection.

Immature, resting DCs normally are important inductors of peripheral CD8 T-cell tolerance. Physiologically, this function prevents autoimmunity and overshooting immune responses but also might promote tolerance to chronic infections and cancer. (Probst et al. 2005; Hawiger et al. 2001) Some studies suggest, that poxviruses impair the maturation of DCs after infection, which could be detrimental for efficient T-cell activation after MVA immunization (Kastenmuller et al. 2006; Engelmayer et al. 1999). Keller et al. (Keller et al. 2009) showed that immature DCs which are endowed by transgenic CD70, change from a tolerogenic to an immunogenic state and lead to tumor control in a murine tumor model. Primary responses were improved in quantity and effector function of CD8 T cells was further improved. This work also provided evidence, that CD70 co-stimulation leads to improved CD8 T cell responses in terms of quantity and quality. Possibly, transgenic CD70 can compensate a lack of maturation of DCs during the MVA boost. These results substantiate, that co-stimulation by CD70 is reasonable in MVA-boost vaccination against CHB.

#### **4.4. Vaccination with transgenic HBc supports clusters of T cells in the livers of HBV1.3tg mice and CD70 enhances this effect**

The livers of vaccinated HBV1.3tg mice were isolated, sliced and immunologically stained to identify cellular immune reactions at the site of HBV-transgene expression. First, the mere number of CD3+ cells (T cells) was counted and revealed that vaccination negligibly increases the number of T cells in the liver (Figure 39, C). This finding is in line with a study in chronically HBV infected patients (Maini et al. 2000): patients with and without viral control had comparable numbers of HBV core-specific CD8 T cells in the liver and Maini et al. suggest, that the control of viral replication is a matter of responsiveness of specific T cells and not of their quantity. It is probable, that in infected patients with viral control, few and scattered HBV-specific cells in the liver can inhibit viral replication by secretion of antiviral cytokines without causing inflammation (Maini et al. 2000; Rehermann 2000). On the other hand, Maini et al. found high numbers of ineffective – since tolerant – T cells in patients with insufficient suppression of viral replication, that furthermore are thought to promote inflammation and liver fibrosis via cytokine-mediated infiltration with a high number of non-specific T cells. In summary, the number of CD3+ T cells in the liver neither allows a statement on quality and effectiveness of the cellular immune response in the liver nor on the likelihood of immunopathology. This explains, why absolute CD3+ T cell counts did not alter between the vaccination experiments in HBV1.3tg mice.

However, the distribution of CD3+ T cells in the liver allows an interpretation of T-cell responsiveness at the site of antigen-presentation (liver): clusters of CD3+ cells were more frequent in livers of vaccinated mice. This effect appeared to be independent from HBeAg levels of mice and was even clearer in mice that were vaccinated with rMVA-C-CD70 (2-fold increase compared to control mice that were vaccinated with MVAwt; Figure 39, E). Clusters of T cells were ki67 positive (a marker for proliferating cells), suggesting that those clusters represent expanding T cells. The histological staining against CD3 and ki67 does not give evidence of specificity of those clustering cells but as they formed primarily after vaccination with HBc, a specificity for HBc is most likely.

Rehermann (Rehermann 2000) described, that in the situation of high antigen levels in the liver, T cells migrate to the liver, where especially CD8 T cells undergo apoptosis within 18 h („graveyard for activated T cells“). High concentrations of HBV antigens in the absence of sufficient co-stimulation might be the cause for this activation-induced cell death. This concept could explain the increased number of T-cell clusters in vaccinated mice. It is plausible that activated antigen-specific T cells from the periphery migrate to the site of antigen presentation in the liver where they respond to antigen stimulation with expansion and antiviral activity. The data of this study suggests that CD70 supports those processes by the prevention of tolerance and the promotion of T-cell survival.

CD8 T cells in liver associated lymphocytes (LAL) from vaccinated HBV1.3tg mice showed an inverse correlation of antigenemia and proportion of HBV core-specific CD8 T cells (Figure 40). This was expected, as it was already described (Backes et al. 2016). Unexpectedly, there could not be observed a correlation between antigenemia and absolute numbers or numbers of T-cell clusters in histological stainings of liver sections (Figure 39, C and D). Of course, only a maximum of 8% of LAL, that were isolated and stained with tetramers, were HBV-core specific (in most mice much less) and hence it could not be expected to find a significant change in the absolute count of CD3+ T cells in liver samples. But since the number of cell clusters is interpreted as immunological responsiveness it would have been consistent if CD3+ T-cell clusters also showed an inverse correlation with antigenemia, but this could not be observed. Further characterization of those intrahepatic T cells (in situ tetramer staining of histological liver cuts for example) could elucidate those questions.

Summarized, those results suggest that vaccination of HBV1.3tg mice against HBc does not increase the number of T cells in the liver but the responsiveness of specific T cells (more precisely: increased expansion and perhaps prolonged survival). Vaccination with rMVA-HBc-CD70 enhanced this effect and confirmed that CD70 is an appropriate component to meet the requirements of an immunotherapeutic vaccination in CHB.

#### **4.5. Therapeutic vaccination with transgenic CD70 boosts the immune response very specifically**

The comparison of MVA-specific and HBV core-specific CD8 T-cell responses of C57Bl/6 mice and HBV1.3tg mice (mice with low HBeAg titers) demonstrated, that the MVA-specific response was only slightly increased while the HBV core-specific response was doubled after co-stimulation with transgenic CD70 (Figure 35, Figure 42). This effect is desirable and argues for the usefulness of transgenic CD70 as a component of the MVA-boost vector.

One reason, why HBV core-specific responses benefited most from the rMVA-C-CD70 boost is the protein prime, which conferred an advantage on the target-specific T-cell response as it is a secondary response – in contrast to the MVA-specific response, which is primary. The recall-response after boost vaccination and not the initial prime has been described to shape the immunodominance hierarchy favoring proteins that are expressed under early promoters (Kastenmuller et al. 2007) and this advantage appeared to be even improvable by CD70 co-expression in C57Bl/6 mice. The importance of the protein prime for HBV core-specific CD8 T-cell responses has been described previously (Backes et al. 2016) and was also evident in this study: after HBc protein-prime/rMVA-boost vaccination of C57Bl/6 mice (Figure 35), the HBV core-specific CD8 T cell response was >10-fold increased in comparison to mice, which received rMVA-core twice without protein prime (Figure 28). A second or additional reason for the observed specificity of CD70 co-stimulation might be the spatial and temporal interrelation of the expression of the transgenes. This hypothesis is underlined by comparison with the results of a study by Bathke et. al., where an MVA-OVA-CD70 vector was constructed with the transgene (OVA) and CD70 under different promoters (the pS promoter for OVA and the pHyb promoter for CD70) (Bathke et al. 2018). After two immunizations with rMVA they found, that MVA-specific CD8 T-cell responses (against B8R) gained more from CD70 co-stimulation than the OVA-specific responses and the total CD8 T-cell response was greater for B8R than for OVA in C57BL/6 mice. As described above, we observed the opposite in our HBc protein-prime/rMVA-boost vaccination experiments with rMVA-C-CD70. Certainly, the main difference in study design is the lacking protein-prime vaccination, which favors HBV core-specific CD8 T-cell immunity during the boost vaccination as explained in the previous section. But the differences in MVA vector design could also be crucial:

the early and equimolar expression of the transgenes CD70 and HBc by utilizing the mutual early promoter mH5 and the post-translational cleavage site P2A (Luke et al. 2008) might concentrate the co-stimulatory effect of CD70 on the target antigen HBc.

#### **4.6. Reduction of HBcAg-expression in the liver of vaccinated HBV1.3tg mice could not be observed in this study**

The HBc-protein-prime/rMVA-boost vaccination without and in particular with co-stimulation by transgenic CD70 did elicit vivid CD8 T-cell responses with effector cells expressing antiviral effector cytokines (Figure 42). In the livers of vaccinated HBV1.3tg mice, the number of T-cell clusters was increased (Figure 39). It was presumed that those cells would decrease HBV core antigen in the liver. Unfortunately, the number of hepatocytes that were positive for HBcAg in the cytoplasm or nucleolus of vaccinated mice and control mice was not significantly different (Figure 47).

The liver histology was taken at day 14 after the MVA boost. Effector phases of CD8 T cells with maximal ALT levels are around day 6 (personal communication with Anna Kosinska). As the HBV genome is integrated into the genome of HBV1.3tg mice, it cannot be eliminated from hepatocytes. Maybe, antigen levels recovered after the initial effector phase to similar levels at day 14. HBcAg levels at earlier time points were not examined in this work.

#### **4.7. An influence of CD70 co-stimulation on the HBV core-specific antibody response could not be observed**

After vaccination of HBV1.3tg mice with a HBc-protein prime and rMVA-HBc-(+/- CD70) boost, we observed, that antibodies against HBc developed mainly after the protein prime. A significant difference of co-stimulation by transgenic CD70 on the development of anti-HBc-antibodies was not detectable.

Taken together, serological effects of CD70 could not be shown in this study. Anti-HBc-antibodies occurred in both groups already after the protein prime and the MVA boost (with or without CD70 co-stimulation) did not add much effect. This was in line with another study, where blockage of CD70 during immunization with MVA did not diminish the MVA-specific antibodies while there was a significant reduction of MVA-specific CD8 T cells (Bathke et al. 2018).

## 4.8. Outlook

The results of the current study leave the following remaining open questions and suggest further experiments:

- To strengthen the data of the vaccination experiments in HBV1.3tg mice, the vaccination experiments could be repeated with a higher number of mice and in groups of mice with comparable levels of HbeAg (low and high).
- Liver histology of HBV1.3tg mice at day 6 after rMVA boost and staining for HBcAg could be performed. It would be interesting to see if HbcAg is reduced due to improved CD8 T-cell function. Alternatively, one could vaccinate another mouse model in which infected cells can be cleared from the virus (e.g. in AAV-HBV-infected mice).
- Vaccination of C57Bl/6 mice with HBc-protein/+/-MVAwt prime and rMVA-HBc±CD70 boost. Evaluation of the HBV core- and MVA-specific CD8 T-cell response could elucidate the question whether CD70 co-stimulation specifically enhances the CD8 T-cell response due to the temporal coupling with the transgene HBc or if CD70 generally is better in boosting already primed T cells than in supporting priming T cells in the first place.

## 4.9. Conclusion: CD70 co-stimulation is a potential improvement for therapeutic vaccination

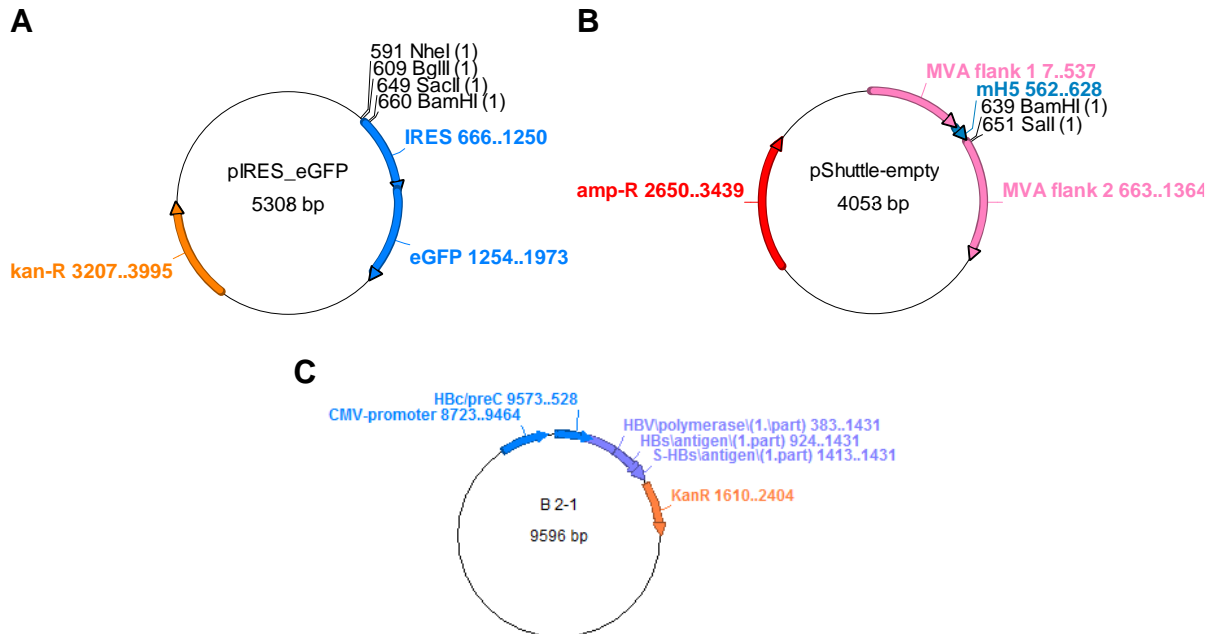
In this work, a recombinant MVA encoding a viral antigen (HBc) and the immunostimulatory molecule CD70 was generated and estimated in a HBc-protein-prime/rMVA-vector boost setting in C57Bl/6 mice and HBV1.3tg mice.

The co-stimulatory molecule CD70 was shown to provide an additional beneficial effect in induction of antigen-specific cellular immune responses, especially in CD8 T cells which are believed to be the key to control or cure CHB. I thus conclude, that CD70 is a promising candidate for co-stimulation in therapeutic vaccination against CHB and maybe other chronic infectious or malignant diseases, which benefit from specific CD8 T cells. Further, this study highlights the importance of the study- and vector design. It confirms the importance of a protein-prime vaccination prior to the rMVA-immunization to enhance the target antigen-specific cellular immunity and suggests, that CD70 co-stimulation is particularly applicable to favor the secondary

CD8 T cell response against the target antigen during boost vaccination. Also, this study points out, that co-stimulation by transgenic CD70 is very specific, when CD70 is spatially and temporarily coupled to the target-antigen by mutual expression under an early promoter. Further, the expression in MVA seems advisable as it limits the time-frame of (co-)stimulation. Together, these considerations lower the risk of adverse or unspecific immune (over)activation while CD70 can improve the target-antigen specific CD8 T-cell response not only in numbers but also by lowering tolerance and improving cytokine production of specific CD8 T cells.

# Appendices

Appendix 1 - **Plasmid charts of plasmids pIRES\_eGFP (A), pShuttle-empty (B) and B2-1 (C)** that were used as backbones for the construction of the Shuttle plasmids for rMVA production. Charts indicate the name and position of each gene as well as the unique restriction sites that were used for cloning by restriction enzyme digest.



Appendix 2 - **DNA sequence and protein translation of the sequence of the CD70 gene, that was used for the production of viral vector rMVA-HBc-CD70.** Upper line shows the genetic code, second line the corresponding amino acid and the lower line the position within the CD70 gene.

```

ATG CCG GAG GAG GGT TCG GGC TGC TCG GTG CGG CGC AGG CCC TAT GGG TGC GTC CTG CGG GCT GCT TTG GTC CCA < 75
M  P  E  E  G  S  G  C  S  V  R  R  P  Y  G  C  V  L  R  A  A  L  V  P
      10          20          30          40          50          60          70

TTG GTC GCG GGC TTG GTG ATC TGC CTC GTG GTG TGC ATC CAG CGC TTC GCA CAG GCT CAG CAG CAG CTG CCG CTC < 150
L  V  A  G  L  V  I  C  L  V  V  C  I  Q  R  F  A  Q  A  Q  Q  Q  L  P  L
      80          90          100         110         120         130         140

GAG TCA CTT GGG TGG GAC GTA GCT GAG CTG CAG CTG AAT CAC ACA GGA CCT CAG CAG GAC CCC AGG CTA TAC TGG < 225
E  S  L  G  W  D  V  A  E  L  Q  L  N  H  T  G  P  Q  Q  D  P  R  L  Y  W
      160         170         180         190         200         210         220

CAG GGG GGC CCA GCA CTG GGC CGC TCC TTC CTG CAT GGA CCA GAG CTG GAC AAG GGG CAG CTA CGT ATC CAT CGT < 300
Q  G  G  P  A  L  G  R  S  F  L  H  G  P  E  L  D  K  G  Q  L  R  I  H  R
      230         240         250         260         270         280         290

GAT GGC ATC TAC ATG GTA CAC ATC CAG GTG ACG CTG GCC ATC TGC TCC TCC ACG ACG GCC TCC AGG CAC CAC CCC < 375
D  G  I  Y  M  V  H  I  Q  V  T  L  A  I  C  S  S  T  T  A  S  R  H  H  P
      310         320         330         340         350         360         370

ACC ACC CTG GCC GTG GGA ATC TGC TCT CCC GCC TCC CGT AGC ATC AGC CTG CTG CGT CTC AGC TTC CAC CAA GGT < 450
T  T  L  A  V  G  I  C  S  P  A  S  R  S  I  S  L  L  R  L  S  F  H  Q  G
      380         390         400         410         420         430         440

TGT ACC ATT GCC TCC CAG CGC CTG ACG CCC CTG GCC CGA GGG GAC ACA CTC TGC ACC AAC CTC ACT GGG ACA CTT < 525
C  T  I  A  S  Q  R  L  T  P  L  A  R  G  D  T  L  C  T  N  L  T  G  T  L
      460         470         480         490         500         510         520

TTG CCT TCC CGA AAC ACT GAT GAG ACC TTC TTT GGA GTG CAG TGG GTG CGC CCC TGA < 582
L  P  S  R  N  T  D  E  T  F  F  G  V  Q  W  V  R  P  *
      530         540         550         560         570         580
  
```





```

      G G P A L G R S F L H G P E L D K G Q L
Seq_1 2401 R I H R D G I Y M V H I Q V T L A I C S
TACGTATCCATCGTATGGCATCTACATGGTACACATCCAGGTGACGCTGGCCATC TGC T 2460
Seq_2 266 TACGTATCCATCGTATGGCATCTACATGGTACACATCCAGGTGACGCTGGCCATC TGT T 325
      R I H R D G I Y M V H I Q V T L A I C S

Seq_1 2461 S T T A S R H H P T T L A V G I C S P A
CCTCCACGACGGCCTCCAGGCACACCCACCCACCCCTGGCCGTGGGAATCTGCTCTCCCG 2520
Seq_2 326 CCTCCACGACGGCCTCCAGGCACACCCACCCACCCCTGGCCGTGGGAATCTGCTCTCCCG 385
      S T T A S R H H P T T L A V G I C S P A

Seq_1 2521 S R S I S L L R L S F H Q G C T I A S Q
CCTCCCGTAGCATCAGCCTGCTGCGTCTCAGCTTCCACCAAGGTTGTACCATTGCCTCCC 2580
Seq_2 386 CCTCCCGTAGCATCAGCCTGCTGCGTCTCAGCTTCCACCAAGGTTGTACCATTGCCTCCC 445
      S R S I S L L R L S F H Q G C T I A S Q

Seq_1 2581 R L T P L A R G D T L C T N L T G T L L
AGCGCCTGACGCCCTGGCCCGAGGGGACACACTCTGCACCAACCTCACTGGGACACTTT 2640
Seq_2 446 AGCGCCTGACGCCCTGGCCCGAGGGGACACACTCTGCACCAACCTCACTGGGACACTTT 505
      R L T P L A R G D T L C T N L T G T L L

Seq_1 2641 P S R N T D E T F F G V Q W V R P * L T
TGCTTCCCGAAACACTGATGAGACCTTCTTTGGAGTGCAGTGGGTGCGCCCTGATTGA 2700
Seq_2 506 TGCTTCCCGAAACACTGATGAGACCTTCTTTGGAGTGCAGTGGGTGCGCCCTGATTGA 565
      P S R N T D E T F F G V Q W V R P * L T

```

Appendix 5 - Alignment of Sequence of p2-1 with Sanger Sequencing result. Primer 10 was used for sequencing of HBc (see chapter 2.1.4 for list of primers). The first few base pairs of sanger sequencing are not accurate due to process limitations. Apart from this, the sequences are identical. Alignment was done with Serial Cloner.

Features [Seq\_1]:

HBc [1455 : 2006 - CW]  
 IRES [2018 : 2602 - CW]

```

Seq_1 1441 S * A T M D I D P Y K E F G A T V E L
GGTCGTGAGCCACATGGACATCGACCCTTATAAAGAA-TTTGGAGCTACTGTGGAG-TT 1498
Seq_2 1 -----GtG-nttTtTtgCTaCTGTGgagnTt 26
X F F A T V E X

Seq_1 1499 L S F L P S D F F P S V R D L L D T A S
ACTCTCGTTTTTGCCCTTCTGACTTCTTTCCTTCAGTACGAGATCTTCTAGATACCGCCTC 1558
Seq_2 27 AcTCTcgtTTTTCCTTCTGACTTCTTTCCTTCAGTACGAGATCTTCTAGATACCGCCTC 86
T L V F A F * L L S F S T R S S R Y R L

Seq_1 1559 A L Y R E A L E S P E H C S P H H T A L
AGCTCTGTATCGGGAAGCCTTAGAGTCTCCTGAGCATTGTTACCTCACCATACTGCACT 1618
Seq_2 87 AGCTCTGTATCGGGAAGCCTTAGAGTCTCCTGagCATTGTTACCTCACCATACTGCACT 146
S S V S G S L R V S * A L F T S P Y C T

Seq_1 1619 R Q A I L C W G E L M T L A T W V G V N
CAGGCAAGCAATTCTTTGCTGGGGGAACCTAATGACTCTAGCTACCTGGGTGGGTGTTAA 1678
Seq_2 147 CAGGCAAGCAATTCTTTGCTGGGGGAACCTAATGACTCTAGCTACCTGGGTGGGTGTTAA 206
Q A S N S L L G G T N D S S Y L G G C *

Seq_1 1679 L E D P A S R D L V V S Y V N T N M G L
TTTGGAAGATCCAGCGTCTAGAGACCTAGTAGTCAGTTATGTCAACACTAATATGGGCCT 1738
Seq_2 207 TTTGGAAGATCCAGCGTCTAGAGACCTAGTAGTCAGTTATGTCAACACTAATATGGGCCT 266
F G R S S V * R P S S Q L C Q H * Y G P

Seq_1 1739 K F R Q L L W F H I S C L T F G R E T V
AAAGTTCAGGCAACTCTGTGGTTTCACATTCTGTCTCACTTTTGGGAAGAGAAACAGT 1798
Seq_2 267 AAAGTTCAGGCAACTCTGTGGTTTCACATTCTGTCTCACTTTTGGGAAGAGAAACAGT 326
K V Q A T L V V S H F L S H F W K R N S

```

```

Seq_1 1799 I E Y L V S F G V W I R T P P A Y R P P 1858
TATAGAGTATTTGGTGTCTTTCGGAGTGTGGATTCGCACTCCTCCAGCTTATAGACCACC
Seq_2 327 TATAGAGTATTTGGTGTCTTTCGGAGTGTGGATTCGCACTCCTCCAGCTTATAGACCACC 386
Y R V F G V F R S V D S H S S S L * T T

Seq_1 1859 N A P I L S T L P E T T V V R R R G R S 1918
AAATGCCCTATCCTATCAACTTCCGGAGACTACTGTTGTTAGACGACGAGGCAGGTC
Seq_2 387 AAATGCCCTATCCTATCAACTTCCGGAGACTACTGTTGTTAGACGACGAGGCAGGTC 446
K C P Y P I N T S G D Y C C * T T R Q V

Seq_1 1919 P R R R T P S P R R R R S Q S P R R R R 1978
CCCTAGAAGAAGAACTCCCTCGCTCGCAGACGAAGGCTCAATCGCCGGTGCAGAAAG
Seq_2 447 CCCTAGAAGAAGAACTCCCTCGCTCGCAGACGAAGGCTCAATCGCCGGTGCAGAAAG 506
P * K K N S L A S Q T K V S I A A S Q K

Seq_1 1979 S Q S R E S Q C * Y S D P P L S L P P P 2038
ATCTCAATCTCGGGAATCTCAATGTTAGTATTTCGGATCCGCCCTCTCCCTCCCCCCCC
Seq_2 507 ATCTCAATCTCGGGAATCTCAATGTTAGTATTTCGGATCCGCCCTCTCCCTCCCCCCCC 566
I S I S G I S M L V F G S A P L P P P P

```

Appendix 6 – **Summary of all vaccination experiments with HBV1.3tg mice performed within the scope of this dissertation.** The experiments were performed in 4 rounds with varying numbers of mice of different HBeAg titers. As the different readouts (ICS, tetramer staining and liver histology) were not performed or data analysis was not applicable for all experiment, the table gives an overview of the performed experimental readouts and which data was used for analysis.

HBV1.3tg mouse vaccinations		round 1			round 2			round 3			round 4		
mice per group	wt	4			1			2			2 (+1 dead*)		
	HBc	4			4			5			6		
	HBc-CD70	3 (+1 nonresp.*)			4			5			5 (+1 dead*)		
		wt	HBc	HBc-CD70	wt	HBc	HBc-CD70	wt	HBc	HBc-CD70	wt	HBc	HBc-CD70
HBeAg titers		2.5	0.5	0.5	40	37	38	80	3.5	3	14.7	21.4	5.8
		2	3.5	2.5		34	45	85	2.5	3	2.9	16.6	20.7
		2.5	1.5	0.7		36	32		4	7	19.2*	3.8	9
		0.5	0.5	3.5*		44	41		7.5	6.5		7.8	20.2
										3	1		22.5
											2.5	16.3*	
tetramer staining	LAL											*2	
	splenocytes												
ICS	LAL											*1	
	splenocytes												
Liver histology													
experiments performed													
experiments performed but excluded from final analysis *1													
*1 wrong buffer in staining - a lot of background in the analysis													
*2 experiment and data acquisition performed by Anna Kosinska													

## List of references

- Aghasadeghi, Mohammad Reza; Velayati, Ali Akbar; Mamishi, Setareh; Nabavi, Mahmood; Aghakhani, Arezoo; Bidari-Zerehpooch, Farahnaz et al. (2016): Low prevalence of hepatitis B vaccine escape mutants among individuals born after the initiation of a nationwide vaccination program in Iran. In: *Archives of virology* 161 (12), S. 3405–3411. DOI: 10.1007/s00705-016-3050-1.
- Anderson, R. J.; Hannan, C. M.; Gilbert, S. C.; Laidlaw, S. M.; Sheu, E. G.; Korten, S. et al. (2004): Enhanced CD8+ T Cell Immune Responses and Protection Elicited against Plasmodium berghei Malaria by Prime Boost Immunization Regimens Using a Novel Attenuated Fowlpox Virus. In: *The Journal of Immunology* 172 (5), S. 3094–3100. DOI: 10.4049/jimmunol.172.5.3094.
- Antoine, G.; Scheiflinger, F.; Dorner, F.; Falkner, F. G. (1998): The complete genomic sequence of the modified vaccinia Ankara strain: comparison with other orthopoxviruses. In: *Virology* 244 (2), S. 365–396. DOI: 10.1006/viro.1998.9123.
- Arens, Ramon; Nolte, Martijn A.; Tesselaar, Kiki; Heemskerk, Bianca; Reedquist, Kris A.; van Lier, Rene A. W.; van Oers, Marinus H. J. (2004): Signaling through CD70 regulates B cell activation and IgG production. In: *Journal of immunology (Baltimore, Md. : 1950)* 173 (6), S. 3901–3908.
- Backes, Simone; Jager, Clemens; Dembek, Claudia J.; Kosinska, Anna D.; Bauer, Tanja; Stephan, Ann-Sophie et al. (2016): Protein-prime/modified vaccinia virus Ankara vector-boost vaccination overcomes tolerance in high-antigenemic HBV-transgenic mice. In: *Vaccine* 34 (7), S. 923–932. DOI: 10.1016/j.vaccine.2015.12.060.
- Barnes, Eleanor (2015): Therapeutic vaccines in HBV: lessons from HCV. In: *Medical microbiology and immunology* 204 (1), S. 79–86. DOI: 10.1007/s00430-014-0376-8.
- Bathke, Barbara; Pätzold, Juliane; Kassub, Ronny; Giessel, Raphael; Lämmermann, Kerstin; Hinterberger, Maria et al. (2018): CD70 encoded by modified vaccinia virus Ankara enhances CD8 T-cell-dependent protective immunity in MHC class II-deficient mice. In: *Immunology* 154 (2), S. 285–297. DOI: 10.1111/imm.12884.
- Baur, Karen; Brinkmann, Kay; Schwenecker, Marc; Patzold, Juliane; Meisinger-Henschel, Christine; Hermann, Judith et al. (2010): Immediate-early expression of a recombinant antigen by modified vaccinia virus ankara breaks the immunodominance of strong vector-specific B8R antigen in acute and memory CD8 T-cell responses. In: *Journal of virology* 84 (17), S. 8743–8752. DOI: 10.1128/JVI.00604-10.
- Bertrand, P.; Maingonnat, C.; Penther, D.; Guney, S.; Ruminy, P.; Picquenot, J. M. et al. (2013): The costimulatory molecule CD70 is regulated by distinct molecular mechanisms and is associated with overall survival in diffuse large B-cell lymphoma. In: *Genes, chromosomes & cancer* 52 (8), S. 764–774. DOI: 10.1002/gcc.22072.
- Block, Timothy M.; Guo, Haitao; Guo, Ju-Tao (2007): Molecular virology of hepatitis B virus for clinicians. In: *Clinics in liver disease* 11 (4), 685-706, vii. DOI: 10.1016/j.cld.2007.08.002.
- Boni, Carolina; Fisicaro, Paola; Valdatta, Caterina; Amadei, Barbara; Di Vincenzo, Paola; Giuberti, Tiziana et al. (2007): Characterization of hepatitis B virus (HBV)-specific T-cell dysfunction in chronic HBV infection. In: *Journal of virology* 81 (8), S. 4215–4225. DOI: 10.1128/JVI.02844-06.
- Bronte, V.; Carroll, M. W.; Goletz, T. J.; Wang, M.; Overwijk, W. W.; Marincola, F. et al. (1997): Antigen expression by dendritic cells correlates with the therapeutic effectiveness of a model recombinant poxvirus tumor vaccine. In: *Proceedings of the National Academy of Sciences of the United States of America* 94 (7), S. 3183–3188.
- Bunse, Till; Kosinska, Anna D.; Michler, Thomas; Protzer, Ulrike (2022): PD-L1 Silencing in Liver Using siRNAs Enhances Efficacy of Therapeutic Vaccination for Chronic Hepatitis B. In: *Biomolecules* 12 (3). DOI: 10.3390/biom12030470.
- Bzowej, Natalie H. (2010): Hepatitis B Therapy in Pregnancy. In: *Current hepatitis reports* 9 (4), S. 197–204. DOI: 10.1007/s11901-010-0059-x.
- Cavanaugh, V. J.; Guidotti, L. G.; Chisari, F. V. (1998): Inhibition of hepatitis B virus replication during adenovirus and cytomegalovirus infections in transgenic mice. In: *Journal of virology* 72 (4), S. 2630–2637.

- Centers for Disease Control and Prevention (Hg.) (2016): Viral Hepatitis - Hepatitis B Information. Perinatal Transmission, zuletzt aktualisiert am 04.10.2016.
- Chahroudi, Ann; Chavan, Rahul; Kozyr, Natalia; Waller, Edmund K.; Silvestri, Guido; Feinberg, Mark B. (2005): Vaccinia virus tropism for primary hemolymphoid cells is determined by restricted expression of a unique virus receptor. In: *Journal of virology* 79 (16), S. 10397–10407. DOI: 10.1128/JVI.79.16.10397-10407.2005.
- Chahroudi, Ann; Garber, David A.; Reeves, Patrick; Liu, Luzheng; Kalman, Daniel; Feinberg, Mark B. (2006): Differences and similarities in viral life cycle progression and host cell physiology after infection of human dendritic cells with modified vaccinia virus Ankara and vaccinia virus. In: *Journal of virology* 80 (17), S. 8469–8481. DOI: 10.1128/JVI.02749-05.
- Chan, Henry Lik-Yuen; Sung, Joseph Jao-Yiu (2006): Hepatocellular carcinoma and hepatitis B virus. In: *Seminars in liver disease* 26 (2), S. 153–161. DOI: 10.1055/s-2006-939753.
- Chisari, F. V.; Ferrari, C. (1995): Hepatitis B virus immunopathogenesis. In: *Annual review of immunology* 13, S. 29–60. DOI: 10.1146/annurev.iy.13.040195.000333.
- Chu, C. M.; Yeh, C. T.; Chien, R. N.; Sheen, I. S.; Liaw, Y. F. (1997): The degrees of hepatocyte nuclear but not cytoplasmic expression of hepatitis B core antigen reflect the level of viral replication in chronic hepatitis B virus infection. In: *Journal of clinical microbiology* 35 (1), S. 102–105.
- Chu, C. M.; Yeh, C. T.; Sheen, I. S.; Liaw, Y. F. (1995): Subcellular localization of hepatitis B core antigen in relation to hepatocyte regeneration in chronic hepatitis B. In: *Gastroenterology* 109 (6), S. 1926–1932.
- Cornberg, Markus; Sandmann, Lisa; Protzer, Ulrike; Niederau, Claus; Tacke, Frank; Berg, Thomas et al. (2021): S3-Leitlinie der Deutschen Gesellschaft für Gastroenterologie, Verdauungs- und Stoffwechselkrankheiten (DGVS) zur Prophylaxe, Diagnostik und Therapie der Hepatitis-B-Virusinfektion – (AWMF-Register-Nr. 021-11). In: *Zeitschrift für Gastroenterologie* 59 (7), S. 691–776. DOI: 10.1055/a-1498-2512.
- Dandri, Maura; Locarnini, Stephen (2012): New insight in the pathobiology of hepatitis B virus infection. In: *Gut* 61 Suppl 1, i6-17. DOI: 10.1136/gutjnl-2012-302056.
- Dembek, Claudia; Protzer, Ulrike (2015): Mouse models for therapeutic vaccination against hepatitis B virus. In: *Medical microbiology and immunology* 204 (1), S. 95–102. DOI: 10.1007/s00430-014-0378-6.
- Dembek, Claudia; Protzer, Ulrike; Roggendorf, Michael (2018): Overcoming immune tolerance in chronic hepatitis B by therapeutic vaccination. In: *Current opinion in virology* 30, S. 58–67. DOI: 10.1016/j.coviro.2018.04.003.
- Denoed, Julie; Moser, Muriel (2011): Role of CD27/CD70 pathway of activation in immunity and tolerance. In: *Journal of leukocyte biology* 89 (2), S. 195–203. DOI: 10.1189/jlb.0610351.
- Depla, E.; van der Aa, A.; Livingston, B. D.; Crimi, C.; Allosery, K.; Brabandere, V. de et al. (2008): Rational design of a multiepitope vaccine encoding T-lymphocyte epitopes for treatment of chronic hepatitis B virus infections. In: *Journal of virology* 82 (1), S. 435–450. DOI: 10.1128/JVI.01505-07.
- Drexler, Ingo; Staib, Caroline; Sutter, Gerd (2004): Modified vaccinia virus Ankara as antigen delivery system: how can we best use its potential? In: *Current opinion in biotechnology* 15 (6), S. 506–512. DOI: 10.1016/j.copbio.2004.09.001.
- Durant, Lydia R.; Pereira, Catherine; Boakye, Aime; Makris, Spyridon; Kausar, Fahima; Goritzka, Michelle; Johansson, Cecilia (2014): DNCR-1 is dispensable for CD8+ T-cell priming during respiratory syncytial virus infection. In: *European journal of immunology* 44 (8), S. 2340–2348. DOI: 10.1002/eji.201444454.
- EASL (2017): Clinical Practice Guidelines on the management of hepatitis B virus infection. In: *Journal of hepatology* 67 (2), S. 370–398. DOI: 10.1016/j.jhep.2017.03.021.
- Engelmayer, J.; Larsson, M.; Subklewe, M.; Chahroudi, A.; Cox, W. I.; Steinman, R. M.; Bhardwaj, N. (1999): Vaccinia virus inhibits the maturation of human dendritic cells: a novel mechanism of immune evasion. In: *Journal of immunology (Baltimore, Md. : 1950)* 163 (12), S. 6762–6768.

- Fiscaro, Paola; Valdatta, Caterina; Massari, Marco; Loggi, Elisabetta; Biasini, Elisabetta; Sacchelli, Luca et al. (2010): Antiviral Intrahepatic T-Cell Responses Can Be Restored by Blocking Programmed Death-1 Pathway in Chronic Hepatitis B. In: *Gastroenterology* 138 (2), 682-693.e4. DOI: 10.1053/j.gastro.2009.09.052.
- Flieswasser, Tal; van den Eynde, Astrid; van Audenaerde, Jonas; Waele, Jorrit de; Lardon, Filip; Riether, Carsten et al. (2022): The CD70-CD27 axis in oncology: the new kids on the block. In: *Journal of experimental & clinical cancer research : CR* 41 (1), S. 12. DOI: 10.1186/s13046-021-02215-y.
- Flores, Joan Ericka; Thompson, Alexander J.; Ryan, Marno; Howell, Jessica (2022): The Global Impact of Hepatitis B Vaccination on Hepatocellular Carcinoma. In: *Vaccines* 10 (5). DOI: 10.3390/vaccines10050793.
- Fofana, Djeneba B.; Somboro, Anou M.; Maiga, Mamoudou; Kampo, Mamadou I.; Diakit , Brehima; Cissoko, Yacouba et al. (2023): Hepatitis B Virus in West African Children: Systematic Review and Meta-Analysis of HIV and Other Factors Associated with Hepatitis B Infection. In: *International journal of environmental research and public health* 20 (5). DOI: 10.3390/ijerph20054142.
- Francis, M. J.; Hastings, G. Z.; Brown, A. L.; Grace, K. G.; Rowlands, D. J.; Brown, F.; Clarke, B. E. (1990): Immunological properties of hepatitis B core antigen fusion proteins. In: *Proceedings of the National Academy of Sciences of the United States of America* 87 (7), S. 2545–2549.
- Ganem, Don; Prince, Alfred M. (2004): Hepatitis B virus infection--natural history and clinical consequences. In: *The New England journal of medicine* 350 (11), S. 1118–1129. DOI: 10.1056/NEJMra031087.
- Gasteiger, Georg; Kastenmuller, Wolfgang; Ljapoci, Ronny; Sutter, Gerd; Drexler, Ingo (2007): Cross-priming of cytotoxic T cells dictates antigen requisites for modified vaccinia virus Ankara vector vaccines. In: *Journal of virology* 81 (21), S. 11925–11936. DOI: 10.1128/JVI.00903-07.
- Gentile, Ivan; Borgia, Guglielmo (2014): Vertical transmission of hepatitis B virus: challenges and solutions. In: *International journal of women's health* 6, S. 605–611. DOI: 10.2147/IJWH.S51138.
- Gerlich, Wolfram H. (2013): Medical virology of hepatitis B: how it began and where we are now. In: *Virology journal* 10, S. 239. DOI: 10.1186/1743-422X-10-239.
- Grewal, Iqbal S. (2008): CD70 as a therapeutic target in human malignancies. In: *Expert opinion on therapeutic targets* 12 (3), S. 341–351. DOI: 10.1517/14728222.12.3.341.
- Guidotti, L. G.; Ishikawa, T.; Hobbs, M. V.; Matzke, B.; Schreiber, R.; Chisari, F. V. (1996): Intracellular inactivation of the hepatitis B virus by cytotoxic T lymphocytes. In: *Immunity* 4 (1), S. 25–36.
- Guidotti, L. G.; Martinez, V.; Loh, Y. T.; Rogler, C. E.; Chisari, F. V. (1994): Hepatitis B virus nucleocapsid particles do not cross the hepatocyte nuclear membrane in transgenic mice. In: *Journal of virology* 68 (9), S. 5469–5475.
- Guidotti, L. G.; Matzke, B.; Schaller, H.; Chisari, F. V. (1995): High-level hepatitis B virus replication in transgenic mice. In: *Journal of virology* 69 (10), S. 6158–6169.
- Hadziyannis, Stephanos J.; Vassilopoulos, Dimitrios (2001): Hepatitis B e antigen–negative chronic hepatitis B. In: *Hepatology* 34 (4), S. 617–624. DOI: 10.1053/jhep.2001.27834.
- Hawiger, D.; Inaba, K.; Dorsett, Y.; Guo, M.; Mahnke, K.; Rivera, M. et al. (2001): Dendritic cells induce peripheral T cell unresponsiveness under steady state conditions in vivo. In: *The Journal of experimental medicine* 194 (6), S. 769–779.
- Hendriks, Jenny; Xiao, Yanling; Borst, Jannie (2003): CD27 promotes survival of activated T cells and complements CD28 in generation and establishment of the effector T cell pool. In: *The Journal of experimental medicine* 198 (9), S. 1369–1380. DOI: 10.1084/jem.20030916.
- Hyams, K. C. (1995): Risks of Chronicity Following Acute Hepatitis B Virus Infection. A Review. In: *Clinical Infectious Diseases* 20 (4), S. 992–1000. DOI: 10.1093/clinids/20.4.992.

- Iborra, Salvador; Izquierdo, Helena M.; Martinez-Lopez, Maria; Blanco-Menendez, Noelia; Reis e Sousa, Caetano; Sancho, David (2012): The DC receptor DNCR-1 mediates cross-priming of CTLs during vaccinia virus infection in mice. In: *The Journal of clinical investigation* 122 (5), S. 1628–1643. DOI: 10.1172/JCI60660.
- Israel, Bruce F.; Gulley, Margaret; Elmore, Sandra; Ferrini, Silvano; Feng, Wen-hai; Kenney, Shannon C. (2005): Anti-CD70 antibodies: a potential treatment for EBV+ CD70-expressing lymphomas. In: *Molecular cancer therapeutics* 4 (12), S. 2037–2044. DOI: 10.1158/1535-7163.MCT-05-0253.
- Jacobs, J.; Deschoolmeester, V.; Zwaenepoel, K.; Rolfo, C.; Silence, K.; Rottey, S. et al. (2015): CD70: An emerging target in cancer immunotherapy. In: *Pharmacology & therapeutics* 155, S. 1–10. DOI: 10.1016/j.pharmthera.2015.07.007.
- Kastenmuller, Wolfgang; Drexler, Ingo; Ludwig, Holger; Erfle, Volker; Peschel, Christian; Bernhard, Helga; Sutter, Gerd (2006): Infection of human dendritic cells with recombinant vaccinia virus MVA reveals general persistence of viral early transcription but distinct maturation-dependent cytopathogenicity. In: *Virology* 350 (2), S. 276–288. DOI: 10.1016/j.virol.2006.02.039.
- Kastenmuller, Wolfgang; Gasteiger, Georg; Gronau, Julian H.; Baier, Robert; Ljapoci, Ronny; Busch, Dirk H.; Drexler, Ingo (2007): Cross-competition of CD8+ T cells shapes the immunodominance hierarchy during boost vaccination. In: *The Journal of experimental medicine* 204 (9), S. 2187–2198. DOI: 10.1084/jem.20070489.
- Keller, Anna M.; Schildknecht, Anita; Xiao, Yanling; van den Broek, Maries; Borst, Jannie (2008): Expression of costimulatory ligand CD70 on steady-state dendritic cells breaks CD8+ T cell tolerance and permits effective immunity. In: *Immunity* 29 (6), S. 934–946. DOI: 10.1016/j.immuni.2008.10.009.
- Keller, Anna M.; Xiao, Yanling; Peperzak, Victor; Naik, Shalin H.; Borst, Jannie (2009): Costimulatory ligand CD70 allows induction of CD8+ T-cell immunity by immature dendritic cells in a vaccination setting. In: *Blood* 113 (21), S. 5167–5175. DOI: 10.1182/blood-2008-03-148007.
- Knolle, Percy A.; Huang, Li-Rung; Kosinska, Anna; Wohlleber, Dirk; Protzer, Ulrike (2021): Improving Therapeutic Vaccination against Hepatitis B-Insights from Preclinical Models of Immune Therapy against Persistent Hepatitis B Virus Infection. In: *Vaccines* 9 (11). DOI: 10.3390/vaccines9111333.
- Knolle, Percy A.; Thimme, Robert (2014): Hepatic immune regulation and its involvement in viral hepatitis infection. In: *Gastroenterology* 146 (5), S. 1193–1207. DOI: 10.1053/j.gastro.2013.12.036.
- Ko, Chunkyu; Michler, Thomas; Protzer, Ulrike (2017): Novel viral and host targets to cure hepatitis B. In: *Current opinion in virology* 24, S. 38–45. DOI: 10.1016/j.coviro.2017.03.019.
- Kosinska, Anna D.; Festag, Julia; Mück-Häusl, Martin; Festag, Marvin M.; Asen, Theresa; Protzer, Ulrike (2021): Immunogenicity and Antiviral Response of Therapeutic Hepatitis B Vaccination in a Mouse Model of HBeAg-Negative, Persistent HBV Infection. In: *Vaccines* 9 (8). DOI: 10.3390/vaccines9080841.
- Kosinska, Anna D.; Johrden, Lena; Zhang, Ejuan; Fiedler, Melanie; Mayer, Anja; Wildner, Oliver et al. (2012): DNA prime-adenovirus boost immunization induces a vigorous and multifunctional T-cell response against hepadnaviral proteins in the mouse and woodchuck model. In: *Journal of virology* 86 (17), S. 9297–9310. DOI: 10.1128/JVI.00506-12.
- Kosinska, Anna D.; Liu, Jia; Lu, Mengji; Roggendorf, Michael (2015): Therapeutic vaccination and immunomodulation in the treatment of chronic hepatitis B: preclinical studies in the woodchuck. In: *Medical microbiology and immunology* 204 (1), S. 103–114. DOI: 10.1007/s00430-014-0379-5.
- Kosinska, Anna D.; Moeed, Abdul; Kallin, Nina; Festag, Julia; Su, Jinpeng; Steiger, Katja et al. (2019): Synergy of therapeutic heterologous prime-boost hepatitis B vaccination with CpG-application to improve immune control of persistent HBV infection. In: *Scientific reports* 9 (1), S. 10808. DOI: 10.1038/s41598-019-47149-w.
- Lau, G. K.; Suri, D.; Liang, R.; Rigopoulou, E. I.; Thomas, M. G.; Mullerova, I. et al. (2002): Resolution of chronic hepatitis B and anti-HBs seroconversion in humans by adoptive transfer of immunity to hepatitis B core antigen. In: *Gastroenterology* 122 (3), S. 614–624.

- Liang, Pu; Yi, Yao; Su, Qiu Dong; Qiu, Feng; Fan, Xue Ting; Lu, Xue Xin; Bi, Sheng Li (2018): Efficient Humoral and Cellular Immune Responses Induced by a Chimeric Virus-like Particle Displaying the Epitope of EV71 without Adjuvant. In: *Biomedical and environmental sciences : BES* 31 (5), S. 343–350. DOI: 10.3967/bes2018.045.
- Liu, Jia; Kosinska, Anna; Lu, Mengji; Roggendorf, Michael (2014a): New therapeutic vaccination strategies for the treatment of chronic hepatitis B. In: *Virologica Sinica* 29 (1), S. 10–16. DOI: 10.1007/s12250-014-3410-5.
- Liu, Jia; Zhang, Ejuan; Ma, Zhiyong; Wu, Weimin; Kosinska, Anna; Zhang, Xiaoyong et al. (2014b): Enhancing virus-specific immunity in vivo by combining therapeutic vaccination and PD-L1 blockade in chronic hepadnaviral infection. In: *PLoS pathogens* 10 (1), e1003856. DOI: 10.1371/journal.ppat.1003856.
- Lok, Anna S.; Zoulim, Fabien; Dusheiko, Geoffrey; Ghany, Marc G. (2017): Hepatitis B cure: From discovery to regulatory approval. In: *Hepatology (Baltimore, Md.)* 66 (4), S. 1296–1313. DOI: 10.1002/hep.29323.
- Luke, Garry A.; Felipe, Pablo de; Lukashev, Alexander; Kallioinen, Susanna E.; Bruno, Elizabeth A.; Ryan, Martin D. (2008): Occurrence, function and evolutionary origins of '2A-like' sequences in virus genomes. In: *The Journal of general virology* 89 (Pt 4), S. 1036–1042. DOI: 10.1099/vir.0.83428-0.
- Maini, M. K.; Boni, C.; Lee, C. K.; Larrubia, J. R.; Reignat, S.; Ogg, G. S. et al. (2000): The role of virus-specific CD8(+) cells in liver damage and viral control during persistent hepatitis B virus infection. In: *The Journal of experimental medicine* 191 (8), S. 1269–1280.
- Mancini-Bourgine, Maryline; Fontaine, Helene; Brechot, Christian; Pol, Stanislas; Michel, Marie-Louise (2006): Immunogenicity of a hepatitis B DNA vaccine administered to chronic HBV carriers. In: *Vaccine* 24 (21), S. 4482–4489. DOI: 10.1016/j.vaccine.2005.08.013.
- Manske, Katrin; Kallin, Nina; König, Verena; Schneider, Annika; Kurz, Sandra; Bosch, Miriam et al. (2018): Outcome of Antiviral Immunity in the Liver Is Shaped by the Level of Antigen Expressed in Infected Hepatocytes. In: *Hepatology (Baltimore, Md.)*. DOI: 10.1002/hep.30080.
- Mason, William S.; Gill, Upkar S.; Litwin, Samuel; Zhou, Yan; Peri, Suraj; Pop, Oltin et al. (2016): HBV DNA Integration and Clonal Hepatocyte Expansion in Chronic Hepatitis B Patients Considered Immune Tolerant. In: *Gastroenterology* 151 (5), 986–998.e4. DOI: 10.1053/j.gastro.2016.07.012.
- Matter, Matthias; Odermatt, Bernhard; Yagita, Hideo; Nuoffer, Jean-Marc; Ochsenbein, Adrian F. (2006): Elimination of chronic viral infection by blocking CD27 signaling. In: *The Journal of experimental medicine* 203 (9), S. 2145–2155. DOI: 10.1084/jem.20060651.
- McMahon, B. J.; Alward, W. L. M.; Hall, D. B.; Heyward, W. L.; Bender, T. R.; Francis, D. P.; Maynard, J. E. (1985): Acute Hepatitis B Virus Infection. Relation of Age to the Clinical Expression of Disease and Subsequent Development of the Carrier State. In: *Journal of Infectious Diseases* 151 (4), S. 599–603. DOI: 10.1093/infdis/151.4.599.
- Meier, Anja; Mehrle, Stefan; Weiss, Thomas S.; Mier, Walter; Urban, Stephan (2013): Myristoylated PreS1-domain of the hepatitis B virus L-protein mediates specific binding to differentiated hepatocytes. In: *Hepatology (Baltimore, Md.)* 58 (1), S. 31–42. DOI: 10.1002/hep.26181.
- Meyer, H.; Sutter, G.; Mayr, A. (1991): Mapping of deletions in the genome of the highly attenuated vaccinia virus MVA and their influence on virulence. In: *The Journal of general virology* 72 (Pt 5), S. 1031–1038. DOI: 10.1099/0022-1317-72-5-1031.
- Michalak, T. I.; Pasquinelli, C.; Guilhot, S.; Chisari, F. V. (1994): Hepatitis B virus persistence after recovery from acute viral hepatitis. In: *The Journal of clinical investigation* 93 (1), S. 230–239. DOI: 10.1172/JC1116950.
- Michler, Thomas; Kosinska, Anna D.; Festag, Julia; Bunse, Till; Su, Jinpeng; Ringelhan, Marc et al. (2020): Knockdown of Virus Antigen Expression Increases Therapeutic Vaccine Efficacy in High-Titer Hepatitis B Virus Carrier Mice. In: *Gastroenterology* 158 (6), 1762–1775.e9. DOI: 10.1053/j.gastro.2020.01.032.
- Peng, Cheng-Yuan; Chien, Rong-Nan; Liaw, Yun-Fan (2012): Hepatitis B virus-related decompensated liver cirrhosis: benefits of antiviral therapy. In: *Journal of hepatology* 57 (2), S. 442–450. DOI: 10.1016/j.jhep.2012.02.033.

- Pol, S.; Lampertico, P. (2012): First-line treatment of chronic hepatitis B with entecavir or tenofovir in 'real-life' settings: from clinical trials to clinical practice. In: *Journal of viral hepatitis* 19 (6), S. 377–386. DOI: 10.1111/j.1365-2893.2012.01602.x.
- Pol, S.; Nalpas, B.; Driss, F.; Michel, M. L.; Tiollais, P.; Denis, J.; Brecho, C. (2001): Efficacy and limitations of a specific immunotherapy in chronic hepatitis B. In: *Journal of hepatology* 34 (6), S. 917–921.
- Prasad, K. V. S.; Ao, Zhaohui; Yoon, Yoosik; Wu, Mei X.; Rizk, Majida; Jacquot, Serge; Schlossman, Stuart F. (1997): CD27, a member of the tumor necrosis factor receptor family, induces apoptosis and binds to Siva, a proapoptotic protein. In: *Proceedings of the National Academy of Sciences of the United States of America* 94 (12), S. 6346–6351.
- Probst, Hans Christian; McCoy, Kathy; Okazaki, Taku; Honjo, Tasuku; van den Broek, Maries (2005): Resting dendritic cells induce peripheral CD8+ T cell tolerance through PD-1 and CTLA-4. In: *Nature immunology* 6 (3), S. 280–286. DOI: 10.1038/ni1165.
- Protzer, Ulrike; Knolle, Percy (2016): "To Be or Not to Be": Immune Tolerance in Chronic Hepatitis B. In: *Gastroenterology* 151 (5), S. 805–806. DOI: 10.1053/j.gastro.2016.09.038.
- Publicover, J.; Gaggar, A.; Nishimura, S.; van Horn, C. M.; Goodsell, A.; Muench, M. O. et al. (2013): Age-dependent hepatic lymphoid organization directs successful immunity to hepatitis B. In: *The Journal of clinical investigation* 123 (9), S. 3728–3739. DOI: 10.1172/JCI68182.
- Pumpens, P.; Grens, E. (2001): HBV core particles as a carrier for B cell/T cell epitopes. In: *Intervirology* 44 (2-3), S. 98–114. DOI: 10.1159/000050037.
- Razavi-Shearer, Devin; Gamkrelidze, Ivane; Nguyen, Mindie H.; Chen, Ding-Shinn; van Damme, Pierre; Abbas, Zaigham et al. (2018): Global prevalence, treatment, and prevention of hepatitis B virus infection in 2016. A modelling study. In: *The Lancet Gastroenterology & Hepatology* 3 (6), S. 383–403. DOI: 10.1016/S2468-1253(18)30056-6.
- Rehermann, B.; Ferrari, C.; Pasquinelli, C.; Chisari, F. V. (1996): The hepatitis B virus persists for decades after patients' recovery from acute viral hepatitis despite active maintenance of a cytotoxic T-lymphocyte response. In: *Nat Med*. 1996.
- Rehermann, Barbara (2000): Intrahepatic T Cells in Hepatitis B: Viral Control versus Liver Cell Injury. In: *The Journal of experimental medicine* 191 (8), S. 1263–1268.
- Rehermann, Barbara; Nascimbeni, Michelina (2005): Immunology of hepatitis B virus and hepatitis C virus infection. In: *Nature reviews. Immunology* 5 (3), S. 215–229. DOI: 10.1038/nri1573.
- Roberts, Drew J.; Franklin, Nathan A.; Kingeter, Lara M.; Yagita, Hideo; Tutt, Alison L.; Glennie, Martin J.; Bullock, Timothy N. J. (2010): Control of established melanoma by CD27 stimulation is associated with enhanced effector function and persistence, and reduced PD-1 expression of tumor infiltrating CD8(+) T cells. In: *Journal of immunotherapy (Hagerstown, Md. : 1997)* 33 (8), S. 769–779. DOI: 10.1097/CJI.0b013e3181ee238f.
- Roose, Kenny; Baets, Sarah de; Schepens, Bert; Saelens, Xavier (2013): Hepatitis B core-based virus-like particles to present heterologous epitopes. In: *Expert review of vaccines* 12 (2), S. 183–198. DOI: 10.1586/erv.12.150.
- Saikia, Nripen; Talukdar, Rupjyoti; Mazumder, Subhasish; Khanna, Sudeep; Tandon, Rakesh (2007): Management of patients with HBeAg-negative chronic hepatitis B. In: *Postgraduate medical journal* 83 (975), S. 32–39. DOI: 10.1136/pgmj.2006.044826.
- Schildknecht, Anita; Miescher, Iris; Yagita, Hideo; van den Broek, Maries (2007): Priming of CD8+ T cell responses by pathogens typically depends on CD70-mediated interactions with dendritic cells. In: *European journal of immunology* 37 (3), S. 716–728. DOI: 10.1002/eji.200636824.
- Schurich, Anna; Khanna, Pooja; Lopes, A. Ross; Han, Ki Jun; Peppas, Dimitra; Micco, Lorenzo et al. (2011): Role of the coinhibitory receptor cytotoxic T lymphocyte antigen-4 on apoptosis-prone CD8 T cells in persistent hepatitis B virus infection. In: *Hepatology (Baltimore, Md.)* 53 (5), S. 1494–1503. DOI: 10.1002/hep.24249.

- Shen, X.; Wong, S. B.; Buck, C. B.; Zhang, J.; Siliciano, R. F. (2002): Direct priming and cross-priming contribute differentially to the induction of CD8+ CTL following exposure to vaccinia virus via different routes. In: *Journal of immunology (Baltimore, Md. : 1950)* 169 (8), S. 4222–4229.
- Song, Jeong Eun; Kim, Do Young (2016): Diagnosis of hepatitis B. In: *Annals of translational medicine* 4 (18), S. 338. DOI: 10.21037/atm.2016.09.11.
- Stephan, Ann-Sophie; Kosinska, Anna D.; Mück-Häusl, Martin; Muschaweckh, Andreas; Jäger, Clemens; Röder, Natalie et al. (2023): Evaluation of the Effect of CD70 Co-Expression on CD8 T Cell Response in Protein-Prime MVA-Boost Vaccination in Mice. In: *Vaccines* 11 (2). DOI: 10.3390/vaccines11020245.
- Su, Jinpeng; Brunner, Livia; Ates Oz, Edanur; Sacherl, Julia; Frank, Geraldine; Kerth, Helene Anne et al. (2023): Activation of CD4 T cells during prime immunization determines the success of a therapeutic hepatitis B vaccine in HBV-carrier mouse models. In: *Journal of hepatology* 78 (4), S. 717–730. DOI: 10.1016/j.jhep.2022.12.013.
- Sunbul, Mustafa (2014): Hepatitis B virus genotypes: global distribution and clinical importance. In: *World journal of gastroenterology* 20 (18), S. 5427–5434. DOI: 10.3748/wjg.v20.i18.5427.
- Tan, Wen Siang (2014): Phage display creates innovative applications to combat hepatitis B virus. In: *WJG* 20 (33), S. 11650. DOI: 10.3748/wjg.v20.i33.11650.
- Tesselaar, Kiki; Arens, Ramon; van Schijndel, Gijs M. W.; Baars, Paul A.; van der Valk, Martin A.; Borst, Jannie et al. (2003a): Lethal T cell immunodeficiency induced by chronic costimulation via CD27-CD70 interactions. In: *Nature immunology* 4 (1), S. 49–54. DOI: 10.1038/ni869.
- Tesselaar, Kiki; Xiao, Yanling; Arens, Ramon; van Schijndel, Gijs M. W.; Schuurhuis, Danita H.; Mebius, Reina E. et al. (2003b): Expression of the murine CD27 ligand CD70 in vitro and in vivo. In: *Journal of immunology (Baltimore, Md. : 1950)* 170 (1), S. 33–40.
- TherVacB project (2020). Online verfügbar unter <https://www.thervacb.eu/>, zuletzt geprüft am 30.01.2023.
- Thimme, Robert; Wieland, Stefan; Steiger, Carola; Ghayeb, John; Reimann, Keith A.; Purcell, Robert H.; Chisari, Francis V. (2003): CD8(+) T cells mediate viral clearance and disease pathogenesis during acute hepatitis B virus infection. In: *Journal of virology* 77 (1), S. 68–76.
- Trevor, K. T.; Hersh, E. M.; Brailey, J.; Balloul, J. M.; Acres, B. (2001): Transduction of human dendritic cells with a recombinant modified vaccinia Ankara virus encoding MUC1 and IL-2. In: *Cancer immunology, immunotherapy : CII* 50 (8), S. 397–407.
- Tscharke, David C.; Karupiah, Gunasegaran; Zhou, Jie; Palmore, Tara; Irvine, Kari R.; Haeryfar, S. M. Mansour et al. (2005): Identification of poxvirus CD8+ T cell determinants to enable rational design and characterization of smallpox vaccines. In: *The Journal of experimental medicine* 201 (1), S. 95–104. DOI: 10.1084/jem.20041912.
- Tuttleman, J. S.; Pourcel, C.; Summers, J. (1986): Formation of the pool of covalently closed circular viral DNA in hepadnavirus-infected cells. In: *Cell* 47 (3), S. 451–460.
- Tzeng, Horng-Tay; Tsai, Hwei-Fang; Liao, Hsiu-Jung; Lin, Yi-Jiun; Chen, Lieping; Chen, Pei-Jer; Hsu, Ping-Ning (2012): PD-1 blockage reverses immune dysfunction and hepatitis B viral persistence in a mouse animal model. In: *PLoS one* 7 (6), e39179. DOI: 10.1371/journal.pone.0039179.
- Utzschneider, Daniel T.; Alfei, Francesca; Roelli, Patrick; Barras, David; Chennupati, Vijaykumar; Darbre, Stephanie et al. (2016): High antigen levels induce an exhausted phenotype in a chronic infection without impairing T cell expansion and survival. In: *The Journal of experimental medicine* 213 (9), S. 1819–1834. DOI: 10.1084/jem.20150598.
- van Lier, R. A.; Borst, J.; Vroom, T. M.; Klein, H.; van Mourik, P.; Zeijlemaker, W. P.; Melief, C. J. (1987): Tissue distribution and biochemical and functional properties of Tp55 (CD27), a novel T cell differentiation antigen. In: *Journal of immunology (Baltimore, Md. : 1950)* 139 (5), S. 1589–1596.

- Vandepapeliere, Pierre; Lau, George K. K.; Leroux-Roels, Geert; Horsmans, Yves; Gane, Edward; Tawandee, Tawesak et al. (2007): Therapeutic vaccination of chronic hepatitis B patients with virus suppression by antiviral therapy: a randomized, controlled study of co-administration of HBsAg/AS02 candidate vaccine and lamivudine. In: *Vaccine* 25 (51), S. 8585–8597. DOI: 10.1016/j.vaccine.2007.09.072.
- Wang, Zhongde; Martinez, Joy; Zhou, Wendi; La Rosa, Corinna; Srivastava, Tumul; Dasgupta, Anindya et al. (2010): Modified H5 promoter improves stability of insert genes while maintaining immunogenicity during extended passage of genetically engineered MVA vaccines. In: *Vaccine* 28 (6), S. 1547–1557. DOI: 10.1016/j.vaccine.2009.11.056.
- Watashi, Koichi; Urban, Stephan; Li, Wenhui; Wakita, Takaji (2014): NTCP and beyond: opening the door to unveil hepatitis B virus entry. In: *International journal of molecular sciences* 15 (2), S. 2892–2905. DOI: 10.3390/ijms15022892.
- Webster, George J. M.; Reignat, Stephanie; Brown, David; Ogg, Graham S.; Jones, Louise; Seneviratne, Suranjith L. et al. (2004): Longitudinal analysis of CD8+ T cells specific for structural and nonstructural hepatitis B virus proteins in patients with chronic hepatitis B: implications for immunotherapy. In: *Journal of virology* 78 (11), S. 5707–5719. DOI: 10.1128/JVI.78.11.5707-5719.2004.
- Wherry, E. John; Kurachi, Makoto (2015): Molecular and cellular insights into T cell exhaustion. In: *Nature reviews. Immunology* 15 (8), S. 486–499. DOI: 10.1038/nri3862.
- WHO (2015): Guidelines for the Prevention Care and Treatment of Persons with Chronic Hepatitis B Virus Infection. Mar-15. Geneva: World Health Organization (DOCUMENTS FOR SALE). Online verfügbar unter <http://gbv.ebib.com/patron/FullRecord.aspx?p=2033880>.
- WHO (2022): Hepatitis B. Fact sheet. Online verfügbar unter <https://www.who.int/news-room/fact-sheets/detail/hepatitis-b>, zuletzt aktualisiert am 24.07.2022, zuletzt geprüft am 29.01.2023.
- Will, H.; Reiser, W.; Weimer, T.; Pfaff, E.; Buscher, M.; Sprengel, R. et al. (1987): Replication strategy of human hepatitis B virus. In: *Journal of virology* 61 (3), S. 904–911.
- Wooddell, Christine I.; Yuen, Man-Fung; Chan, Henry Lik-Yuen; Gish, Robert G.; Locarnini, Stephen A.; Chavez, Deborah et al. (2017): RNAi-based treatment of chronically infected patients and chimpanzees reveals that integrated hepatitis B virus DNA is a source of HBsAg. In: *Science translational medicine* 9 (409). DOI: 10.1126/scitranslmed.aan0241.
- Wyatt, Linda S.; Earl, Patricia L.; Xiao, Wei; Americo, Jeffrey L.; Cotter, Catherine A.; Vogt, Jennifer; Moss, Bernard (2009): Elucidating and Minimizing the Loss by Recombinant Vaccinia Virus of Human Immunodeficiency Virus Gene Expression Resulting from Spontaneous Mutations and Positive Selection. In: *Journal of virology* 83 (14), S. 7176–7184. DOI: 10.1128/JVI.00687-09.
- Xia, Yuchen; Stadler, Daniela; Lucifora, Julie; Reisinger, Florian; Webb, Dennis; Hösel, Marianna et al. (2016): Interferon- $\gamma$  and Tumor Necrosis Factor- $\alpha$  Produced by T Cells Reduce the HBV Persistence Form, cccDNA, Without Cytolysis. In: *Gastroenterology* 150 (1), S. 194–205. DOI: 10.1053/j.gastro.2015.09.026.
- Yalcin, K.; Acar, M.; Degertekin, H. (2003a): Specific hepatitis B vaccine therapy in inactive HBsAg carriers: a randomized controlled trial. In: *Infection* 31 (4), S. 221–225.
- Yalcin, K.; Danis, R.; Degertekin, H.; Alp, M. N.; Tekes, S.; Budak, T. (2003b): The lack of effect of therapeutic vaccination with a pre-S2/S HBV vaccine in the immune tolerant phase of chronic HBV infection. In: *Journal of clinical gastroenterology* 37 (4), S. 330–335.
- Yan, Huan; Zhong, Guocai; Xu, Guangwei; He, Wenhui; Jing, Zhiyi; Gao, Zhenchao et al. (2012): Sodium taurocholate cotransporting polypeptide is a functional receptor for human hepatitis B and D virus. In: *eLife Sciences* 1, e00049. DOI: 10.7554/eLife.00049.
- Yang, F-Q; Yu, Y-Y; Wang, G-Q; Chen, J.; Li, J-H; Li, Y-Q et al. (2012): A pilot randomized controlled trial of dual-plasmid HBV DNA vaccine mediated by in vivo electroporation in chronic hepatitis B patients under lamivudine chemotherapy. In: *Journal of viral hepatitis* 19 (8), S. 581–593. DOI: 10.1111/j.1365-2893.2012.01589.x.

Yang, S-H; Lee, C-G; Park, S-H; Im, S-J; Kim, Y-M; Son, J-M et al. (2006): Correlation of antiviral T-cell responses with suppression of viral rebound in chronic hepatitis B carriers: a proof-of-concept study. In: *Gene therapy* 13 (14), S. 1110–1117. DOI: 10.1038/sj.gt.3302751.

Zelenay, Santiago; Keller, Anna M.; Whitney, Paul G.; Schraml, Barbara U.; Deddouche, Safia; Rogers, Neil C. et al. (2012): The dendritic cell receptor DNGR-1 controls endocytic handling of necrotic cell antigens to favor cross-priming of CTLs in virus-infected mice. In: *The Journal of clinical investigation* 122 (5), S. 1615–1627. DOI: 10.1172/JCI60644.

## Danksagungen

Mein herzlicher Dank gilt folgenden Personen, die mich während der Erarbeitung meiner Doktorarbeit unterstützt haben:

An erster Stelle möchte ich meiner Doktormutter Prof. Dr. Ulrike Protzer danken für die Möglichkeit, am Institut für Virologie zu promovieren. Danke für die hervorragende Betreuung und die wissenschaftliche Unterstützung während der gesamten Zeit meiner Promotion.

Meinem zweiten Betreuer Prof. Dr. Percy Knolle danke ich besonders für das konstruktive Feedback während der Mentoratstreffen.

Meiner Mentorin Dr. Claudia Dembek kann ich vermutlich gar nicht genug danken: für die Idee und die Konzeption meines Promotionsprojekts, das gemeinsame Durchführen von Experimenten, das Einführen in die für mich unbekannte Welt des virologischen Labors, die vielen Gespräche, wenn es mal nicht weiterging und fürs Dranbleiben während Durststrecken. Ihre herzliche und offene Art hat wesentlich dazu beigetragen, dass ich mich im Labor sehr wohlfühlt habe und ihr mehrfaches Korrigieren der Monographie und des Papers waren maßgeblich dafür, dass alles zu einem guten Ende kam.

Auch Dr. Anna Kosinska gilt mein herzlicher Dank für die Durchführung eines zusätzlichen Mausexperiments und die häufigen bereichernden Gespräche, insbesondere bezüglich des strukturellen Aufbaus des Papers und meiner Monographie, der FACS-Färbungen und der Auswertung der Mausdaten. Natalie Röder danke ich für die Hilfe bei den Mausexperimenten, Dr. Martin Mück-Häusl und Dr. Andreas Muschawekh für das Zurverfügungstellen von Material und Wissen für die Herstellung von MVA, sowie Prof. Dr. Mathias Heikenwälder und seinen Mitarbeitern für das Herstellen der histologischen Schnitte und Färbungen. Dr. Florian Rosenberger und Dr. Oliver Quitt danke ich für das sorgfältige Korrekturlesen meines Papers. Nicht unerwähnt bleiben sollen alle weiteren Mitglieder des Trogerstraßenlabors und der „Schnecke“, die mir inhaltlich oder methodisch weitergeholfen haben.

Miriam Büxenstein, Stefanie Rosenberger und Maria Fritsch danke ich für die treue Freundschaft und für den moralischen Beistand in allen Lebenslagen.

Meiner Mama danke ich von Herzen für die aufopfernde Erziehung und die Förderung meiner verschiedenen Interessen, sowie dafür, dass sie mich im Verfolgen meiner persönlichen und beruflichen Ziele bedingungslos mit Rat und Tat unterstützt. Ohne ihre finanzielle Rückendeckung hätte ich dieses Promotionsvorhaben nicht so zuversichtlich in Angriff nehmen können. Mit Dankbarkeit denke ich auch an meinen Vater, der mir immer ein Vorbild war und ohne den ich vermutlich nicht in der Medizin gelandet wäre.

Meinen Geschwistern Johannes und Friederike danke ich für die Freundschaft und Verbundenheit und für so manches motivierende Gespräch, als der Berg an Arbeit noch hoch und der Weg noch weit war.

Meinem Mann Emanuel möchte ich unter anderem für seine Geduld und Hingabe danken, wenn es darum ging, Präsentationen, Texte und Abbildungen zu verbessern. Das genaue Zuhören und Nachfragen und seine treffsicheren Verbesserungsvorschläge waren mir eine große Hilfe. Doch natürlich möchte ich dir, Emanuel, nicht

nur für diese praktische Unterstützung und deine Zeit danken, sondern auch für die Liebe und den Rückhalt, die du mir schenkst. Ich schätze mich sehr glücklich, dich bei diesem Projekt und allen kommenden Abenteuern an meiner Seite zu haben.